Analytical Methods

Diffusion NMR Spectroscopy in Supramolecular and Combinatorial Chemistry: An Old Parameter—New Insights

Yoram Cohen, Liat Avram, and Limor Frish*

Keywords:
combinatorial chemistry · host–guest chemistry · molecular recognition · NMR spectroscopy · supramolecular chemistry

Dedicated to Professor Mordecai Rabinovitz on the occasion of his 70th birthday

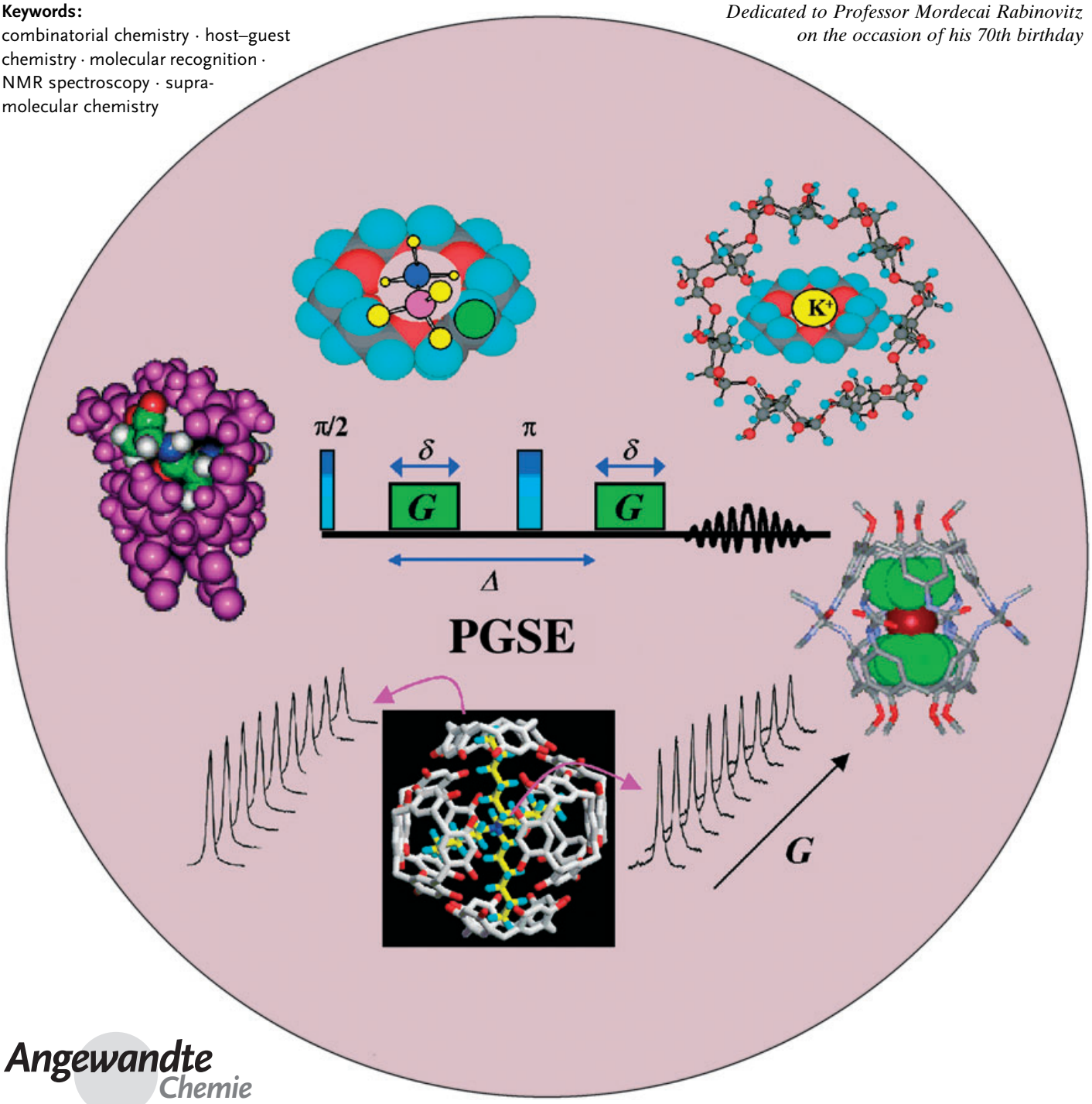

DOI: 10.1002/anie.200300637

Intermolecular interactions in solution play an important role in molecular recognition, which lies at the heart of supramolecular and combinatorial chemistry. Diffusion NMR spectroscopy gives information over such interactions and has become the method of choice for simultaneously measuring diffusion coefficients of multicomponent systems. The diffusion coefficient reflects the effective size and shape of a molecular species. Applications of this technique include the estimation of association constants and mapping the intermolecular interactions in multicomponent systems as well as investigating aggregation, ion pairing, encapsulation, and the size and structure of labile systems. Diffusion NMR spectroscopy can also be used to virtually separate mixtures and screen for specific ligands of different receptors, and may assist in finding lead compounds.

From the Contents

1. Introduction

1.1. Measuring High-Resolution Diffusion by NMR Spectroscopy

Over the last decade, pulsed field-gradient (PFG) NMR spectroscopy has become the method of choice for measuring diffusion in solutions in both chemical and biological systems. In principle, the diffusion coefficient of a certain molecular species under given conditions (for example, solvent and temperature) depends on its "effective" molecular weight, size, and shape. Therefore, it is evident that diffusion can be used to map intermolecular interactions that play an important role in both chemistry and biology in solution and which lie at the heart of molecular recognition, a process which is essential to supramolecular and combinatorial chemistry.[1–3] Nevertheless, chemists working in these fields have only recently started to use diffusion NMR spectroscopy to study their systems.

The fact that molecular diffusion can be measured by NMR methods was realised in the early days of NMR spectroscopy.[4] The most practical pulse sequence for measuring diffusion coefficients by NMR spectroscopy was introduced by Stejskal and Tanner in 1965,[5a] long before the advent of 2D NMR spectroscopy,[6–8] which is currently routinely used by chemists worldwide. Indeed, diffusion NMR measurements have increasingly been used since 1965, and most of these applications in solution up until 1987 were reviewed by Stilbs and Kärger et al.[9,10a]

The last decade has witnessed an explosion in the utilization of gradients in all areas of NMR spectroscopy, ranging from coherence selection in high-resolution NMR spectroscopy[11] to magnetic resonance imaging (MRI).[12] Indeed, the use of diffusion MRI of the central nervous systems (CNS) has, in particular, increased considerably over the last decade.[13] This is partially a result of the surprising efficacy of diffusion-weighted MRI in the early diagnosis of a stroke[14] and the opportunities that diffusion tensor imaging (DTI) provides in mapping the fiber tracts in the CNS.[15]

In view of the above, it may seem quite surprising that the application of diffusion NMR spectroscopy as a tool for studying molecular interactions in the context of supramolecular and combinatorial chemistry only began being implemented over the last few years. One reason for this is probably the fact that gradient sets, which are needed for the pulsed gradient spin echo (PGSE) experiment used to measure diffusion by NMR spectroscopy, were not commercially available until recently. However, with the advent of high-resolution gradient-enhanced spectroscopy[11] and the technological improvement in gradient performance, mainly because of the development of MRI, such gradient sets became commercially available and are currently conventional accessories of standard modern high-resolution NMR spectrometers. These gradient-containing high-resolution probes provide a means to simultaneously determine the diffusion coefficient for the entire set of signals in a high-resolution spectrum with high sensitivity and accuracy. It should be noted that diffusion NMR spectroscopy, as will be demonstrated herein, provides a means for studying diffusion in systems in equilibrium where no concentration gradients exist. In addition, new pulse sequences and methodologies, some of which will be briefly discussed herein, were developed, thus enabling modern NMR spectrometers to routinely perform simple and complex NMR diffusion experiments.

1.2. Applications of Diffusion NMR Spectroscopy

Diffusion NMR measurements are used in many different fields ranging from the medical sciences[12–15] to material sciences.[16–18] Recently, with the advent of high-resolution

[*] Prof. Y. Cohen, L. Avram, Dr. L. Frish
School of Chemistry
Tel Aviv University
Ramat Aviv, Tel Aviv 69978 (Israel)
Fax: (+972) 3-6409-293
E-mail: ycohen@post.tau.ac.il

 DOI: 10.1002/anie.200300637

gradient enhanced spectroscopy, some general reviews dealing with the theoretical and practical aspects of gradient NMR specroscopy have been published.[11,17] In addition, more-specific reviews on diffusion in polymers,[16b] zeolites and porous systems,[16a,18] surfactants,[19] and liquid crystals and membranes[20] have also been published. Since diffusion NMR spectroscopy is a totally non-invasive technique it is particularly suited to studying molecular dynamics and translational diffusion, and hence structural details in biological and physiological systems. Indeed, the application of diffusion NMR spectroscopy to membrane transport was recently reviewed,[21] and several reviews dealt with diffusion in restricted geometries.[17] q-Space diffusion NMR spectroscopy[22] laid the foundations for the utilization of such experiments to obtain structural information and compartment size. In addition, because of the non-invasiveness of the technique and the fact that the current technology is suitable for studying compartments of only a few microns in size, q-space diffusion MR was recently used to study biological systems.[23–25] Very recently, we expanded this approach to q-space MRI of the CNS.[26,27] Callaghan and others have used diffusion NMR spectroscopy and MRI to study complex fluids.[28] Van As and co-workers, for example, used these techniques to study flow in porous materials used for chromatography.[29]

In this Review the applications of high-resolution diffusion NMR spectroscopy in solution will be discussed, with special emphasis on applications in the fields of supramolecular and combinatorial chemistry. The Review will concentrate on the applications in these fields of chemistry rather than on an extensive description of the theory of diffusion NMR experiments which can be found in many of the recently published reviews.[9–11,16–21,28] We shall include a brief description of diffusion in the context of NMR measurements (Section 2) and a basic description of the NMR methods used to measure diffusion, with emphasis mainly on the most simple and commonly ones used to study diffusion in isotropic solutions (Section 3). In the main body of this Review (Sections 4 and 5) we shall describe different applications of diffusion NMR spectroscopy to demonstrate, through selected literature examples, the potential of simple diffusion NMR measurements in supramolecular and combinatorial chemistry. The final section gives future prospects for diffusion NMR spectroscopy (Section 6).

2. Concepts of Molecular Diffusion

2.1. Translational Diffusion in Isotropic Systems—"Free Diffusion"

Translational diffusion is one of the most important modes of molecular transport.[30] Self-diffusion is the random translational motion of ensembles of particles (molecules or ions) as a consequence of their thermal energy. In the case of self-diffusion, no (net) force acts on the molecular particles and, consequently, no net displacement is observed. In an isotropic homogeneous system the conditional probability $P(r_0,r,t_d)$ of finding a molecule, which was initially at position r_0, at position r after a time t_d is given by Equation (1), where D is

$$P(r_0,r,t_d) = (4\pi D t_d)^{-3/2} \exp\left(-\frac{(r-r_0)^2}{4 D t_d}\right) \quad (1)$$

the self-diffusion coefficient. This equation shows that the volume occupied by a molecule, originally at position r_0 relative to an arbitrary reference position, in a nonrestricted system is a Gaussian distribution that broadens with the increase in the diffusion time t_d (Figure 1). Therefore, the mean displacement of a particle under these conditions in all three directions by random walk is zero. However, the self-diffusion root-mean-square displacement $(\langle X^2\rangle)^{1/2}$ in such systems is given by the Einstein equation [Eq. (2)], where n is

$$(\langle X^2\rangle)^{1/2} = (n D t_d)^{1/2} \quad (2)$$

2, 4, or 6 for the cases of one-, two- and three-dimensional diffusion. From this equation it follows that the mean displacement for free diffusion increases linearly with the square root of the diffusion time.[31]

In addition, it is well known that diffusion is closely related to molecular size, as seen from the Einstein–Smoluchowski equation [Eq. (3)],[21,30] where k_b is the Boltzmann

$$D = \frac{k_b T}{f} = \frac{R T}{N f} \quad (3)$$

constant, T is the absolute temperature, f is the so-called hydrodynamic frictional coefficient, N is Avogadro's number, and R is the gas constant. For a sphere in a continuous

Yoram Cohen was born in 1956 in Israel and received his BSc (1981) and a PhD (1987) from the Hebrew University of Jerusalem under the supervision of Professors M. Rabinovitz and J. Klein. He then spent three years with Professor Tom James at the University of California at San Francisco (UCSF) as a Fulbright postdoctoral fellow. He joined the faculty of the School of Chemistry at Tel Aviv University in 1992 as a lecturer and was appointed senior lecturer in 1996 and associate professor in 2000. His research interests encompass NMR spectroscopy of supramolecular systems and MRS/MRI of the CNS with an emphasis on diffusion MR.

Limor Frish was born in Ramat Gan, Israel, in 1973 and received her BSc in chemistry from the School at Chemistry of Tel Aviv University in 1997. She has just received her PhD, which was carried out under the supervision of Prof. Yoram Cohen. Her main interest is the applications of diffusion NMR spectroscopy in supramolecular chemistry.

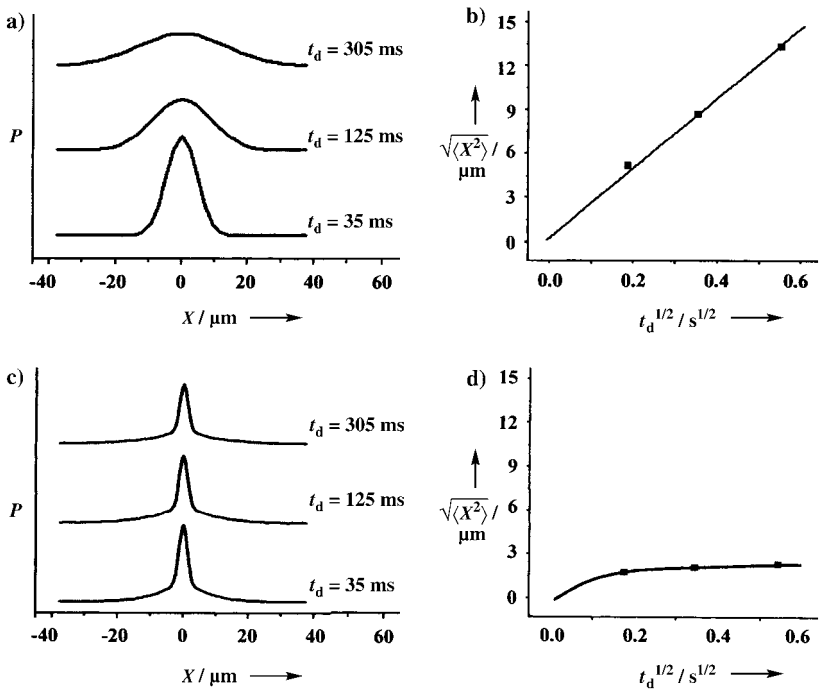

Figure 1. a), b) Free diffusion in a solution of *tert*-butanol; c), d) restricted diffusion (water in optic nerve). a), c) displacement distribution profiles; b), d) root-mean-square of the displacement *X* calculated from the full width at half height of the displacement distribution profiles shown in (a) and (c), respectively, against the square root of the diffusion time The slope of the straight line in (b) provides the self-diffusion coefficient of *tert*-butanol (2.7×10^{-6} $cm^2 s^{-1}$).[26c].

medium of viscosity η, f is given by the Stokes Equation [Eq. (4)].[30] In this equation, r_s is the hydrodynamic radius,

$$f = 6\pi\eta r_s \tag{4}$$

often called the Stokes' radius. Combining Equations (3) and (4) leads to the familiar Stokes–Einstein equation [Eq. (5)]. It

$$D = \frac{k_b T}{6\pi\eta r_s} \tag{5}$$

should be noted, however, that, different theories are needed to describe the hydrodynamic frictional coefficient f for molecular species of different geometries.[30]

Liat Avram was born in Tel Aviv, Israel, in 1977 and received her BSc and MSc in 1999 and 2001, respectively, from the School of Chemistry at Tel Aviv University. Since October 2001 she has been pursuing a PhD under the supervision of Prof. Yoram Cohen. She is a Charles Clore PhD Scholar.

Equation (5) indicates that, by measuring the self-diffusion coefficient of a given molecular species under controlled conditions, one may obtain information on its effective size or weight and, therefore, on the specific interactions of the species with its molecular environment. Thus, the diffusion coefficients are sensitive to structural properties of the observed molecular species such as weight, size, and shape, as well as binding phenomena, aggregation, and molecular interactions. In addition, there is no need for further interpretation of the diffusion coefficients, the values of which are directly related to the translational molecular displacement in the laboratory frame when diffusion occurs in a homogeneous medium that allows free and isotropic diffusion. However, in nonhomogeneous samples, where different modes of diffusion prevail, the extraction of diffusion coefficients from diffusion NMR experiments is a much more difficult task.

2.2. Other Modes of Diffusion: Restricted and Anisotropic Diffusion

As will be shown in Section 3, the spins are tagged at at least two time points in the different NMR methods used to study diffusion.[5,9–10,13–29] Therefore, the signal decay in a diffusion NMR experiment depends on the mean displacement of the particles during a certain time, called the diffusion time. Figure 1 shows the displacement distribution profiles for different diffusion times for free and restricted diffusion (Figure 1 a and c), as well as the mean displacement as a function of the square root of the diffusion time for free isotropic diffusion and restricted diffusion (Figure 1 b and d). For the case of free diffusion, the mean displacement experienced by the diffusing molecular species increases linearly with the square root of the diffusion time, as expected from Equation (2). By plotting the mean displacement as a function of the square root of the diffusion time, a linear graph is obtained, the slope of which reflects the diffusion coefficient (Figure 1 b). In a system where there are barriers which prohibit free diffusion, a situation may be envisaged in which an increase in the diffusion time does not translate into an increase in the mean displacement of the diffusing species. In such a situation there is no longer a linear relationship between the mean displacement and the square root of the diffusion time as shown in Figure 1 d. Restricted diffusion prevails in this situation and only an apparent diffusion coefficient can be obtained.[14,15] It is clear that such a restriction will occur when the diffusion time t_d is larger than $l^2/2D$, where l is the length of the compartment and D the diffusion coefficient of the diffusing molecular species. This means that the extracted apparent diffusion coefficients in such systems may be affected by the diffusion time t_d of the diffusion NMR experiment. Anisotropic diffusion may be

found in cases where the barriers which impose restriction are not uniformly distributed.[15] Both restricted and anisotropic diffusion are extremely important phenomena in heterogeneous systems such as porous materials and biological systems and provide, under certain experimental conditions, a means for obtaining structural information on the investigated system.[22–29] Since these phenomena are much less important in homogeneous solutions, we shall not elaborate any further on these modes of diffusion.

3. NMR Methods for Measuring Diffusion

In recent years diffusion NMR methods have replaced the traditional way of measuring self-diffusion coefficients with radioactive tracers, since NMR methods are easier to perform, are totally non-invasive, and allow simultaneous determination of diffusion coefficients in multicomponent systems. In the next section we shall outline the effect of magnetic field gradients on the measured NMR signal.[5a,9–11,16–18] Thereafter, we shall outline some of the most useful NMR methods for measuring diffusion in solution.

3.1. The Modified Spin-Echo Experiment: The Pulse Gradients Spin Echo Experiment

The basis for diffusion measurements is the fact that magnetic field gradients can be used indirectly to label the position of NMR-active nuclei through their Larmor frequency. This is done by applying an external gradient of the magnetic field, which is described by Equation (6), where $\hat{i}$, $\hat{j}$,

$$G = \frac{\partial Bz}{\partial x}\hat{i} + \frac{\partial Bz}{\partial y}\hat{j} + \frac{\partial Bz}{\partial z}\hat{k} \tag{6}$$

and $\hat{k}$ are the unit vectors in the x, y, and z directions, respectively. Thus, the total external magnetic field at position r is given by Equation (7). Spins precess with an angular

$$B(r) = B_0 + G\,r \tag{7}$$

frequency according to Equation (8). The acquired phase angle depends linearly on both $B(r)$ and the duration of the

$$\omega(r) = -\gamma B(r) \tag{8}$$

gradient δ. In the following, we assume that only a z gradient is present; hence, the gradient produces the position-dependent phase angle $\Phi(z)$ [Eq. (9)]. From these equations it is

$$\Phi(z) = -\gamma B(z)\delta \tag{9}$$

clear that the magnetic field gradient can be used to label the z position of the spins.

The most common approach to measuring diffusion is to use the pulsed gradient spin echo (PGSE) NMR technique,[5a] which is a modification of the Hahn spin echo pulse sequence.[4] In this sequence, two identical gradient pulses are inserted, one into each period τ of the spin-echo sequence (Figure 2).[5a,17a] The PGSE sequence and a schematic representation of its effect on the magnetization of an ensemble of spins are shown in Figure 2. The net magnetization at the beginning of the experiment is oriented along the z-axis,

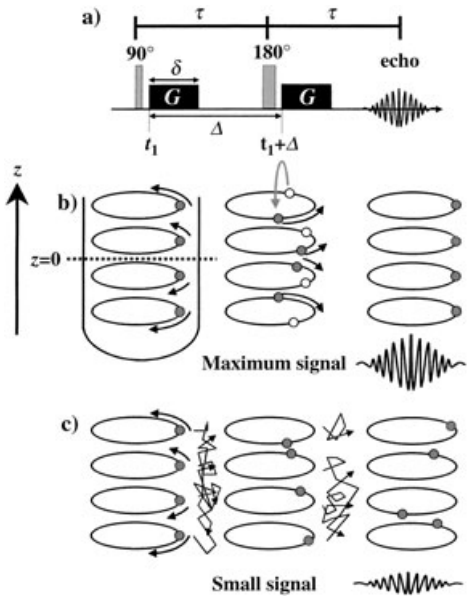

Figure 2. a) The PGSE pulse sequence.[5a] G is the amplitude of the pulsed gradient, δ its duration, and Δ the separation between the leading edges of the pulsed gradients. Also shown is the effect of the absence (b) and presence (c) of diffusion on the phase shift and signal intensity in a PGSE experiment. In the sequence shown in (a), the term $(\Delta-\delta/3)$ is the diffusion time. Adapted with permission from Ref. [17a].

which means that the ensemble of spins are in thermal equilibrium. A 90° radiofrequency (RF) pulse is then applied and, as a consequence, the magnetization rotates from the z-axis to the x-y plane. A pulse gradient of duration δ and magnitude G is then applied at a time point t_1. As a result, each spin experiences a phase shift according to Equation (10) at the end of the first period τ, just before

$$\Phi i(\tau) = \gamma B_0 \tau + \gamma G \int_{t_1}^{t_1+\delta} z_i(t)\mathrm{d}t \tag{10}$$

application of the 180° RF pulse. The left term is the phase shift arising from the static magnetic field, and the term on the right is the phase shift arising from the applied magnetic gradient pulse.

The next step is the application of a 180° RF pulse, which causes the reversal of the sign of the processing and the sign of the phase angle as depicted in Figure 2 (hollow circles become filled circles). A second gradient, equal in magnitude and duration to the first, is applied at time $t_1+\Delta$. At this point, two different scenarios can be considered. In the first scenario (Figure 2b) the spins do not undergo any translational motion along the z-axis, that is, there is no diffusion during the time interval. In this case, the phase shift of each spin after the first period τ is equal in magnitude to the phase shift of each spin

after the second period τ. Hence, the effects of the two pulsed gradients cancel out and all the spins refocus. In this case, a maximum echo signal is obtained. In the presence of diffusion (the second scenario, Figure 2c), however, the phase shift of each spin after the first period τ is different in magnitude from the phase shift of each spin after the second period τ. This effect occurs since, in the presence of diffusion, each species is located in a different position along the z-axis at times t_1 and $t_1+\Delta$, and hence each species is situated in a different magnetic field [Eq. (7)]. Therefore, the spins precess with altered angular frequencies in these different periods of time [Eq. (8)]. Thus, the phase angle fans out (at least partially) in the presence of diffusion, and the echo signal is consequently smaller. It can be intuitively deduced that larger diffusion is reflected by poorer refocusing of the spins and, consequently, by a smaller echo signal.

From these equations, it is apparent that the stronger and longer the phase of the pulsed gradients are, the poorer the refocusing of the spins and the smaller the recovered echo signal for diffusing spins. In addition, it is clear that the larger the Δ value is (the duration between the pulsed gradients) the smaller the echo intensity will be. Thus, without presenting the complete mathematical manipulations, it is clear that the signal intensity should be described by Equation (11), where

$$I_{(2\tau,G)} = I_{(0,0)}\exp\left(-\frac{2\tau}{T_2}\right)f(\delta,G,\Delta,D) = I_{(2\tau,0)}f(\delta,G,\Delta,D) \tag{11}$$

$I_{(0,0)}$ and $I_{(2\tau,0)}$ are the signal and echo intensity that would be observed immediately after the first 90° RF pulse and at 2τ, respectively, and $f(\delta,G,\Delta,D)$ is a function that represents the signal attenuation as a result of diffusion.

If the PGSE experiment is preformed such that τ is kept constant, then it is possible to separate the T_2 relaxation time and the diffusion contributions. Hence, after normalizing out the attenuation arising from T_2 relaxation, only the attenuation arising from the diffusion remains [Eq. (12)]. Stejskal

$$\frac{I_{(2\tau,G)}}{I_{(2\tau,0)}} = f(\delta,G,\Delta,D) \tag{12}$$

and Tanner have shown that the signal intensity for a single free-diffusing component is described in the case of rectangular pulse gradients by Equation (13),[5] and gives Equation (14), where γ is the gyromagnetic ratio, G is the pulsed

$$\begin{aligned} I_{(2\tau,G)} &= I_{(0,0)}\exp\left(\frac{-2\tau}{T_2}\right)\exp(-\gamma^2 G^2\delta^2(\Delta-\delta/3)D) \\ &= I_{(2\tau,0)}\exp(-\gamma^2 G^2\delta^2(\Delta-\delta/3)D) \end{aligned} \tag{13}$$

$$\ln\left(\frac{I_{(2\tau,G)}}{I_{(2\tau,0)}}\right) = -\gamma^2 G^2\delta^2(\Delta-\delta/3)D = -b\,D \tag{14}$$

gradient strength, Δ is the time separation between the pulsed-gradients, δ is the duration of the pulse, and D is the diffusion coefficient. The product $\gamma^2G^2\delta^2(\Delta-\delta/3)$ is termed the b value. Thus, a plot of $\ln(I_{(2\tau,G)}/I_{(2\tau,0)})$ versus the b values for an isotropic solution should give a straight line, the slope of which is equal to $-D$. In principle, any of the parameters δ, Δ, and G can be increased during the experiment to obtain increased signal attenuation. However, technical factors and the relaxation charactarictics of the sample may limit the choice. The term $(\Delta-\delta/3)$ is generally refered to as the diffusion time.[5b]

Figure 3 shows the results for a PGSE experiment in which the strength of the gradient pulse was incremented

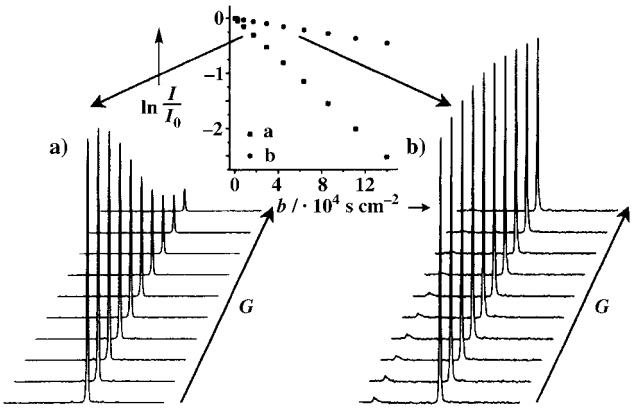

Figure 3. Signal decays as a function of G of the following diffusion coefficients: a) $D=1.81\times10^{-5}$ cm^{2}s^{-1} and b) $D=0.33\times10^{-5}$ cm^{2}s^{-1} together with the corresponding graphical analysis of the data; $\ln(I/I_0)\equiv\ln(I_{(2\tau,G)}/I_{(2\tau,0)})$.

from 0 to approximately 30 G cm^{-1} in ten steps while δ and Δ were kept constant. Figure 3a shows the signal attenuation of a small molecule, the diffusion coefficient of which is 1.81×10^{-5} cm^{2}s^{-1}, while Figure 3b shows the signal attenuation of another molecule having a diffusion coefficient of 0.33×10^{-5} cm^{2}s^{-1}. This figure shows that there is a more prononced attenuation of the signal intensity for the fast diffusing species as reflected by the steeper slope of the graph of $\ln(I_{(2\tau,G)}/I_{(2\tau,0)})$ versus the b values. It should be noted that $\ln(I_{(2\tau,G)}/I_{(2\tau,0)})$ is generally abreviated as $\ln(I/I_0)$.

3.2. The Stimulated Echo Diffusion Sequence

The standard stimulated echo (STE) diffusion experiment is shown in Figure 4a.[32] This sequence contains three 90° pulses; the echo after the third RF pulse was named by Hahn[4] as the "stimulated echo". The signal intensity of the STE diffusion experiment with rectangular pulse gradients is thus given by Equation (15).[32] From this equation it is clear

$$\begin{aligned} I_{(T_M+2\tau,G)} &= (I_{(0,0)}/2)\exp\left[\left(\frac{-2\tau}{T_2}\right)-\left(\frac{T_M}{T_1}\right)\right] \\ \exp(-\gamma^2 G^2\delta^2(\Delta-\delta/3)D) &= I_{(T_M+2\tau,0)}\exp(-\gamma^2 G^2\delta^2(\Delta-\delta/3)D) \end{aligned} \tag{15}$$

that the effects of relaxation and diffusion can again be separated in the signal decay. It was shown by performing the diffusion experiments with constant time intervals that the normalized signal decay in the STE diffusion experiments has the same dependency as the PGSE experiment.[5a,32] Comparison of Equation (15) with the expression for the signal

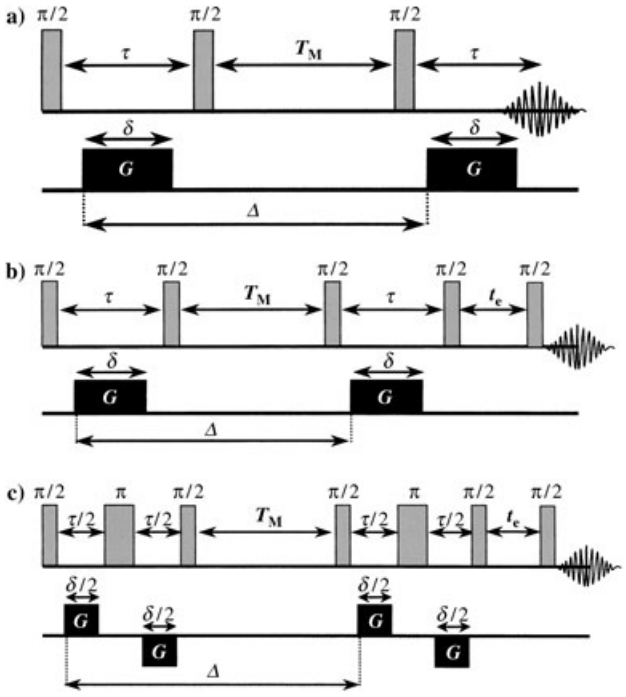

Figure 4. a) The STE diffusion pulse sequence,[32] b) the LED pulse sequence,[33] and c) the bipolar LED (BPLED) pulse sequence.[35a]

intensity of the PGSE [Eq. (13)] reveals two differences between the two equations: the reduction of the amplitude by a factor of two and—more importantly in the context of diffusion—the relaxation attenuation of the stimulated echo is dependent on T_1 during most of the diffusion interval (that is, during the time interval between the second and the third 90° pulses). This observation implies that one can use a STE diffusion sequence to obtain diffusion spectra of systems characterized by short T_2 times. This is an advantage since, in many systems, T_1 is significantly longer than T_2. The STE diffusion sequence allows an increase of the diffusion weighting by "paying" in the T_1 and not the T_2 relaxation time. The use of longer diffusion times is required for increasing the b values when measuring low diffusion coefficients and in situations where the diffusion coefficients may be dependent on the diffusion times (that is, in the cases of chemical exchange or restricted diffusion). In addition, the stimulated echo diffusion sequence is more suitable for measuring diffusion of spin–spin coupled systems.

The PGSE and STE diffusion sequences were introduced long before the advent of 2D NMR spectroscopy, but an important technical development at the beginning of the 1990s was that of diffusion ordered spectroscopy (DOSY), which was introduced by Johnson, Jr. and co-workers.[33–35]

3.3. The DOSY Technique

DOSY provides a means for "virtual separation" of compounds, by providing a 2D map in which one axis is the chemical shift while the other is that of the diffusion coefficient.[34–35] It is based on the longitudinal eddy-current delay (LED) and bipolar LED sequences and, more recently, 3D DOSY experiments have also been presented. We shall provide only a brief introduction to DOSY and the interested reader should refer to the comprehensive review recently published.[34]

3.3.1. The Basic LED and BPLED Experiments

An important requirement of the DOSY technique is the ability to discriminate between diffusion coefficients even when signals for similar-sized molecules overlap. To accomplish this goal it is essential to minimize spectral distortions that may result from eddy currents, which are induced from the gradient pulses and may, consequently, generate spectral distortions. The best way to avoid the effects of eddy currents is to prevent their formation in the first place. However, in spite of the best efforts, they may still be significant, especially when strong gradient pulses are used with short delays. Therefore, the LED sequence,[33] which is a modification of the stimulated echo sequence shown in Figure 4a, was introduced (Figure 4b).

As shown in Figure 4, the difference between these two sequences is the addition of two 90° pulses and a delay t_e at the end of the stimulated echo sequence. As a result of the fourth 90° pulse, the magnetization is stored in the longitudinal direction while the eddy currents decay. After the eddy current settling period t_e, the magnetization is recalled with an additional 90° pulse and an acquisition takes place (Figure 4b).

The bipolar LED (BPLED) sequence,[35a] which is a modification of the LED sequence, is shown in Figure 4c. In this sequence, each gradient pulse in the LED sequence is replaced by two pulses of different polarity separated by a 180° pulse. There are two advantages to using the BPLED over the LED experiment: Firstly, eddy currents are reduced to a minimum and, secondly,[35b] the effective gradient output is doubled. Thus, this sequence is useful in cases where large gradients are required to measure relatively low diffusion coefficients. For these reasons BPLED is the sequence of choice at present for many DOSY experiments. The DOSY sequence was also coupled into other methods such as INEPT and DEPT.[36]

3.3.2. The 2D DOSY Technique

The diffusion experiments presented above can be processed and displayed as a 2D matrix with chemical shifts plotted along one axis and diffusion coefficients plotted along the perpendicular axis (Figure 5). While the chemical shift information is obtained by fast Fourier transformation (FFT) of the time domain data, the diffusion information is obtained by an inverse Laplace transformation (ILT) of the signal decay data (Figure 6). The goal of the DOSY experiment is to separate species spectroscopically (not physically) present in a mixture of compounds. In this sense, the use of the DOSY experiment is reminiscent of the physical separation of compounds by chromatography. Thus, DOSY is also termed "NMR chromatography".[37] Figure 5 illustrates this concept. Each horizontal line represents a distinct diffusion coefficient

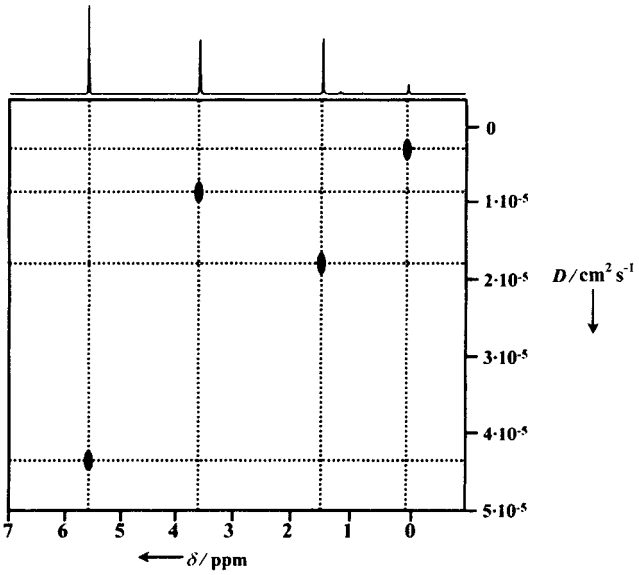

Figure 5. 2D DOSY spectrum showing four different species characterized by four different diffusion coefficients.

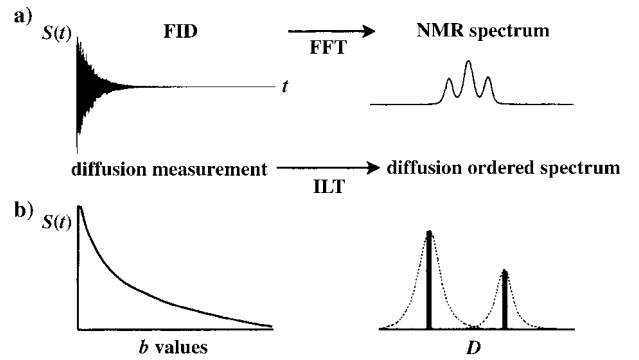

Figure 6. Comparison of FFT and ILT transformations. In contrast to the FT for the inverse laplace transform (ILT), there is not a single solution. Adapted with permission from Ref. [34].

and, hence, all the peaks on this horizontal line correlate with signals in the chemical shifts dimension, and should be attributed to a specific molecular species.

At a certain frequency, where a continuum of diffusion coefficients should be considered, the data sets $I(s)$, which describe the attenuation of this signal, should be described as Equation (16) ($\lambda = D(\Delta - \delta/3)$ and $s = \gamma^2\delta^2 G^2$). From Equation (16) it can be seen that $I(s)$ is the Laplace transform of $a(\lambda)$ and that $a(\lambda)$ is the Laplace spectrum of the diffusion coefficients. Thus, the desired spectrum $a(\lambda)$ is the inverse Laplace transform (ILT) of the decay function $I(s)$.

$$I(s) = \int_0^\infty a(\lambda)\exp(-\lambda s)\mathrm{d}\lambda \qquad (16)$$

It should be noted that a perfect transform produces the Laplace transform of delta functions and the inverse transformation should therefore exist. The required situation is that a unique transformation will exist as in the case of the FT shown in Figure 6a. However, there is no perfect transformation and the dotted lines in Figure 6b are the practical results which depict this statement. Hence, when running a DOSY experiment it is preferable that the diffusion coefficients differ as much as possible from one another and the standard errors in the diffusion coefficients be as marginal as possible.

3.3.3. *The 3D DOSY Technique*

In 3D DOSY experiments a diffusion coordinate is added to the conventional 2D map. Like the conventional 2D applications, these experiments reduce the probability of spectral overlap by spreading the NMR signals of the same species over an entire 2D plane[6–8] rather than along a single axis, while spreading the different species on a third axis on the basis of their diffusion coefficients. Indeed, in the first 3D DOSY experiment,[38] which was a DOSY-NOESY sequence, the overlapping peaks from a DNA duplex and a dinucleotide were resolved.

Figure 7a shows the pulse sequence for a DOSY-COSY experiment.[39a] This pulse sequence is constructed by linking the BPLED and the COSY sequences, with an eddy current delay t_e introduced between the BPLED and COSY sequences. Other 3D DOSY sequences, for example, DOSY-TOCSY[39b] and DOSY-HMQC,[39c] have been reported following the same rationale. Figure 7b shows a schematic representation of the results of a 3D DOSY sequence, and depicts the ability of this sequence to "virtually separate"

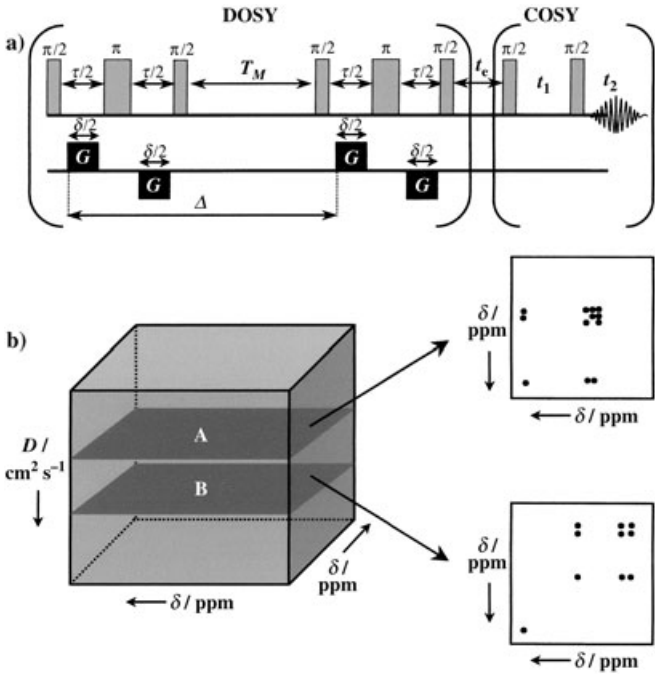

Figure 7. a) The DOSY-COSY pulse sequence[38] and b) a schematic representation of a 3D DOSY data obtained from a pulse sequence such as the one shown in (a). The DOSY-COSY experiment gives, after 3D transformation, a 2D COSY spectrum in each plane of the cube. Each plane in the cube represents a different diffusion coefficient. Adapted with permission from Ref. [34].

different components. The various compounds are spectroscopically separated according to their different diffusion coefficients. Thus, the planes at different altitudes on the diffusion axis of the cube represents the 2D spectrum of a different species. Figure 7b shows two schematic COSY spectra of compounds A and B, which clearly differ in their diffusion coefficients. It should be kept in mind that a 3D DOSY experiment is a time-consuming method, as are all 3D NMR methods. Indeed this is one of the major disadvantages of the 3D DOSY method.

4. Applications of NMR Diffusion Measurements in Supramolecular Chemistry

4.1. Molecular Interactions

Molecular interactions, which are so essential in supramolecular and combinatorial chemistry, have been studied by many different spectroscopic methods.[40] Despite the major role played by NMR spectroscopy in these fields, diffusion NMR spectroscopy, which we believe has great potential in assisting the characterization of such systems, is still not fully exploited. However, an increasing number of applications have demonstrated this potential in recent years. Some of these applications will be outlined below in a way that emphasizes the chemical information that can be obtained from such measurements.

4.1.1 Binding and Association Constants

The association constant K_a is a valuable measure that quantifies molecular interactions. In recent decades, tens of thousands of such constants have been determined by many different methods.[40,41] Despite the fact that NMR spectroscopy has become an important tool for studying association constants over the last two decades, diffusion NMR spectroscopy was not even mentioned as a possible option for studying host–guest systems in many of these reviews.[40a,42] Only a few very recent reviews devoted a short paragraph to the use of diffusion NMR spectroscopy for determining association constants.[43]

It was suggested many years ago that diffusion can be used to determine association constants.[44] The first example of such an application on a system that can be classified as an organic host–guest system was reported by Stilbs et al., who pioneered diffusion NMR spectroscopy of chemical systems by using a home-built gradient system.[45] In 1983 they measured the K_a values of different alcohols with α- and β-cyclodextrins (α-CD (**1**) and β-CD (**2**)) in D_2O.[46] The experimental errors for the determined association constants were relatively high in some cases.[46] However, the advancement of gradient technology has made such measurements much more accurate and reliable today.

In fact, since NMR diffusion coefficients can be directly observed by NMR spectroscopy, it can be used in a very similar way as chemical shifts to determine the stoichiometry and association constants of complexes.[43,44,46,47] For the simple case of a 1:1 stoichiometric host–guest complex

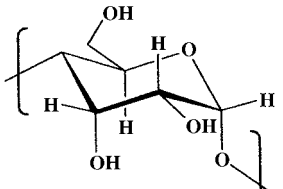

1 $n = 6$
2 $n = 7$
3 $n = 8$

(HG) formed between a host (H) and a guest (G), K_a is determined by Equation (17), where [H], [G], and [HG] are

$$K_a = \frac{[HG]}{[H]\,[G]} \tag{17}$$

the concentrations of the host, guest, and host–guest complex formed at equilibrium, respectively. In the case of slow exchange on the NMR time scale, the association constant can be determined by simple integration of the peaks of a solution of known concentrations. In these cases, diffusion measurements can only be used to probe the association between the different molecular species, however, numerical values of K_a cannot be obtained. However, in the case of fast exchange, the numerical value of the association constant can be determined.

The rationale behind the extraction of the bound fraction from diffusion NMR measurement is simple:[43,44,46,47] The host and guest have their own diffusion coefficients in the free state that reflect their molecular weight and shape. However, when a complex is formed and the host and guest are tightly bound, they should have the same diffusion coefficient since they diffuse as a single molecular entity.[44,46,47] In the case of a weak or negligible association, the diffusion coefficients of the host and the guest will remain unchanged. For any other case, assuming fast exchange on the NMR time scale, the observed (measured) diffusion coefficient (D_{obs}) is a weighted average of the free and bound diffusion coefficients (D_{free} and D_{bound}, respectively) and can, therefore, be used to calculate the bound fraction X, as shown in Equation (18), in the same

$$D_{obs} = X\,D_{bound} + (1-X)\,D_{free} \tag{18}$$

way that chemical shifts are used. Therefore, in principle, the same graphical and curve-fitting methodologies used to obtain K_a values from changes in chemical shifts in titration experiments[43] can be used to obtain association constants from diffusion NMR measurements. The most important difference between the two methods is that in many cases a complete titration to find D_{bound} for the guest is not a necessity with the former method. This is true in cases where there is a large difference between the molecular weight of the host and the guest (usually the guest has a significantly lower molecular weight) and, hence, one can predict, a priori, that the D_{bound} value of the guest will be very similar to the D_{free} value of the much larger host.[47]

One of the first examples of the determination of an association constant in the context of supramolecular chemis-

try by diffusion NMR spectroscopy using a conventional high-resolution NMR probe on a commercial instrument was the determination of the association constants of methylammonium chloride with [18]crown-6 (**4**) and [2.2.2]cryptand (**5**) in

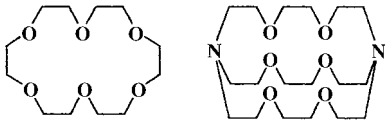

4 **5**

water and methanol.[47] Figure 8 shows the signal decay of **4** and methylammonium chloride in the absence and presence of **4** in methanol as a function of the gradient strength (G).

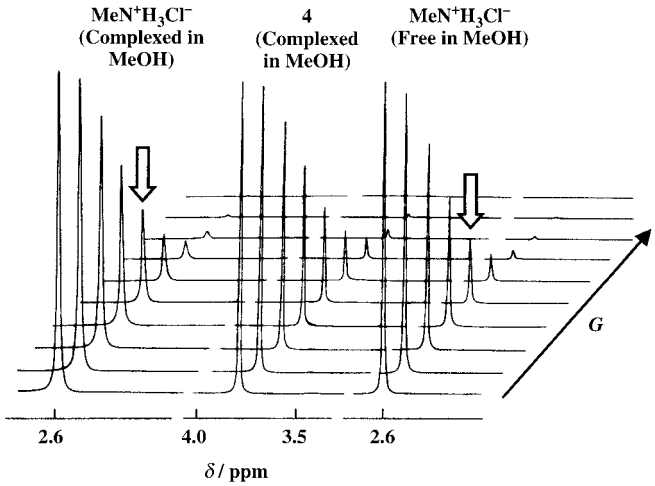

Figure 8. The signal decays in the Stejskal–Tanner diffusion experiments performed on a 50 mM solution of **4** and $MeNH_3^+Cl^-$ (1:1) in CD_3OD (middle and left) and on a 50 mM solution of free $MeNH_3^+Cl^-$ in CD_3OD (right). The arrows point to the difference in the intensities of the tetramethylammonium signal in the presence and absence of **4**. Reprinted with permission from Ref. [47].

This plot demonstrates that the signal attenuation of methylammonium chloride as a function of G in the presence of **4** is significantly smaller because of the formation of a complex with **4**. Here, the diffusion coefficients were extracted using the Stejskal–Tanner equation [Eq. (14)]. Figure 9 shows the normalized signal decays of **4**, methylammonium chloride, and their 1:1 mixture in CD_3OD as a function of G^2. The diffusion coefficients of these species and their 1:1 mixture, as well as the extracted association constants determined from the changes in the diffusion coefficients, are given in Table 1. The changes in the chemical shifts in the complexation of methylammonium chloride with **4** were small, thus making diffusion NMR spectroscopy an attractive alternative for determining the association constant.[47]

In principle, the determination of association constants using diffusion NMR measurements has advantages and limitations arising from the fact that this is an NMR-based

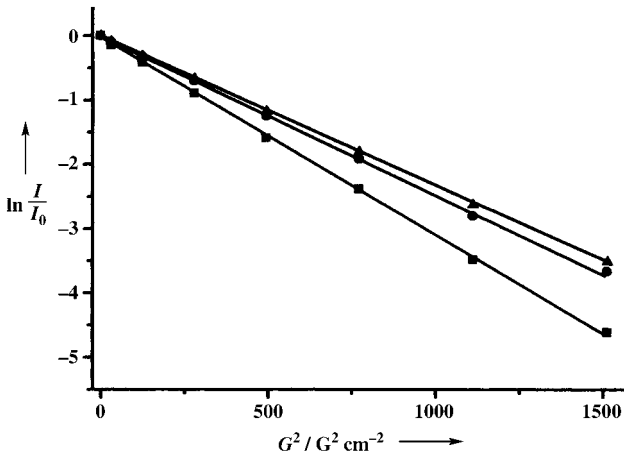

Figure 9. Normalized signal decay as a function of G^2 for methylammonium chloride in CD_3OD and methylammonium chloride and **4** (1:1) in 50 mM CD_3OD solution. ■: $MeNH_3^+Cl^-$ (free), ●: $MeNH_3^+Cl^-$ (complexed), ▲: **4**.

Table 1: Diffusion coefficients D and logarithm of the association constants K_a for the methylammonium chloride complex of [18]crown-6 (**4**) and [2.2.2]cryptand (**5**)[a] in D_2O and CD_3OD at various temperatures.[47]

Substance	Solvent	T/K	D_m [10^{-5} cm^2 s^{-1}]	$D_{MeNH_3^+}$ [10^{-5} cm^2 s^{-1}]	lg K_a [M^{-1}]
4 + $MeNH_3^+$	D_2O	298	0.55 ± 0.01	1.23 ± 0.02	0.67
4	D_2O	298	0.56 ± 0.01	–	
$MeNH_3^+$	D_2O	298	–	1.36 ± 0.01	
4 + $MeNH_3^+$	CD_3OD	298	1.34 ± 0.01	1.37 ± 0.02	3.69
4	CD_3OD	298	1.35 ± 0.02	–	
$MeNH_3^+$	CD_3OD	298	–	1.70 ± 0.01	
5 + $MeNH_3^+$	D_2O	298	0.46 ± 0.02	0.95 ± 0.04	1.53
5	D_2O	298	0.45 ± 0.04	–	
$MeNH_3^+$	D_2O	298	–	1.38 ± 0.01	
5 + $MeNH_3^+$	D_2O	277	0.21 ± 0.01	0.59 ± 0.01	1.67
5	D_2O	277	0.20 ± 0.01	–	
$MeNH_3^+$	D_2O	277	–	0.72 ± 0.01	
5 + $MeNH_3^+$	CD_3OD	298	1.14 ± 0.03	1.14 ± 0.03	> 4
$MeNH_3^+$	CD_3OD	298	–	1.64 ± 0.01	
5 + $MeNH_3^+$	CD_3OD	213	0.28 ± 0.01	0.29 ± 0.01	> 4
$MeNH_3^+$	CD_3OD	213	–	0.42 ± 0.06	

[a] All experiments were performed three times and the reported values are means ± standard deviation. m = macrocycle.

method.[43] Therefore, on the one hand, this method is less prone to misinterpretation because of minor impurities than methods based on UV and fluorescence, for example.[48] On the other hand, diffusion NMR spectroscopy is only suitable for measuring, in a direct way, association constants in the range of 10–10^5 M^{-1}. However, one of the main advantages of using diffusion NMR measurements to extract association constants, as compared with other NMR-based techniques such as chemical-shift titrations, is the elimination of one of the main possible sources of error in such techniques, namely, confusing acid–base chemistry with binding processes.[47] It should be noted, however, that in contrast to chemical shifts, proton transfer has only a marginal effect on the measured

diffusion coefficient.[47] This property enabled simple extraction of the association constant between methylammonium chloride and **5**, where partial protonation of **5** occurred as expected.

Since the diffusion of a certain molecular species depends on its effective molecular size, which should change with any intermolecular interaction, it is clear that diffusion coefficients are intuitively related to aggregation and intermolecular interactions. This means that only in diffusion measurements can the observable parameters of the bound guest be predicted a priori, thus reducing the need for a complete titration. The main limitation of the diffusion coefficient D as a parameter for the determination of the association constant is in systems where the interacting species happen to have similar diffusion coefficients in the free state, thus making the method much less sensitive or even impractical.

Particularly interesting host–guest systems are those in which the guest itself can act as the host for yet another smaller guest. Early examples of such systems are the macrocycle complexes with γ-CD (**3**) introduced by Vögtle and Muller as early as 1979.[49] These systems, subsequently analyzed by X-ray crystallography,[50,51] were recently studied in solution by diffusion NMR measurements.[52] In this study, complexation of [12]crown-4 (**6**), cyclen (**7**), and 1,4,7,10-tetrathiacyclododecane (**8**) with γ-CD were studied in the presence and absence of salts in various solvents and in D_2O at various pH values.[52] Although the ^{1}H NMR chemical shift changes were found to be very small in these systems, the difference in the molecular weight of the different macrocycles and that of γ-CD (**3**) enabled accurate determination of these relatively weak and modest association constants.[52] Figure 10 shows the normalized signal decay of **6** in the absence and presence of γ-CD before and after addition of lithium acetate (LiOAc) as an example. The diffusion coefficients of these systems, along with the extracted association constants, are given in Table 2. Interestingly, it was found that the presence of alkali metal salts decreased the association between the macrocycles and the γ-CD and that the pH value had practically no effect on the extracted association constants, thus suggesting that hydrogen bonding is not a dominant factor governing the association constant in these host–guest systems.[52] It was also found in these complexes that hydrophobic interactions, which are the major driving force of many of the complexes formed from cyclodextrins and organic systems in water, are not the major factor responsible for complexation.[52,53] In these systems, the changes in the chemical shifts were rather small and both the cation and the γ-CD had some effect on the chemical shift of the macrocycles, which made the extraction of association constants from this parameter very difficult and problematic. This example emphasizes the advantage of using diffusion coefficients to map the interaction of many molecular species simultaneously.

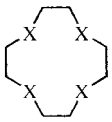

6 X = O
7 X = N
8 X = S

Table 2: Diffusion coefficients D and calculated association constants K_a of the γ-CD:macrocycle, macrocycle:salt, and the three-component systems at 298 K.[a],[b][52]

System	D_3 [10^{-5} cm^2 s^{-1}]	D_m [10^{-5} cm^2 s^{-1}]	D_{OAc^-} [10^{-5} cm^2 s^{-1}]	K_a [M^{-1}]
6 + **3** + LiOAc	0.27 ± 0.01	0.56 ± 0.01	0.86 ± 0.02	11
6 + **3**	0.27 ± 0.01	0.48 ± 0.01	–	187
6	–	0.68 ± 0.02	–	
3	0.32 ± 0.02	–	–	
LiOAc	–	–	1.02 ± 0.01	
6 + LiOAc	–	0.60 ± 0.01	0.90 ± 0.01	40
7 + **3** + LiOAc	0.30 ± 0.01	0.53 ± 0.01	0.96 ± 0.01	19
7 + **3**	0.29 ± 0.01	0.42 ± 0.01	–	165
7	–	0.60 ± 0.01	–	
3	0.32 ± 0.02	–	–	
LiOAc	–	–	1.09 ± 0.01	
7 + LiOAc	–	0.58 ± 0.01	0.96 ± 0.01	29
8 + **3** + LiOAc	0.19 ± 0.02	0.36 ± 0.02	0.82 ± 0.01	21
8 + **3**	0.19 ± 0.01	0.34 ± 0.02	–	69
8	–	0.41 ± 0.02	–	
3	0.24 ± 0.02	–	–	
LiOAc	–	–	0.87 ± 0.02	
8 + LiOAc	–	0.39 ± 0.01	0.84 ± 0.01	10

[a] All experiments were performed three times and the reported values are averages ± standard deviation. [b] Systems with **6** and **7** were measured in a D_2O solution at pD = 7.6 while the system with **8** was measured in [D_6]DMSO. m = macrocycle.

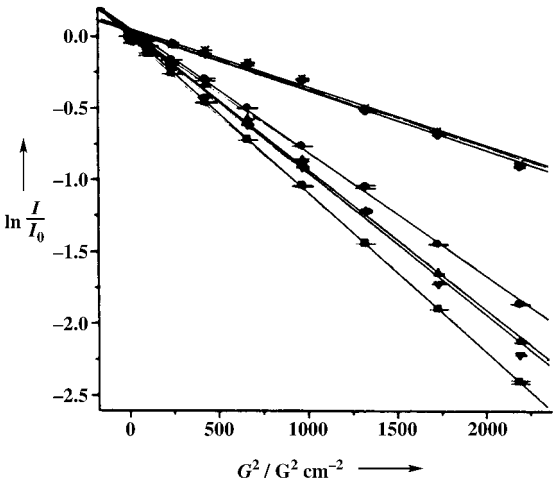

Figure 10. Normalized signal decay as a function of the gradient strength squared (G^2) in D_2O,; ■: **6**, ●: **6** (+ **3**), ▲: **6** (+ LiOAc + **3**), ▼: **6** (+ LiOAc), ◆: **3** (+ LiOAc + **6**), ⋆: **3** (+ **6**). All measurements were performed at 298 K and pD = 7.6. Adapted with permission from Ref. [52].

Gafni et al. demonstrated for the first time that diffusion NMR measurements provide a means to probe enantiomer discrimination by lipophilic cyclodextrins.[54] It was found that the α-cyclodextrin derivative **9** and its β analogue (**10**) show some chiral discrimination when complexed with amphetamine (**12**), ephedrine (**13**), and propranolol (**14**). The highest $K_{(+)}/K_{(-)}$ value was found for propranolol (**14**) with **10**. Interestingly, when the 3-position of **9** and **10** were blocked, as in **11**, no enantiomeric preference could be found.[54] Both the changes in the chemical shifts and the T_1 relaxation times were also measured in these systems. Complex formation resulted in these parameters changing in different directions,

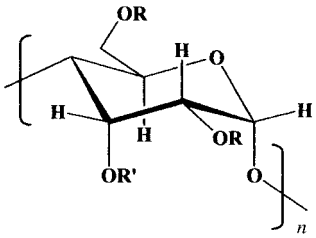

9: R = $C_{12}H_{25}$ R′ = H $n = 6$
10: R = $C_{12}H_{25}$ R′ = H $n = 7$
11: R = $C_{12}H_{25}$ R′ = CH_3 or C_8H_{17} $n = 7$

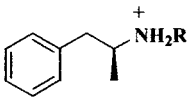

(*S*) - (+) - **12**
R = H

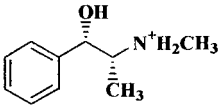

(1*S*,2*R*) - (+) - **13**

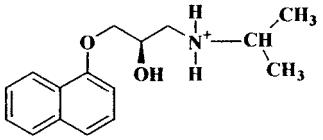

(*R*) - (+) - **14**

and the diffusion coefficient, which changed uniformly for all signals, was found to be the most robust parameter for characterization of the association constant for these systems.

As previously stated, one of the main advantages of using diffusion coefficients to extract the association constants of host–guest systems, as compared with chemical shifts for example, is the fact that D_{bound} for the guest is usually not very different from that of D_{free} of the host since the host is much larger than the guest in most host–guest systems. This may, in some cases (but not all), eliminate the need for a complete titration to describe the binding curve. It is clear that the larger the difference in the size of the interacting molecules, the better this approximation, and Cameron and Fielding recently tested this assumption both theoretically and experimentally.[55] It was found that when β-CD ($M_r = 1135$) forms a complex with cyclohexylacetic acid (**15**, $M_r = 136$) with $K_a = 1800 \pm 100$ there is a small gradual reduction in the diffusion

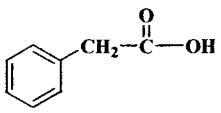

15

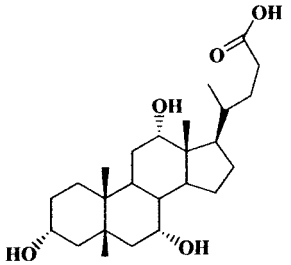

16

coefficient of β-CD upon addition of **15**, but these changes were on the order of the error bars of the diffusion measurements. However, much more significant changes in the value of D_{host} were found following the addition of cholic acid (**16**, $M_r = 420$) as the guest, which implies that $D_{complex}$ differs from D_{host} and thus emphasizing the need for a complete titration, or at least measurement at several different mixing ratios, to obtain the binding curve in this complex. These results clearly indicate that a single binding experiment using diffusion NMR spectroscopy needs to be viewed with caution in cases where the different partners of the host–guest systems are similar in size.[43,51,55]

Diffusion measurements were used recently to probe the interactions of α-CD-based pseudorotaxanes with diaminoalkanes (**17**).[56a] The motivation of this study included the

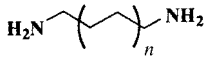

17a: $n = 1$ **17f:** **17a** · 2HCl
17b: $n = 2$ **17g:** **17b** · 2HCl
17c: $n = 3$ **17h:** **17c** · 2HCl
17d: $n = 4$ **17i:** **17d** · 2HCl
17e: $n = 5$ **17j:** **17e** · 2HCl

verification of whether protonation could convert these pseudorotaxanes into rotaxanes,[57] and hence there was a need to determine the association constants of the different diaminoalkanes before and after protonation.[56a] Since the changes in chemical shifts upon the formation of these pseudorotaxanes are small, and to avoid attributing chemical shift changes arising from protonation to binding phenomena (in the case of the protonated amines), diffusion measurements rather than NMR chemical shift titrations were used. Representative diffusion coefficients in these systems along with the $\lg K_a$ values extracted for these systems are shown in Table 3. Only in the last entry, which describes the formation of the pseudorotaxanes from α-CD and **17e**, was a small effect on the diffusion coefficient of **1** observed. A dependency was found between the length of the diaminoalkanes and the association constants to **1** (Figure 11).[56a] It was found that protonation considerably reduced the stability of the pseudorotaxanes formed with the shorter diaminoalkanes. Only with the longest diaminoalkane studied, that is, diaminododecane (**17e**), were the same association constants found for the diaminoalkane and its corresponding disalt.

The simple PGSE technique was also used to study the binding affinity of the peptidocalixarene **18**,[58] a vancomycin mimic prepared by Ungaro and co-workers.[59] Vancomycin is an important antibiotic that acts by binding to the mucopeptide precursors of the cell wall through the terminal D-alanyl-D-alanine sequence.[60] Recently, however, resistance toward this class of antibiotics has been reported and the need for synthetic analogues of vancomycin has emerged.[61] Since **18**, like vancomycin, contains several functional groups of different types, its interaction with the D-alanyl-D-alanine residue may be a superposition of electrostatic and/or hydrophobic interaction and may also involve π–hydrogen and dipole–dipole interactions or hydrogen bonds. Therefore, the association constant had to be determind in different solvents with guests having or lacking the D-alanyl-D-alanine residue (**19**–**24**). Diffusion NMR spectroscopy was used since NMR titration was difficult to apply and gave inconsistant results with relatively large errors. From the changes in the diffusion coefficients of a series of guests, some of which contain one or two alanine residues, upon addition of **18** in different solvents it was concluded that[58] in $CDCl_3$ **18** forms a complex of

Table 3: Diffusion coefficients D and the computed $\lg K_a$ values of host α-CD and guests **17a**, **17b**, **17c**, **17d**, **17e** in D_2O at 298 K.[56a]

System	D_{amine} [$\times 10^{-5}$ cm^{2}s^{-1}]	D_{CD} [$\times 10^{-5}$ cm^{2}s^{-1}]	D_{water} [$\times 10^{-5}$ cm^{2}s^{-1}]	X[a]	$\lg K_a$ [M^{-1}]
α-CD [2.8 mM]		0.30 ± 0.01	1.96 ± 0.01	–	–
17a	0.76 ± 0.01	–	1.97 ± 0.01	–	–
17a:α-CD (1:2.9)	0.71 ± 0.01	0.29 ± 0.01	1.97 ± 0.01	0.11 ± 0.03	1.18 ± 0.14
17b	0.65 ± 0.01	–	1.96 ± 0.01	–	–
17b:α-CD (1:5.1)	0.49 ± 0.02	0.30 ± 0.01	1.96 ± 0.01	0.46 ± 0.04	1.81 ± 0.07
17c	0.60 ± 0.01	–	1.96 ± 0.01	–	–
17c:α-CD (1:0.8)	0.47 ± 0.01	0.29 ± 0.01	1.95 ± 0.01	0.42 ± 0.05	2.83 ± 0.21
17d	0.55 ± 0.01	–	1.96 ± 0.01	–	–
17d:α-CD (1:0.7)	0.38 ± 0.01	0.29 ± 0.01	1.96 ± 0.01	0.65 ± 0.06	4.13 ± 0.30
17e	0.50 ± 0.01	–	1.94 ± 0.01	–	–
17e:α-CD (1:0.9)	0.32 ± 0.01	0.26 ± 0.01	1.94 ± 0.01	0.75 ± 0.10	3.85 ± 0.27

[a] The bound molar fraction.

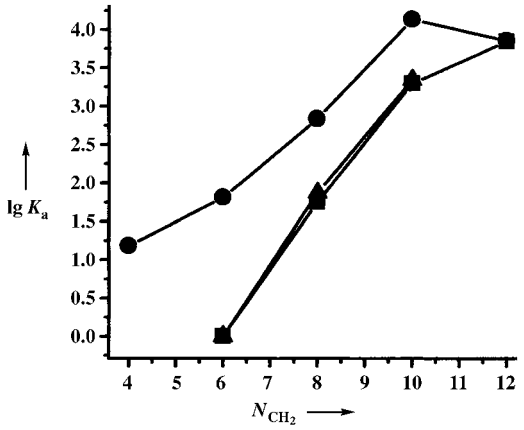

Figure 11. $\lg K_a$ values determined from diffusion data as a function of the number of CH_2 groups N_{CH_2} in the α-CD pseudorotaxanes of α,ω-diaminoalkanes (**17a**–**e**; ●) as well as their respective disalts before (▲) and after the addition of DCl (■). These experiments were performed on approximately 3 mM samples with an acquisition time of 20 minutes. Reproduced with permission from Ref. [56a].

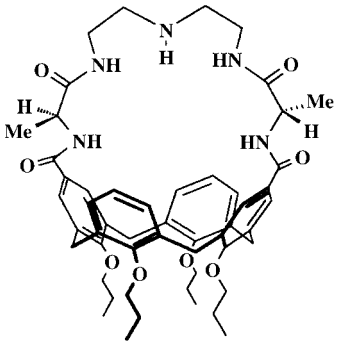

18

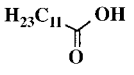

19

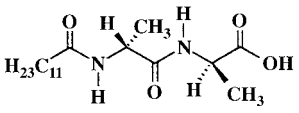

22

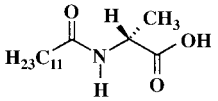

20

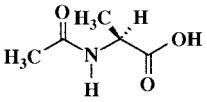

23

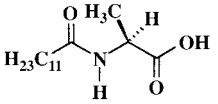

21

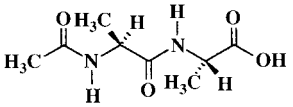

24

moderate stability with lauric acid (**19**; $\lg K_a = 2.7 \pm 0.2$) and stronger complexes with guests containing alanine residues ($\lg K_a \sim 4.0$). Hydrogen-bond-competing solvents resulted in a decrease in the K_a values, with this decrease being more pronounced in complexes formed between **18** and guests **20**, **23**, and **24**, which contain the alanine group, than in the complex of **18** with **19**. The K_a values determined by diffusion NMR spectroscopy for the various guests in the different solvents are consistant with the fact that hydrogen bonds (amongst other factors) play a significant role in these complexes in chloroform. This study was the first direct quantitative evaluation of the binding constant of **18** with dipeptides, since it was not possible to determine the K_a values of these complexes by classical ^{1}H NMR experiments. This result demonstrates that diffusion measurements may be superior to standard NMR techniques for determination of the association constants when complexation is associated with proton exchange.

A demonstration of the ability of a quick qualitative measurement of diffusion coefficients in determining the mutual interaction between different molecular species in solution is the study of the *p-tert*-butylcalix[4]arene–Cs–CH_3CN complex **25** in $CDCl_3$.[62] The solid-state structure of this complex, in which a CH_3CN molecule was found to be coordinated to the cesium ion, was said to maintain its structure in solution based on its cesium NMR spectrum.[63] The ^{1}H NMR spectrum of the isolated crystals and a side view of the crystal structure of **25** are shown in Figure 12a and Figure 12b, respectively. Figure 12c shows the signal decays for the signals of the *tert*-butyl group of **25**, the CH_3CN molecules originating from the dissolved crystals of complex **25**, and the signal decay of the solvent ($CHCl_3$). This figure clearly demonstrates that the CH_3CN molecules have a much higher diffusion coefficient than the complex, which is the

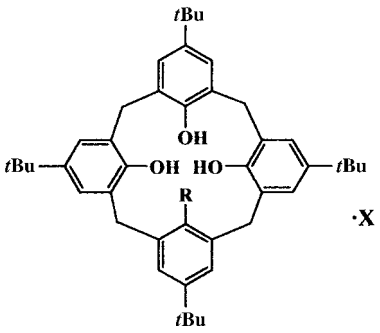

25 R : O^- X : Cs^+ ···· N≡C–CH_3

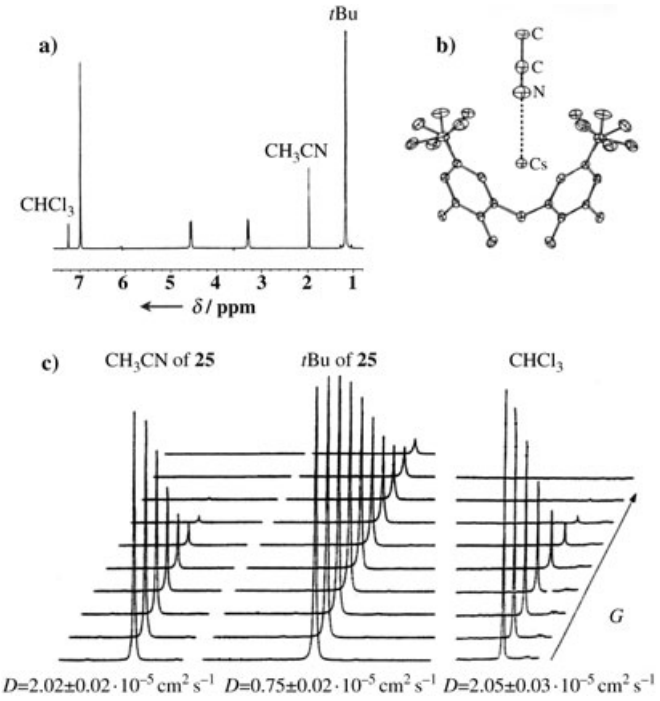

Figure 12. a) Section of the ^{1}H NMR spectrum (500 MHz) of **25** (crystallized from CH_3CN) in a $CDCl_3$ solution; b) side view of the crystal structure of **25**;[63] and c) the signal decay in a PGSE experiment of the *tert*-butyl signal of **25**, the CH_3CN originating from complex **25**, and $CHCl_3$ as a function of the gradient strength (*G*). The diffusion coefficient extracted for each signal is indicated.[62]

expected result if there is no interaction between the small CH_3CN molecule and the much larger complex. Comparison of the diffusion coefficient of the CH_3CN signal originating from the crystals of **25** with the diffusion coefficient of CH_3CN in $CDCl_3$ ($2.01 \pm 0.02 \times 10^{-5}$ $cm^2 s^{-1}$) led to the conclusion that, as expected, there is practically no interaction between the CH_3CN molecules and the complex in $CDCl_3$.[62] In fact, a clear visualization of the lack of interaction is obtained conclusively from Figure 12c. It should be noted that the entire diffusion experiment shown in Figure 12c, which proves unequivocally that there is no interaction between CH_3CN and the other part of complex **25**, was acquired in 10 minutes, thus demonstrating the robustness of this approach for determining molecular interactions in solution. In contrast, the acquisition of only a single ^{133}Cs NMR spectrum of the same sample, just to ascertain that complex **25** was indeed obtained, required several hours.

The determination of association constants by using diffusion NMR spectroscopy is based on the fact that there is a fast exchange between the free and bound states of the guest. However, there are important applications of diffusion measurements, even in the case of slow exchange—such as for the study of molecular capsules and the encapsulation phenomenon outlined in the next section.

4.1.2. Encapsulation and Molecular Capsules

Molecular capsules in general,[64,65] and those obtained by self-assembly in particular, are intriguing molecular systems that have attracted considerable attention over the last decade.[64–66] Molecular capsules are molecules that can accommodate smaller molecules in their cavity, thus isolating them from the immediate bulk, and can therefore, be regarded as microreactors.[67] Indeed, in recent years, such systems have been used to stabilize reactive intermediates[67a] and enhance the rate of some reactions.[67b,c]

The diffusion coefficient should be a powerful tool for detecting and probing encapsulation,[68] since the encapsulated guests are generally much smaller molecular species than the capsule itself and, therefore, should have a much higher diffusion coefficient in its free state. Moreover, the encapsulated molecules, which are in slow exchange with the bulk, should have the same diffusion coefficient as the capsule itself since the capsule and the encapsulated molecules diffuse as a single molecular entity.[68]

Such a diffusion-based argument was used recently to probe benzene encapsulation in the tetraureacalix[4]arene dimer (**26**·**26**).[68] Figure 13a shows part of the ^{1}H NMR

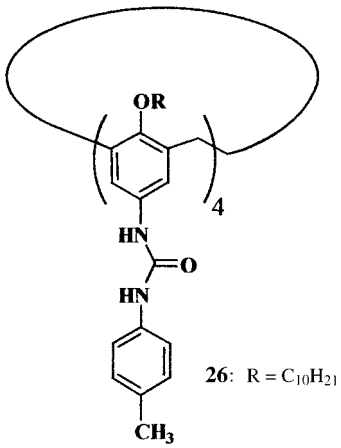

26: R = $C_{10}H_{21}$

spectrum of dimer **26**·**26** prepared in a 80:20 mixture of C_6H_6 and C_6D_6. The signal at about $\delta = 4.4$ ppm was suspected to be that of the encapsulated benzene. Figure 13b shows the decay of this signal, the signal of "free" benzene (at $\delta = 7.15$ ppm), and one representative signal of the dimer (at $\delta = 1.95$ ppm) as a function of the diffusion gradient strength *G*. This figure

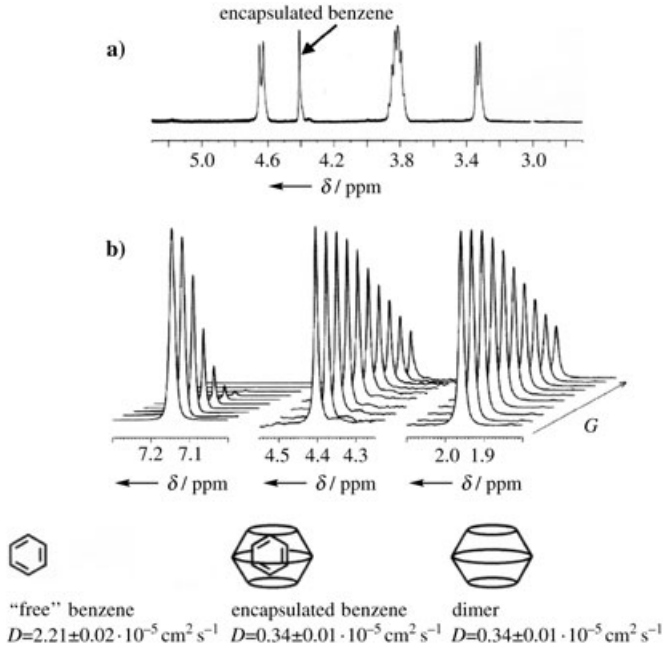

Figure 13. a) Section of the ^{1}H NMR spectrum (500 MHz) of **26** in an 80/20 (v/v) solution of benzene and C_6D_6. b) ^{1}H NMR spectra (500 MHz) of the same sample (recorded with a Stejskal–Tanner diffusion experiment). The figure shows the decay of the signal intensity as a function of *G*. For clarity, only the signal of **26** at $\delta = 1.95$ ppm and the signals attributed to the "free" and encapsulated benzene at $\delta = 7.15$ and 4.4 ppm, respectively, are shown.[68]

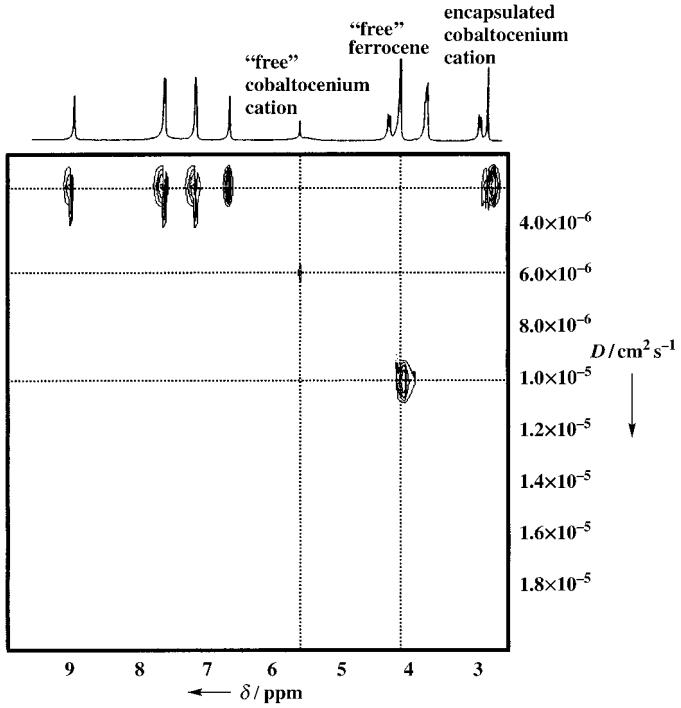

Figure 14. The DOSY spectrum (400 MHz, 298 K) of a solution containing **26**, ferrocene, and cobaltocenium cation in $C_2D_4Cl_2$. The signal at $\delta = 2.72$ ppm, suspected to be the encapsulated cobaltocenium cation, has the same diffusion coefficient as all the signals of **26**·**26**. The signals of the free ferrocene and cobaltocenium cation at $\delta = 4.06$ and 5.61 ppm, respectively, were found to have much higher diffusion coefficients, as expected.

demonstrates that the signal at $\delta = 4.4$ ppm has a much lower diffusion coefficient than that of the free benzene, and that the extracted diffusion coefficient for this signal ($0.34 \pm 0.01 \times 10^{-5}$ cm^2 s^{-1}) was exactly the same as the one determined for the dimer[68] and illustrates that, as expected, the encapsulated benzene and the dimer diffuse as a single molecular entity. A titration experiment in which the diffusion coefficients of the dimer and the DMSO molecules added to the benzene solution of **26**·**26** were followed demonstrated that it was possible to determine by diffusion NMR spectroscopy that about four DMSO molecules per molecule of **26** are required to disrupt the dimer.[68]

Frish et al. subsequently used a similar approach to probe the encapsulation of a tropylium cation by **26**·**26** in an attempt to evaluate the relative importance of electronic effects, namely, the importance of π–cation interactions[69], in determining the guest affinity for the cavity of the dimer. It was found that π–cation interactions indeed play an important role in determining the relative affinity toward the dimer cavity, as it was found that the tropylium cation affinity is about four orders of magnitude larger than that of benzene, which happens to have a very similar size.[70a] The same approach was recently used to demonstrate that the affinity of the cobaltocenium cation is at least five orders of magnitude larger than that of ferrocene.[70b] The DOSY spectrum shown in Figure 14 demonstrates how easy and simple the analysis and mapping of the mutual interactions was between the different molecular species that prevail in the solution, that is, between ferrocene, the cobaltocenium cation (bound and free), and the dimer **26**·**26**.

These small complexes are relatively simple systems that are assembled, in most cases, from only three molecular species. However, as will be demonstrated, the advantage of using diffusion NMR spectroscopy to map the interactions between different molecular species may be even more important in systems that contain multiple molecular species and interactions.

Recently, the potential of simple diffusion NMR experiments in mapping the different molecular interactions in the spectacular resorcinarene hexamer capsule,[71] first characterized by Atwood and co-workers,[72] was demonstrated. Atwood's group showed that **27a** forms a hexamer of the type $[(\mathbf{27a})_6(H_2O)_8]$ in the solid state.[72] It was shown subsequently by Shivanyuk and Rebek that **27b** forms such a hexamer in the presence of suitable guests in water-saturated $CDCl_3$.[73] It was found that the cation of tetrahexylammonium bromide (THABr, **29**) is encapsulated in the large cavity of the hexamer.[73] The addition of THABr to **27b** resulted in a change in the chemical shifts of **27b** and the appearance of very high field signals at $\delta \sim -1.00$ ppm. On the basis of chemical shifts arguments, it was logically assumed that guest **29** induces the formation of the hexameric capsule. However, simple diffusion measurements demonstrated that this is not the case in these systems. Diffusion measurements of **27b**, before and after the addition of **29**, showed that the

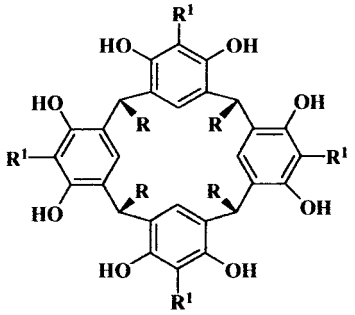

27a: R = CH_3 R^1 = H
27b: R = $C_{11}H_{23}$ R^1 = H
28: R = $C_{11}H_{23}$ R^1 = OH

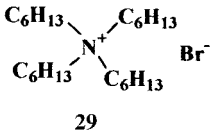

29

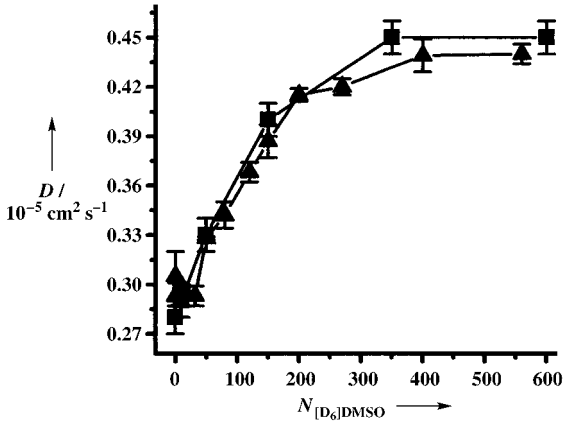

Figure 15. Changes in the diffusion coefficients *D* for the water-saturated $CDCl_3$ solutions of **27b** (■) and **27b** in the presence of **29** (▲) as a function of the addition of [D_6]DMSO ($N_{[D_6]DMSO}$: number of equivalents of added [D_6]DMSO). Adapted with permission from Ref. [71].

same diffusion coefficients (that is, $0.28 \pm 0.01 \cdot 10^{-5}$ $cm^2 s^{-1}$ for a 3 mM solution at 298 K) are obtained, within experimental error, for the two systems. This result clearly contradicted the notion that **27b** is a monomer that self-assembles into a hexamer in the presence of **29** in $CDCl_3$. Therefore, it was suggested that **27b** self-assembles spontaneously into a hexameric capsule in water-saturated $CDCl_3$.[71] Indeed, when **27b** was subsequently dissolved in water-saturated $CHCl_3$, new high-field singlets appeared at about 4.8–5.1 ppm. The peaks were tentatively assigned to encapsulated $CHCl_3$ molecules. These singlets were found to have the same diffusion coefficient as that of the resorcinarene moiety, thus further supporting the assignment of these singlets to encapsulated chloroform molecules. Moreover, addition of **29** to this chloroform solution resulted in the immediate disappearance of these signals, thus corroborating the conclusion that **27b** spontaneously self-assembles into a hexameric capsule in water-satuated $CDCl_3$. Very recently Shivanyuk and Rebek came to the same conclusion by using a different methodology.[74]

The results of titration experiments in which the diffusion coefficient of the resorcinarene moiety was measured as a function of the amount of DMSO added to the $CDCl_3$ solution are shown in Figure 15.[71] This study demonstrated that there is an increase in the diffusion coefficient of **27b** with the addition of DMSO. Very similar titration curves were found for the hexamer in the presence and absence of **29**.[71] The fact that the minor changes in the chemical shifts observed upon addition of DMSO is accompanied by an increase in the diffusion coefficient of **27b** (an increase in the viscosity of the solution is expected because of this addition) strongly supports the interpretation that the process followed is the disruption of the hexamer into its monomer.

The role of water in the formation of the hexameric capsule of **27b** and **28** in water-saturated chloroform was also studied by measuring the diffusion coefficient of the water signal and the hexamer signals in solutions with different **27b**,**28**/H_2O ratios. Only a single water signal was observed in these samples, thus indicating that the different observable water pools are in fast exchange on the NMR time scale.[75a,c] However, since the chemical shift and width of the water signal were found to be very sensitive to different parameters and to conditions other than the **27b**/H_2O ratio (Figure 16a), the measurement of diffusion coefficients was selected as an alternative method to evaluate the role of water molecules in these hexameric capsules. Figure 16b shows the effect of the **27b**/H_2O ratios on the diffusion coefficients of water and of **27b** in the presence and absence of THABr.[75a] It was found that there was a decrease in the diffusion coefficient of the water signal as the relative amount of H_2O decreased. Interestingly, the diffusion coefficient for the water signal was nearly twice that of the hexamer even when the **27b**/H_2O ratio was 6:8.4. However, the diffusion coefficient of the water signal was found to be equal to that of the hexamer when that ratio was less than 6:8 (for example, 6:7.2). It was found for the **29**@$\mathbf{27b}_6$ system that the diffusion coefficient of the water signal is still several times that of the hexamer, even when the **27b**/H_2O ratio was less than 6:8 (Figure 16b).[75b] The diffusion NMR measurements seem to indicate that the water molecules play a different role in the two capsules. In $CDCl_3$ solution and in the absence of THABr the water molecules seem to be part of the supramolecular structure of the capsule. Indeed, it was found that about eight water molecules per six molecules of **27b** have the same diffusion coefficient as **27b** in the hexamer. It should be noted, however, that diffusion measurements cannot distinguish between encapsulated water molecules and water molecules which are part of the hexamer since the water diffusion coefficient in both situations should be equal to the diffusion coefficient of the hexamer when slow exchange occurs. However, because of the fast exchange of H_2O with bulk water and the fact that $[(\mathbf{27b})_6(H_2O)_8]$-type capsules were observed in the solid state,[72] the more plausible explanation seems to be that the eight water molecules which have the same diffusion coefficient as the hexamer are part of the supramolecular structure in the solution. However, it seems that in the presence of THABr there is no need for water molecules for the construction of the supramolecular capsule.[75b] By using the same methodology (Figure 16c) it was found that water has no role in the construction of the hexameric capsule of **28** in $CDCl_3$ solutions,[75c] an observation in line with the results of X-ray crystallographic analysis of

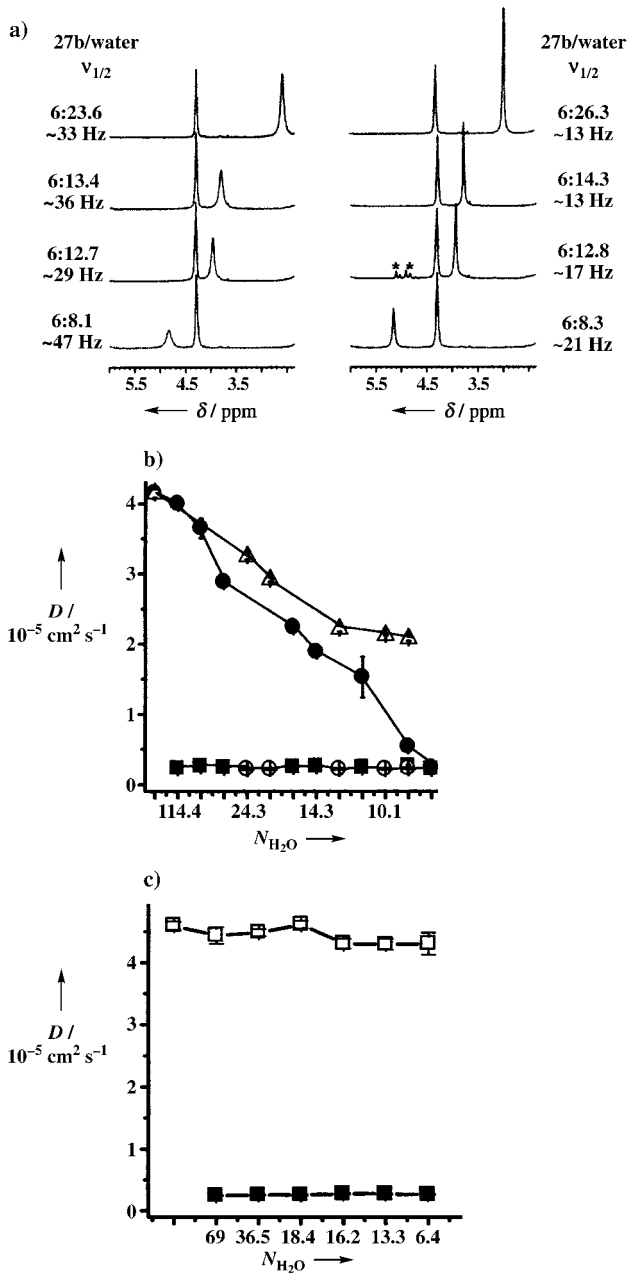

Figure 16. a) Sections of the ^{1}H NMR spectra from different studies of **27b** as a function of the **27b**/H_2O ratios for $CDCl_3$ solutions. Both the line shape and chemical shift may be very different even when the **27b**/H_2O ratio is very similar. b) Diffusion coefficients of **27b** and the water signal in the presence of **29** (○ and △, respectively) and absence of **29** (■ and ●, respectively) as a function of the number of water equivalents (N_{H_2O}) per six equivalents of **27b**.[75b] c) Diffusion coefficients of **28** and the water signal (■ and □, respectively) as a function of the number of water equivalents (N_{H_2O}) per six equivalents of **28**. Figure 16b and c are adapted with permission from Ref. [75b,c].

this system.[75d,e] In addition, it was found by combining the results from chemical shift experiments and diffusion NMR spectroscopy that **27b** encapsulates trialkylamines and tetraalkylammonium salts. However, **28** was shown to encapsulate only trialkylamines which are ejected from the cavity of the hexamer of **28** following addition of DCl and the in situ formation of ammonium salts.[75f] These examples demonstrate the ability of diffusion NMR spectroscopy to provide a simple means to map the molecular interactions in such multicomponent systems. The maps of some of the molecular interactions that prevail in these systems are summarized graphically in Figure 17.[71,75a–c]

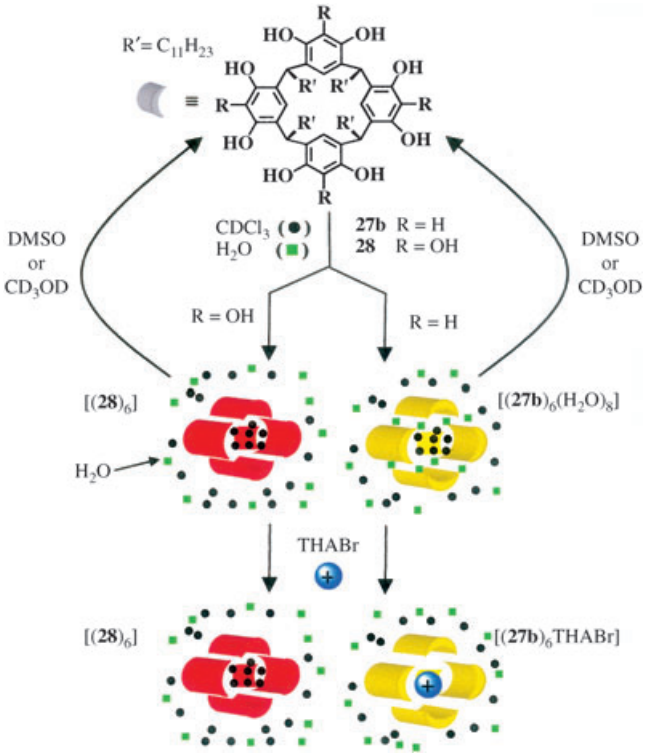

Figure 17. Schematic representation of some of the different molecular interactions and aggregation modes identified in these capsules by diffusion NMR spectroscopy.[71,75a–c]

The evaluation of the interaction of the water molecules with the organic systems in this section indicates that the interaction of water molecules with organic systems in nonaqueous solutions could, in principle, be approached by diffusion NMR measurements—this is briefly outlined in the next section.

4.1.3. Hydrogen Bonds and Water Hydration in Organic Solutions

Many NMR methods have been used to study the interaction of water molecules with biomolecules, since such interactions are of prime importance.[76] Hydration of biomolecules has been approached by NMR methods based on the nuclear Overhauser effect (NOE) and magnetic relaxation dispersion (MRD).[77,78] In principle, the interaction of water molecules with a biomolecule should be easy to probe by diffusion NMR spectroscopy because of the large difference in the sizes and molecular weights of the small water

molecules and the large biomolecule. Interactions between water molecules and biomolecules in an aqueous solution is beyond the scope of the present review, and we shall restrict ourselves to the few studies that measured the interaction of water with organic species in non-aqueous media.[76–78]

In addition to the studies described in Section 4.1.2 regarding the role of water molecules in the hydrogen-bonded capsule,[75a–c] an early report dealt with the hydration, or more accurately the interaction of water molecules with [18]crown-6 (**4**) and its KI complex ($\mathbf{4}_{KI}$) in water-saturated $CDCl_3$ solutions.[79] In this study, the process was followed by comparing the changes observed in the chemical shift and the diffusion coefficient of the water signal upon changing the H_2O:**4** and the H_2O:$\mathbf{4}_{KI}$ ratios. It was found that the average fraction of bound water molecules was independent of the H_2O:$\mathbf{4}_{KI}$ ratio but increased considerably when the H_2O:**4** ratio was increased. In this study, similar conclusions were obtained from the chemical shift titrations and the diffusion NMR measurements.[79] The results of this study (Figure 18)

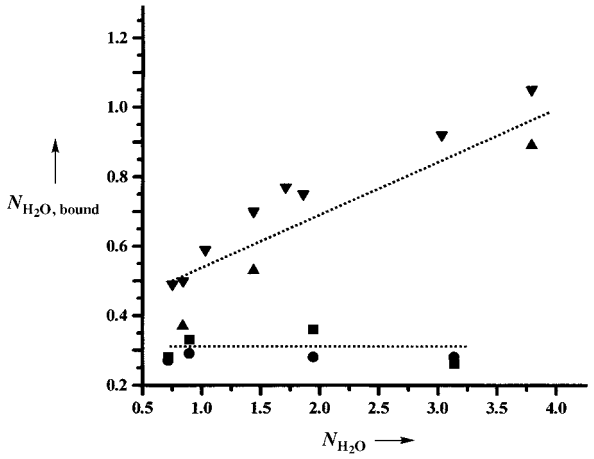

Figure 18. Average number of water molecules ($N_{H_2O,\,bound}$) interacting with **4** and $\mathbf{4}_{KI}$ in $CDCl_3$ solutions. The numbers were calculated from the changes in the chemical shift (δ) and diffusion coefficients (D) of the water signal as a function of the number of water equivalents present N_{H_2O} in $CDCl_3$. ■: $\mathbf{4}_{KI}$ (from D), ●: $\mathbf{4}_{KI}$ (from δ), ▲: **4** (from D), ▼: **4** (from δ).[79]

show that the bound fraction of water molecules was higher in the case of the noncomplexed crown ether. An average of about 0.3 water molecules per complex molecule were obtained for the $\mathbf{4}_{KI}$ system, which was consistent with the finding of Iwachido et al. who found that the potassium complex of **4** can extract on average 0.3 water molecules per complex molecule into nitromethane while **4** can extract up to 1.6 water molecule per molecule.[80] These results imply that **4** acts as an efficient solvation shell for the potassium ion. In the case of **4**, the fraction of bound H_2O was found to depend on the H_2O:**4** ratio. In this case, it was suggested that complexation of the water molecules into the empty cavity of **4** cannot be ruled out.

The hydration of macromolecules in aqueous media is very complex and different types of hydration spheres have been evoked on the basis of their average lifetime in the bound state.[76–78] One of the main problems in aqueous media is to avoid the large signal of the bulk water, which is in most cases in fast exchange with the water molecules that do interact with the (bio)molecules. This problem is much less severe in organic solvents, however. Nevertheless, it should be noted that diffusion measurements give only an average picture. A bound fraction of 0.3 may well be one molecule that spends 30% of its lifetime in the bound state or two molecules that each spend only 15% of their lifetimes in the bound state and so on.[79]

Hydrogen bonds have well-established effects in NMR spectroscopy,[81] such as downfield shifts,[82a] an intermolecular NOE effect,[82b] and spin–spin coupling which may be observed through such hydrogen bonds in some cases.[82c] Recently, Berger and co-workers demonstrated how DOSY could be used to qualitatively study the strength of hydrogen bonds between different species in solutions.[83] The principle behind the measurement is clear: The formation of a hydrogen bond will decrease the diffusion coefficient of a certain molecule from that expected from its molecular weight and shape in a given medium at a given temperature. DOSY was used for this purpose because it has the advantage of visualizing the effect very clearly even in complex mixtures.[83a]

It was shown that the addition of DMSO (a known H-bond acceptor) results in a more pronounced decrease in the diffusion coefficient of phenol than that of cyclohexanol. These different responses were attributed to the higher tendency of phenol, which is the more acidic compound, to form hydrogen bonds with the added DMSO molecules.[83a] A similar phenomenon was observed for a mixture of phosphorus-containing compounds: The four compounds studied by using the ^{31}P DOSY technique were trimethyl phosphate (**30a**), triphenylphosphine oxide (**30b**), triethylphosphine oxide (**32**), and dibutylphosphite (**31**). The results of the DOSY spectra of these systems obtained before and after the addition of triethanolamine are shown in Figure 19a and b, respectively. It can be seen that the largest change in the diffusion coefficients were observed for **32**, which is expected to form the strongest hydrogen bonds. However, a closer look at the data shows that the addition of triethanolamine caused a decrease in the diffusion coefficients of all the solutes in both samples thus suggesting that the addition of the H-bond acceptor affected the solutions viscosity. More recently, the same research group suggested the use of tetramethylsilane (TMS) as a reference for studying this effect in a more quantitative manner by using the ratios of the diffusion coefficients relative to the diffusion coefficients of TMS before and after addition of an H-bond acceptor. This was done since TMS is considered to be unaffected by hydrogen bonds and can therefore be used to report on the effect of the change in viscosity on the measured diffusion coefficients.[83b]

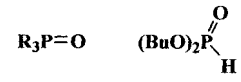

30a: R = OCH_3 **31**
30b: R = Ph
32: R = Et

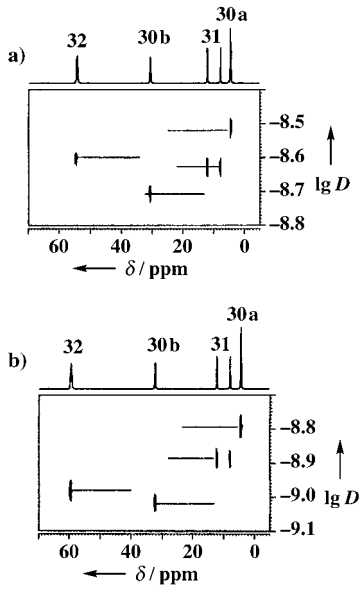

Figure 19. a) The ^{31}P DOSY spectrum of a mixture of trimethyl phosphate (**30a**), triphenylphosphine oxide (**30b**), triethylphosphine oxide (**32**), and dibutyl phosphite (**31**); b) the ^{31}P DOSY spectrum of the same mixture containing triethanolamine as an additional component. The spectrum was recorded using the BPLED sequence with gradient strengths of 2 ms in 32 steps. Reproduced with permission from Ref. [83a].

4.2. Molecular Size and Shape

Diffusion coefficients, being intuitively related to the effective radius of the molecular species through the Stokes–Einstein equation [see Eq. (5)], have also been used to determine the size and shape of different supramolecular entities called rosettes.[84,85] The pulsed gradient spin echo (PGSE) sequence was used to characterize several rosettes prepared by the research group of Reinhoudt.[86] In this study, single, double, and tetrarosettes of the type shown in Scheme 1 were classified on the basis of their diffusion coefficients.[86] Relatively good agreement was found between the hydrodynamic diameter extracted from diffusion NMR measurements and those obtained from gas-phase-minimized structures.[86] More importantly, by measuring the diffusion coefficient of the single rosette (**33a**$_3$·**34**$_3$) to which **33a** was added, it was possible to show that these rosettes are kinetically labile and in fast exchange with their components on the NMR time scale under the given conditions (2 mM sample in $CDCl_3$, 298 K, 500 MHz). In addition, it was also possible to determine by using this approach which of the double rosettes were in fast exchange with their components and which were kinetically less labile. This information was difficult to obtain from conventional NMR spectroscopic analysis of these systems.

In another recent application, Stang and co-workers[87a] used the PGSE sequence to corroborate the formation of their spectacular dodecahedra constructed from 50 predesigned components (Scheme 2). The diffusion coefficients of the two dodecahedra **40** and **41**, the molecular weights of

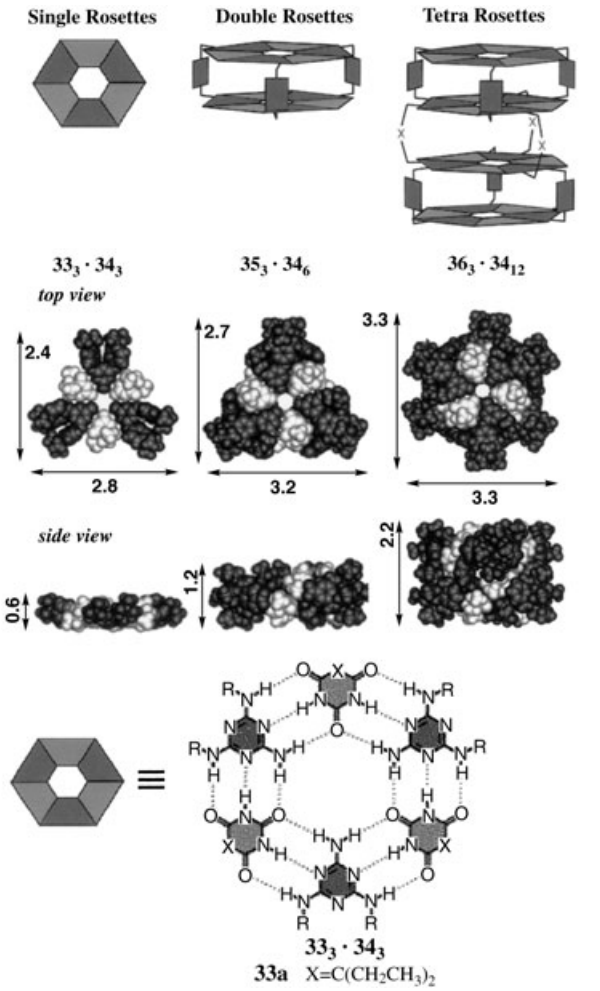

Scheme 1. Single (**33**$_3$·**34**$_3$), double (**35**$_3$·**34**$_6$), and tetrarosettes (**36**$_3$·**34**$_{12}$), which could be characterized by their diffusion coefficients.

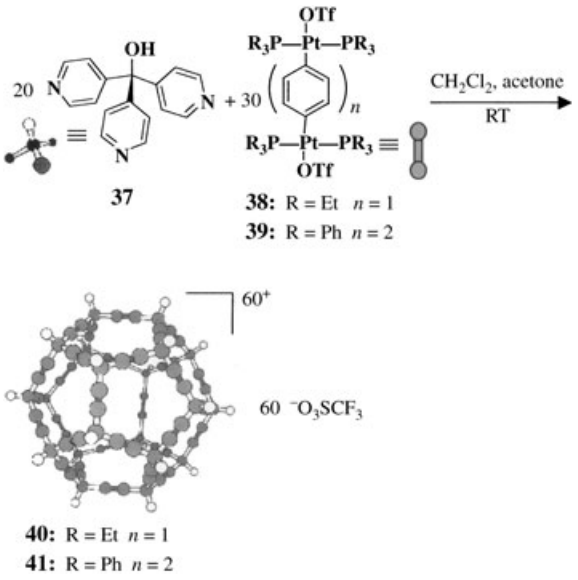

Scheme 2. Synthesis of the dodecahedra **40** (R = Et, n = 1, M_r = 41 656 Da) and **41** (R = Ph, n = 2, M_r = 61 955 Da) from 20 monomers of **37** with 30 monomers of **38** (R = Et, n = 1) and **39** (R = Ph, n = 2), respectively.[87a]

which were calculated to be 41656 and 61955 Da, were found to be $0.18 \pm 0.005 \times 10^{-5}$ and $0.13 \pm 0.006 \times 10^{-5}$ $cm^2 s^{-1}$, respectively, in a mixture of acetone and dichloromethane.[87a] Simulation of the motion with such diffusion coefficients through that medium (taking into account its viscosity) enabled them to extract diameters of 5.2 and 7.5 nm, which are in good agreement with the estimated calculated diameters of 5.5 and 7.5 nm, respectively. Recently, Viel et al. demonstrated by using DOSY that π–π stacking interactions occurred in the hydrophobic compound metolachlor (**42**) in concentrated aqueous solutions.[87b] These authors reached the conclusion that the polymer formed was held together by π–π interactions from the much lower diffusion coefficient of the extra signals observed at high concentration.[87b] Comparison of the surprising DOSY data with other NMR methods (such as 2D NOESY) led to the conclusion that, indeed, the formed aggregate is not a dimer or a trimer but a polymer.[87b]

Diffusion NMR spectroscopy was used to corroborate the formation of double-stranded helicates in solutions in several cases.[88a,b] Larive and co-workers recently used diffusion NMR measurements to characterize a series of ligands (**43**–**47**) and rhenium complexes that were used as

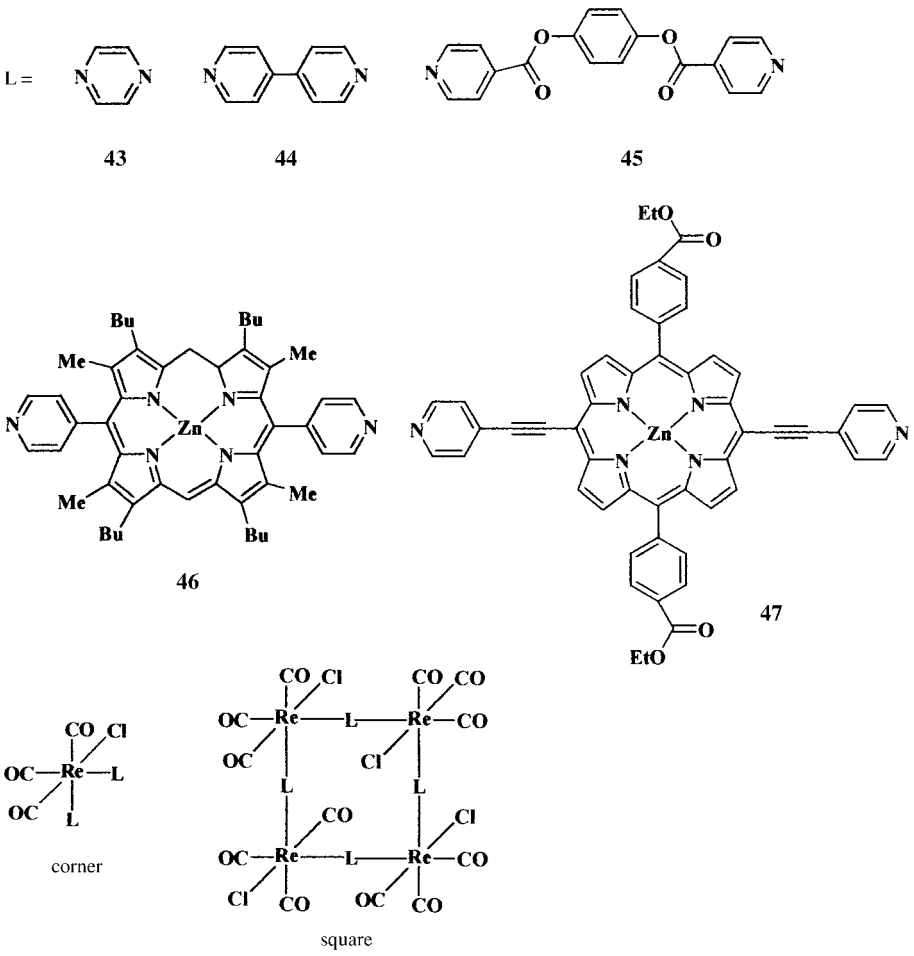

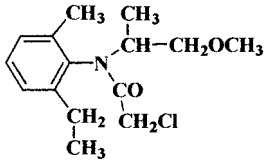

building units for the construction of molecular squares, which could not be characterized by mass spectrometry.[88c] In this case, a good correlation was found between the diffusion coefficient and the reciprocal of the estimated stokes radii ($1/r_s$), as shown in Figure 20. The authors also concluded on the basis of the diffusion NMR measurements that the complexity of some of the spectra are intrinsic characteristics of the supramolecular systems prepared rather than contamination from species of low-molecular weight.[88c] The data extracted from these diffusion NMR experiments are presented in Table 4.

A specific field where size determination by diffusion NMR spectroscopy can assist the characterization of the obtained system in solution is dendrimer chemistry, in which generations can be probed easily by using diffusion NMR spectroscopy, as demonstrated briefly in the next section.

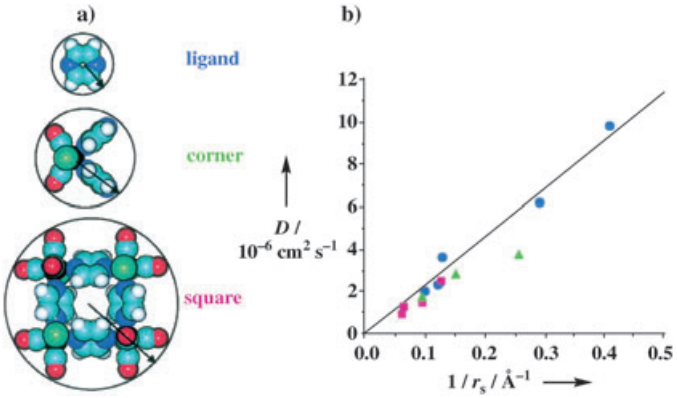

Figure 20. a) Approximated molecular radii of ligands **43**–**47** as well as their respective monomers (corners) and square complexes; b) the correlation between their diffusion coefficients and the reciprocal of the estimated Stokes radii ($1/r_s$) for ligands (●), corners (▲), and squares (■). Reproduced with permission from Ref. [88c].

4.3. Dendrimers and Dendrons: Size, Shape, and Function

Diffusion NMR measurements may assist in characterizing dendrimers[89] and it is surprising that, until recently, relatively few studies have used this technique to characterize

Table 4: Molecular diffusion coefficients D of the ligands **43**–**47** and their rhenium complexes.[88c]

Molecule	D_{43} [$\times 10^{-6}$ cm^2 s^{-1}]	D_{44} [$\times 10^{-6}$ cm^2 s^{-1}]	D_{45} [$\times 10^{-6}$ cm^2 s^{-1}]	D_{46} [$\times 10^{-6}$ cm^2 s^{-1}]	D_{47} [$\times 10^{-6}$ cm^2 s^{-1}]
ligand	9.68 ± 0.09	6.03 ± 0.04	3.53 ± 0.04	2.24 ± 0.02	1.94 ± 0.06
corner	3.62 ± 0.08	2.69 ± 0.02		1.61 ± 0.03	
square	2.37 ± 0.11	1.42 ± 0.05	0.87 ± 0.02	1.20 ± 0.04	1.04 ± 0.03

dendrimers.[90–94] One of the early applications of diffusion NMR spectroscopy in the field of dendrimers was reported on the first, second, third, and fourth generations of dentritic aliphatic polyesters based on 2,2-bis(hydroxymethyl)propionic acid and 1,1,1-tris(hydroxyphenyl)ethane.[91] The signal decays for these dendrimers were fitted to a modified Stejskal–Tanner equation as shown in Equation (19), where

$$I_{(2\tau,G)} = I_{(2\tau,0)} \exp(-\gamma^2 G^2 \delta^2 (\Delta - \delta/3) D_{app})^{\beta} \quad (19)$$

D_{app} represents the apparent diffusion coefficient and β is a measure of the width of the distribution ($0 < \beta < 1$). In the fitting procedure, β was found to be 1, thus indicating that the dendrimers are nearly monodisperse. By assuming that the dendrimers had a spherical shape, these authors were able to compute the hydrodynamic radii r_s of the dendrimers by using the Stokes–Einstein equation. The values estimated were 7.8, 10.3, 12.6, and 17.1 Å for the first, second, third, and fourth generation dendrimers, respectively, and were said to be in good agreement with those obtained from molecular modeling studies.[91]

One of the earliest applications of DOSY demonstrated that diffusion NMR measurements are sensitive to the structural changes induced by the external stimulation of dendrimers.[90b] Indeed, it was shown that the diffusion coefficients, and hence the hydrodynamic radii, can give information on the structural changes induced in these materials by a pH change. It was shown that the dendrimers with terminal CO_2H groups swell at neutral pH values and shrink in acidic conditions. The dendrimers with terminal CH_2NH_2 groups shrank in basic pH conditions, while those with terminal CH_2OH groups were practically insensitive to pH changes.[90b] Interestingly, the changes in the chemical shifts in these systems as a result of the pH changes were marginal. These findings imply that diffusion NMR spectroscopy has the potential to relate structural changes and the packing mode of dendrimers with their functional performances.

Gorman et al. combined diffusion NMR measurements with the determination of electron-transfer rate constants and molecular modeling studies in an attempt to determine the relationships between molecular structure and electron transfer in dendritic systems.[92] Interestingly, these diffusion NMR measurements carried out on the flexible and inflexible electroactive dendrimers **48**–**52** (Scheme 3) and **53**–**57** (Scheme 4), respectively, showed a dramatic effect of the solvent on the hydrodynamic radii of only the flexible dendrimers. For the flexible dendrimers **48**–**52**, a better correlation between the hydrodynamic radii and the radii of gyration, calculated using molecular dynamics simulation, was obtained for the diffusion measurements performed on the DMF solutions, where the dendrimers have compact hard-sphere-like structures, and not in THF, where some swelling seems to occur.[92] Moreover, the correlation between these two parameters for the inflexible dendrimers was less significant, thus implying that these electroactive rigid dendrimers **53**–**57** have a nonspherical/noncompact shape. A comparison of the structural features of these two classes of dendrimers in the different solvents with the electron-transfer rates in these systems led the authors to evoke a molecular structure/property relationship for the attenuation of the electron transfer in these systems.[92]

Riley et al. studied the relationship between the diffusion characteristics of pyrene-labeled poly(aryl ether) monodendrons[93] (Scheme 5) and their photophysical performance. Interestingly, it was found that the increase in the Stokes radii with the increase in dendron generation is much more pronounced in THF than in CH_3CN (Table 5). However, comparison of the experimental data with theoretical values showed that the dendrons are not fully extended ($r_s < R_{theory}$), even in THF, and that the smaller dendrons are more open and flexible than the larger ones. The structures are much more collapsed in CH_3CN, and there is a structural change between G2 (**60**) and G3 (**61**), with G3 (**61**) apparently having the more compact structure. Comparison of the structural information obtained from the diffusion NMR measurements and the quenching experiments revealed that G0–G3 (**58**–**61**) in THF and G0–G2 (**58**–**60**) in acetonitrile have a minimal barrier to the passage of the dioxygen-quenching molecules, while the larger dendrons G4 (**62**) in THF as well as G3 and G4 in CH_3CN are more dense and less permeable. The structure is even more collapsed in cyclohexane.[93] The change in the diffusion behavior in THF occurs between G2 and G3, while the quenching data shows the change in behavior occurs between G3 and G4. The authors pointed out that the different breaking points arise from the different probes used in both processes (THF or dioxygen).[93]

The last two examples demonstrate how diffusion NMR spectroscopy gives a better insight into the solution structure of dendritic materials, which, in turn, may affect their properties, and demonstrate the potential of such measurements to establish the structure/functional activity of such complex systems.[93]

4.4. Reactive Intermediates, Ion Pairing, and Organometallic Systems

The interactions of different ions with different systems and polyelectrolytes, their binding to micelles, and their involvement in the formation of microemulsions have been studied extensively by diffusion NMR spectroscopy and are

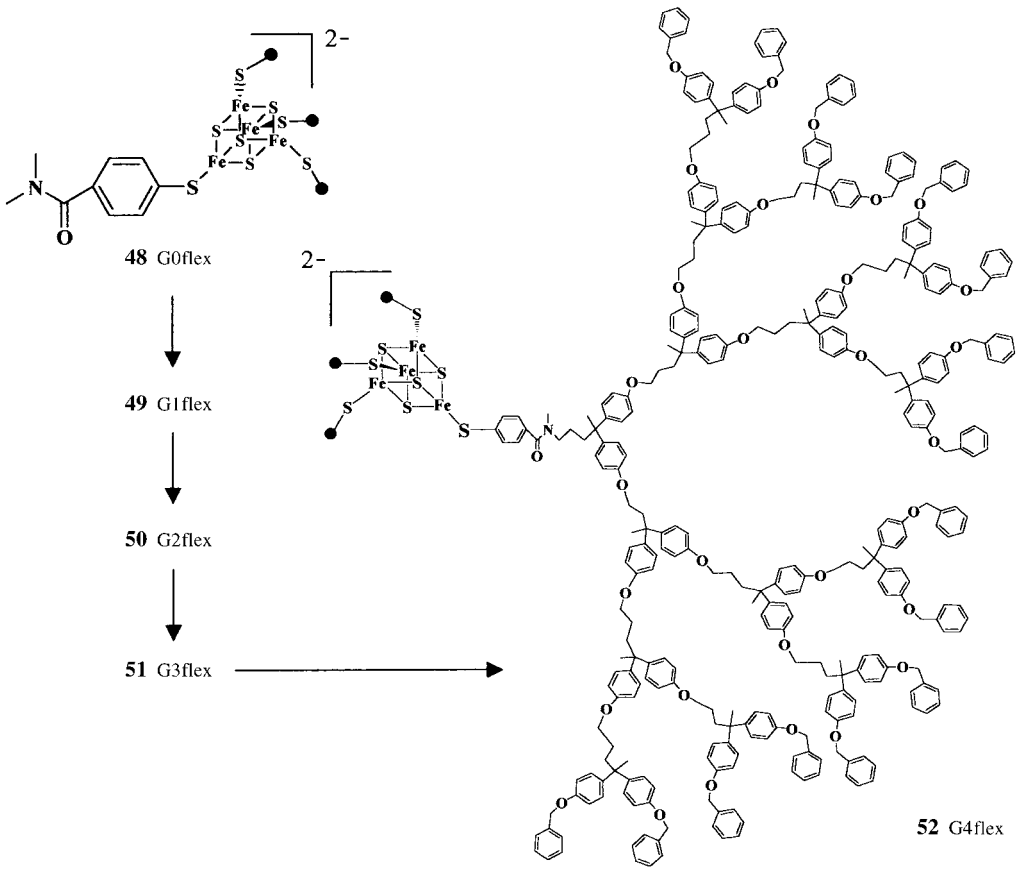

Scheme 3. A strong influence of the solvent on the hydrodynamic radii was found for the flexible electroactive dendrimers **48**–**52** (compact structure in DMF, slightly swollen structure in THF).

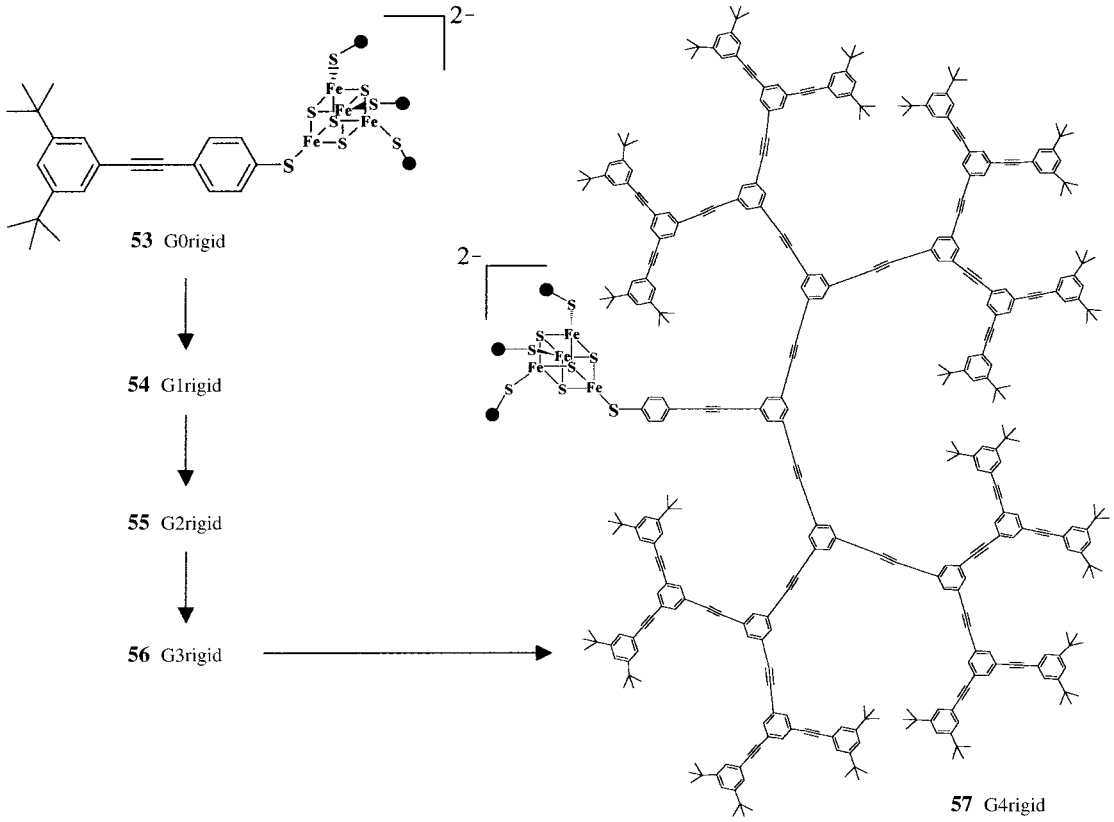

Scheme 4. The rigid electroactive dendrimers **53**–**57** probably have a nonspherical and noncompact structure.

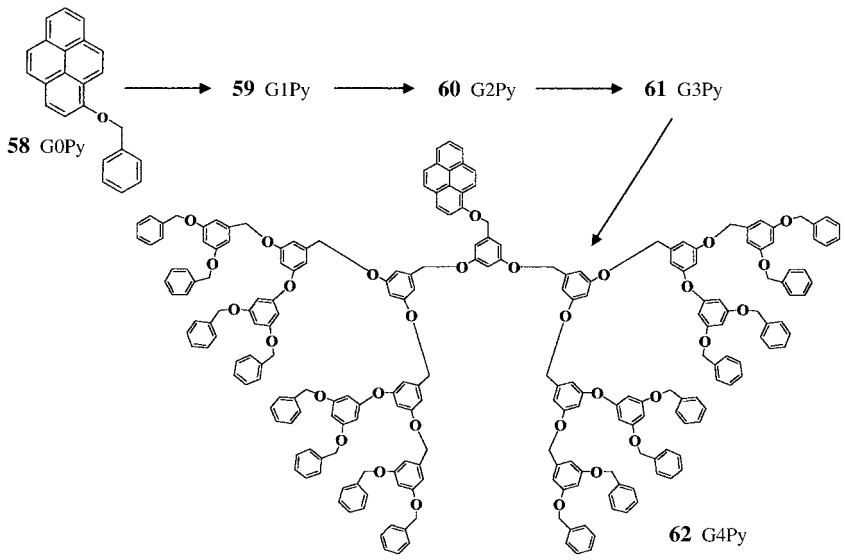

Scheme 5. Pyrene-labeled poly(aryl ether) monodendrons **58**–**62**.

Table 5: Diffusion coefficients D, radii r, volumes V, and densities ρ from pulsed-field-gradient NMR experiments.[93]

Compound	M_r	D_{py} [$cm^2 s^{-1}$][a]	r_s [Å][b]	V_{stokes} [$Å^3$][c]	ρ_{stokes} [$Da Å^{-3}$][d]	R_{theory} [Å][e]	V_{theory} [$Å^3$][f]
			tetrahydrofuran				
pyrene	82	1.7×10^{-5}	2.8	92	2.19	(3.5)	180
58	308	1.3×10^{-5}	3.7	210	1.47	7.2	1560
59	521	0.97×10^{-5}	4.9	490	1.06	10.1	4320
60	932	0.78×10^{-5}	6.1	950	0.99	13.0	9200
61	1822	0.48×10^{-5}	10	4200	0.43	15.9	16800
62	3495	0.34×10^{-5}	14	11500	0.30	18.8	27800
			acetonitrile				
pyrene	82	2.3×10^{-5}	2.6	74	2.72	(3.5)	180
58	308	1.8×10^{-5}	3.3	150	2.06	7.2	1560
59	521	1.4×10^{-5}	4.1	289	1.80	10.1	4320
60	932	1.2×10^{-5}	4.9	490	1.92	13.0	9200
61	1822	1.1×10^{-5}	5.4	660	2.72	15.9	16800
			cyclohexane				
pyrene	82	9.4×10^{-6}	2.6	74	2.73	(3.5)	180
58	308	8.7×10^{-6}	2.8	92	2.52	7.2	1560

[a] Calculated from NMR diffusion data. [b] Calculated from Equation (4) using, $\eta = 4.56\times10^{-4}$ Pa s for THF. [c] Calculated from R_{Stokes} given above, $V_{Stokes} = {}^4/_3\pi(R_{Stokes})^3$. [d] Calculated from V_{Stokes} given above and M_r, $\rho_{Stokes} = M_r/V_{Stokes}$. [e] Radii of fully extended structures calculated from models. [f] Volume of fully extended structures, from radii given above, $V_{theory} = {}^4/_3\pi(R_{theory})^3$. Measurements were performed at 298 K.

beyond the scope of the present Review.[9,10,19,20,95] Some selected examples of the applications of diffusion NMR spectroscopy in the field of organic reactive intermediates, ion pairs, and organometallic systems which bear some relevance to supramolecular chemistry are outlined below. In fact, diffusion NMR spectroscopy should make an important contribution in the field of reactive intermediates since most of these species are unstable and therefore classical methods for measuring diffusion, such as Rayleiigh interferometry[96] or radioactive tracer techniques,[97] are impractical. Diffusion NMR spectroscopy, which provides a means for studying diffusion without perturbating the systems or the need for any chemical modification, is much more suitable for measuring the diffusion characteristics of such unstable species. In addition, many ions and organometallic systems tend to dimerize and self-aggregate, thus making diffusion an intuitively important parameter for such systems. Therefore, it seems surprising that diffusion NMR spectroscopy of such systems only became popular over the last few years.

One of the first applications of high-resolution diffusion NMR spectroscopy in the study of reactive intermediates was the determination of the diffusion coefficients of a series of polycyclic systems, such as compounds **63**–**69**, and their respective doubly and quadruply charged derivatives.[98] In this study, both external and internal references were used since it was anticipated that the reduction of the polycyclic systems into their respective charged derivatives would affect the solution viscosity and hence the diffusion coefficient, and would limit the utility of the diffusion coefficient as a characterizing parameter of the systems. Indeed, a pronounced decrease in the diffusion coefficients of the polycycles was observed upon reduction (Table 6), with only a small change in the viscosity seen. Since the two-electron reduction has no effect on the molecular weight of the systems, it is clear that the decrease in the diffusion coefficients should be attributed to a superposition of the higher solvation and the probable partial self-aggregation of the charged systems.[98] The dilithium, disodium, and dipotassium salts of the tetracene dianion ($\mathbf{65}^{2-}$), for example, were found to have very similar diffusion coefficients, thus implying that the ion-pair phenomenon had only a marginal effect on these systems under the experimental conditions used.[98] An interesting point that emerged from the comparison of the diffusion coefficients of the charged systems with their respective noncharged parent systems was that a larger decrease in the diffusion coefficients was observed for systems that are more suited to self-aggregation. A decrease in the diffusion coefficients to nearly 50% of their initial values was found and attributed to partial self-aggregation in these systems.[98] Indeed, the corannulene tetranion $G3^{4-}$, which showed a pronounced decrease in the diffusion coefficient, was previously shown to form dimers.[99] The conclusion of this study was that self-aggregation and dimerization in these systems might be more important than previously thought.[98]

Rabinovitz and co-workers subsequently showed through the use of diffusion NMR spectroscopy that there is a fair to good correlation between $1/D$ and the van der Waals radii of neutral polycyclic compounds.[100a] A somewhat weaker correlation was found between the Stokes–Einstein radii

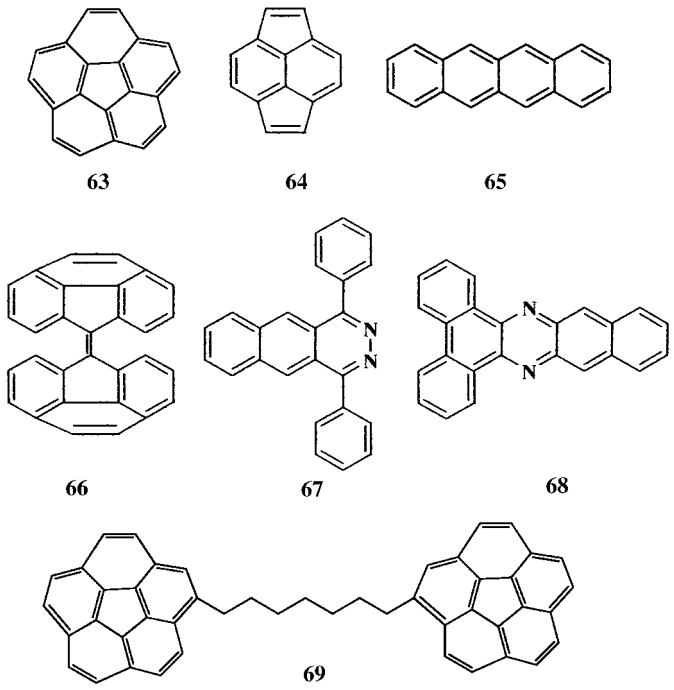

Table 6: Diffusion coefficients *D* of polycyclic systems and their anions in [D_8]THF at 298 K.[98]

System	*D* (CH_2Cl_2; ext. stand.) [10^{-5} cm^2s^{-1}]	*D* (benzene; int. stand.) [10^{-5} cm^2s^{-1}]	*D* (polycyclic system) [10^{-5} cm^2s^{-1}]
63	3.73 ± 0.002	2.87 ± 0.017	1.57 ± 0.017
$\mathbf{63}^{4-}$/4 Li^+	3.73 ± 0.002	2.90 ± 0.041	0.84 ± 0.017
65	3.83 ± 0.031	2.96 ± 0.027	1.83 ± 0.032
$\mathbf{65}^{2-}$/2 Li^+ (2 mg)	3.79 ± 0.006	2.86 ± 0.039	0.96 ± 0.038
$\mathbf{65}^{2-}$/2 Li^+ (20 mg)	3.78 ± 0.000	2.39 ± 0.043	0.71 ± 0.020
		2.86 ± 0.039	0.86 ± 0.017[a]
$\mathbf{65}^{2-}$/2 Na^+	3.80 ± 0.003	2.74 ± 0.014	0.94 ± 0.015
$\mathbf{65}^{2-}$/2 K^+	3.79 ± 0.004	[b]	0.94 ± 0.014
64	3.82 ± 0.017	2.86 ± 0.025	1.90 ± 0.011
$\mathbf{64}^{2-}$/2 Li^+	3.78 ± 0.015	2.82 ± 0.048	1.06 ± 0.057
66	3.80 ± 0.002	2.97 ± 0.014	1.38 ± 0.021
$\mathbf{66}^{2-}$/2 Na^+	3.82 ± 0.002	2.99 ± 0.003	1.05 ± 0.014
67	3.79 ± 0.000	2.85 ± 0.041	1.17 ± 0.008
$\mathbf{67}^{2-}$/2 Na^+	3.72 ± 0.030	2.84 ± 0.003	0.93 ± 0.030
68	3.79 ± 0.002	2.90 ± 0.015	1.38 ± 0.010
$\mathbf{68}^{2-}$/2 Na^+	3.80 ± 0.002	2.97 ± 0.032	1.10 ± 0.026

[a] After correcting for viscosity changes. [b] Very broad signal for benzene, undetectable in the spin echo.

obtained from the diffusion coefficients and the van der Waals radii for the neutral polycyclic systems. The authors suggested that this is partially a result of the fact that the Stokes–Einstein equation does not hold very well when the diffusing particles are less than about five times the radius of the solvent molecules in which the diffusion takes place. There was practically no correlation between $1/D$ and the extracted Stokes–Einstein radii for the charged systems.[100a] This may be a consequence of the different solvation of the anions studied, which also differed in their number of charges. In a different study,[100b] the same research group used diffusion NMR spectroscopy to try to verify whether or not the octaanion of **69** forms dimers. They found that the diffusion coefficient of $\mathbf{69}^{8-}$ is 0.55×10^{-5} cm^2s^{-1} while that of the dimer of $\mathbf{63}^{4-}$ is 0.76×10^{-5} cm^2s^{-1} in [D_8]THF solutions, and concluded that $\mathbf{69}^{8-}$ forms an intermolecular sandwich.[100b]

Pochapsky et al., who studied the phenomenon of ion pairing by NMR spectroscopy quite extensively,[101] recently used diffusion NMR spectroscopy to study the aggregation of tetrabutylammonium chloride (**70**).[102a] In this study the diffusion coefficient ratios of **70** were compared with that of tetrabutylsilane (**71**), a non-aggregating standard with a similar molecular weight and shape, as a function of the concentration. Pochapsky et al. found that this ratio decreased when the concentration was decreased, and achieved a value of nearly 1.0 in very dilute solutions ($\sim 10^{-4}$ M). The aggregation number for **70** was estimated to be 3 at a concentration of about 30 mM in $CDCl_3$.[102a] Subsequently, Pochapsky et al. used the same rationale to study the ion pairs of tetrabutylammonium tetrahydrobrate (**72**) by simultaneously monitoring the diffusion coefficients of the cation and the anion.[102b] They showed that the diffusion coefficients of the cation and anion in $CDCl_3$ are not very different and are much lower than that of tetrabutylsilane (**71**). The interpretation was that, indeed, a tight ion pair is formed. The fact that the diffusion coefficient ratio was found to be concentration-dependent clearly indicated that this ion pair forms aggregates in $CDCl_3$, which is to be expected because of the low solvating power of the solvent.[102b] Recently, Keresztes and Williard demonstrated by diffusion NMR experiments that the tetramer and dimer of *n*-butyllithium can be identified in [D_8]THF.[103] This was accomplished by comparing the diffusion coefficients obtained experimentally from diffusion NMR measurements with the those expected from known X-ray parameters of these species. The data was also presented in a DOSY form.[103]

Organometallic chemistry, where ligand insertion and/or dissociation and aggregation may play an important role, is an additional field in which diffusion NMR spectroscopy may complement other NMR methods for the characterization of species in solution. Since this field was recently reviewed by Pregosin and co-workers,[104] we shall only outline a few examples here. Beck et al. have claimed on the basis of diffusion NMR experiments that the formation of ion quadruples (B) from simple ion pairs (A), as shown in Scheme 6, is probably more important than previously thought in zirconocene-based catalytic systems.[105] This was concluded by measuring the diffusion coefficient of the zirconocenes **73–77** (Scheme 6), and by comparing the findings with the diffusion coefficient obtained for a series of ion pairs such as **73a/b** and **77a/b** with the diffusion coefficient of **73c**, for which the binuclear structure was previously established by X-ray crystallogra-

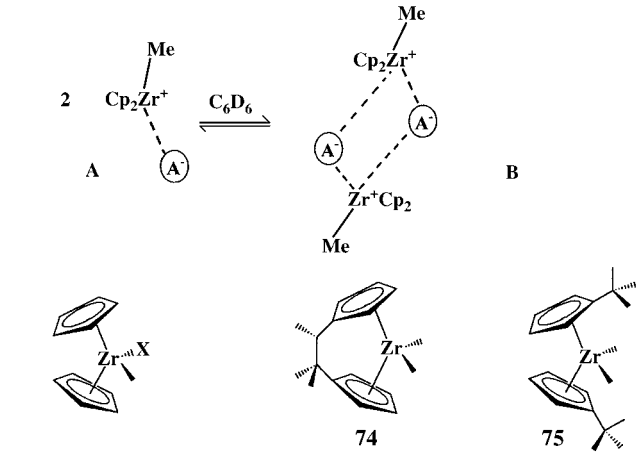

73 X = Me
73a X = $MeB(C_6F_5)_3^-$
73b X = $B(C_6F_5)_4^-$
73c X = (μ–Me)[$(C_2H_5)_2ZrMe^+$][$B(C_6F_5)_4$]$^-$

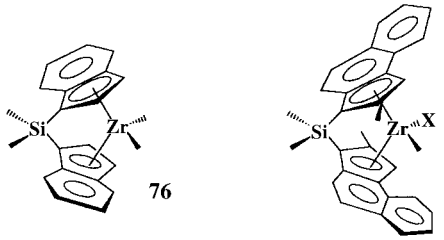

77 X = Me
77a X = $MeB(C_6F_5)_3^-$
77b X = $B(C_6F_5)_4^-$

[$Me_2Si(Me_4Cp)(tBuN)TiMe$]$^+$[$MeB(C_6F_5)_3$]$^-$ **78**
[Me_2C(fluorenyl)(Cp)ZrMe]$^+$[$MeB(C_6F_5)_3$]$^-$ **79**
[$(Me_5Cp)_2ThMe$]$^+$[$B(C_6F_5)_4$]$^-$ **80**
[$(Me_2SiCp)_2ZrMe$]$^+$[$MeB(C_6F_5)_3$]$^-$ **81**
[Cp_2ZrMe]$^+$[$MeB(C_6F_5)_3$]$^-$ **82a**
[$(Me_5Cp)_2ZrMe$]$^+$[$MeB(C_6F_5)_3$]$^-$ **82b**

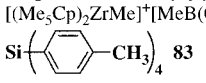

83

Scheme 6. Possible formation of ion quadruples (B) from simple ion pairs (A).

phy.[106a] Since the diffusion coefficient of **73b** deviated from that of **73** and **74**, and was similar to that of the dinuclear complex of **73c**, it was concluded that **73b** is an ion quadruple (structure **8** in Scheme 6). These measurements were performed in benzene in the 1.6–4.7 mM concentration range. However, a very recent study on very similar complexes (**78**–**82**) and with (*p*-tolyl)$_4$Si (**83**) as a reference (Scheme 6) demonstrated that there is a good correlation between the hydrodynamic volumes of these complexes, as obtained from the PGSE diffusion data, and the van der Waals volumes computed for 1:1 ion pairs from the crystal structures of these complexes (Figure 21).[106b] The concentrations of the studied metalocenes were well above the 10^{-4}–10^{-5} M range generally used in polymerizations and it was therefore concluded that aggregation of the metallocenium catalysts is unlikely to be of major importance for chain growth in olefin polymerization.[106b]

Zuccaccia et al. measured the diffusion coefficients of the cationic complex **84** and its neutral analogue **85** in different solvents at various concentrations.[107] In this study, the simple STE pulsed gradient sequence was used for the diffusion

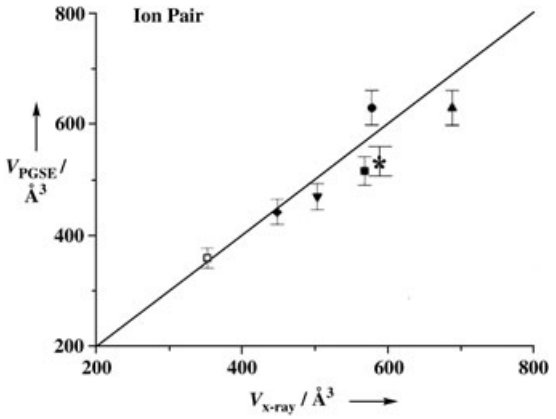

Figure 21. Plot of PGSE-derived hydrodynamic volumes V_{PGSE} for the metallocenium ion pairs versus van der Waals volumes $V_{X\text{-}ray}$ computed for 1:1 ion pairs from the corresponding crystal structures. The straight line represents the equation $V_{PGSE} = V_{X\text{-}ray}$. ■: **78**, ●: **79**, ▲: **80**, ▼: **81**, ◆: **82a**, ⋆: **82b**, □: (*p*-tolyl)$_4$Si (**83**). Adapted with permission from Ref. [106b].

measurements. The results clearly indicated that compound **84** exists as a tight ion pair in $CDCl_3$. It seems that the equilibrium is shifted to a looser ion pair in CD_3NO_2, as witnessed by the higher diffusion coefficient of BPh_4^- relative to the cation. In this solvent, there was only about a 10% difference between the diffusion coefficient of **84** and **85**;[107] in the $CDCl_3$ and CD_2Cl_2 solutions, however, the difference between these diffusion coefficients was much more pronounced and found to be concentration-dependent.[107] The authors suggested on the basis of these results that higher aggregates were involved in these solutions. It should be noted that reference **85** has a lower molecular weight than **84**, for which the molecular weight of the ion pair (cation and

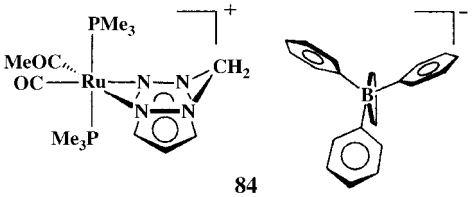

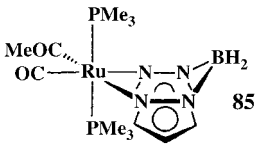

anion) should be taken into account. In addition, compound **85** is probably less solvated than **84** since **85** is an uncharged molecule and therefore should have a somewhat higher diffusion coefficient. However, the fact that the changes in the diffusion coefficients are smaller in solvents with higher solvating power and the fact that the difference in diffusion coefficients are concentration-dependent favors the explanation of higher aggregates in the case of **84** in the chlorinated solvents under the experimental conditions used.[107]

In a recent application Pregosin and co-workers reported the diffusion coefficients of a series of Pd^{II}–arsine complexes of the type $[PdCl_2L_2]$ (**86–89**; $L = AsMe_xPh_{3-x}$ ($x = 3$–0)) and some other organometallic complexes of different sizes (**90–93**; Tp′ = hydrotris(3,5-dimethylpyrazolyl)borate, Ar = *p*-tolyl, dba = *trans,trans*-dibenzylideneacetone), from which they calculated their hydrodynamic radii r_s by using the

$[PdCl_2(AsMe_2Ph)_2]$ **86**

$[PdCl_2(AsMePh_2)_2]$ **87**

$PdCl_2(AsMe_3)_2$ **88**

$PdCl_2(AsPh_3)_2$ **89**

$[Tp'W(CO)_3H]$ **90**

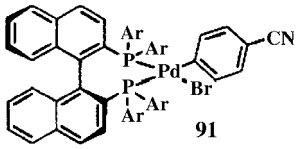

91

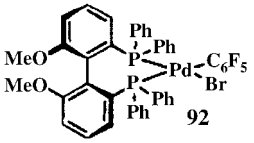

92

$Pd_2(dba)_3$ **93**

Stokes–Einstein equation [see Eq. (5)].[108a] They found a good correlation between the r_s values and the estimated radii compiled from the X-ray structures of these systems (Figure 22).[108a] This approach was further extended to ruthenium(II) complexes through the use of ^{19}F and ^{1}H PGSE measurements.[108b]

A recent demonstration of how diffusion NMR spectroscopy could be used to characterize organometallic reactive intermediates in solution was recently given by Berger and coworkers, who provided a snapshot of the reaction of $^{13}CO_2$ with $[Cp_2Zr(Cl)H]$ (**94**) by using ^{13}C diffusion NMR spectroscopy (Scheme 7).[109] The authors used $^{13}CO_2$ to increase the sensitivity, and combined the DOSY sequence with the INEPT sequence to enhance the signal of the protonated

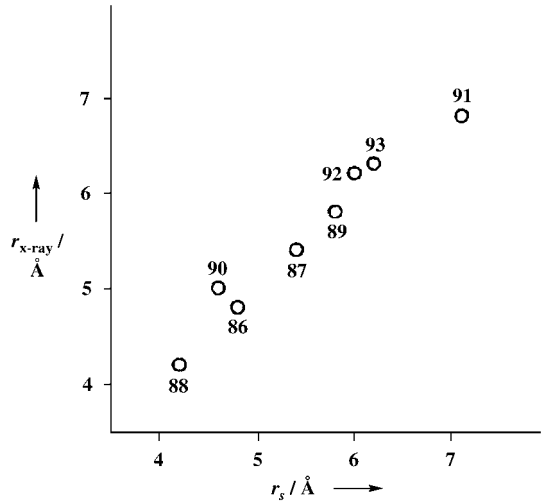

Figure 22. Plot of the hydrodynamic radii (r_s) versus the radii $r_{X\text{-ray}}$ calculated from the crystallographic data for **86–93**. The radii of **86–89** in the solid state were estimated from reported structures for the analogous phosphine, instead of arsine. Adapted with permission from Ref. [108a].

carbon atoms formed during the course of the reaction.[110] The dimeric nature of intermediate **96** was elucidated by comparing the diffusion coefficients, and hence the hydrodynamic radii, of the formed intermediates with those of a series of known zirconocenes, such as **97–99** (see Table 7).

Table 7: Experimental and calculated diffusion coefficients *D* and hydrodynamic radii r_s of the studied zirconium complexes.[109]

	Experimental		Calculated	
	r_s [Å][a]	D [$cm^2 s^{-1}$]	r_s [Å]	D [$cm^2 s^{-1}$][a]
99	3.0	1.61×10^{-5}	3.1[b]	1.55×10^{-5}
97	3.7	1.31×10^{-5}	3.9[b]	1.30×10^{-5}
98	4.2	1.55×10^{-6}	3.6[c]	1.81×10^{-6}
96	6.3	1.05×10^{-6}	6.1[c]	1.07×10^{-6}

[a] Calculated from the Stokes–Einstein equation. [b] Calculated from X-ray structure data under the assumption of a spherical shape. [c] Calculated from the minimized gas-phase structure (PM3).

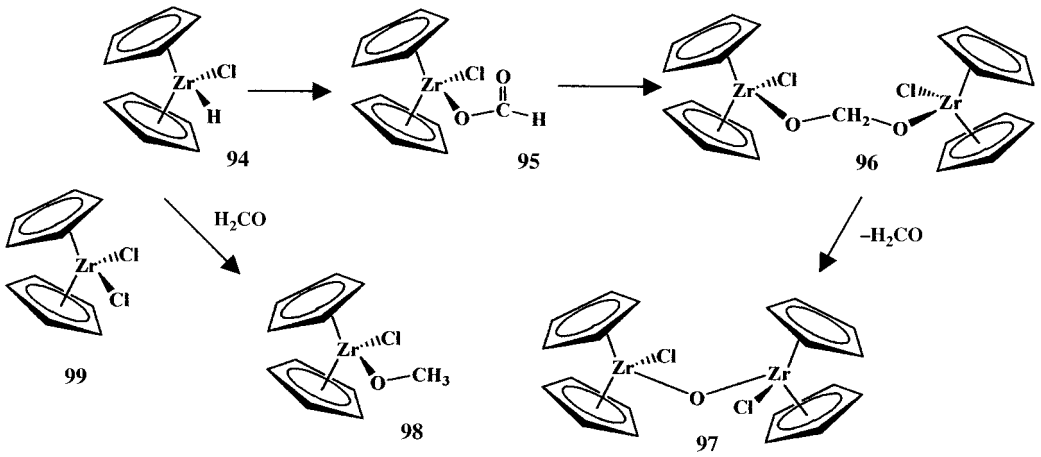

Scheme 7. The combination of DOSY and INEPT sequences enabled the structure of the dimeric intermediate **96** in the reaction of CO_2 with $[Cp_2Zr(Cl)H]$ to be elucidated.

This study demonstrates the tremendous utility of diffusion NMR spectroscopy in probing the structure of organometallic complexes where aggregation, dimerization, and ligand insertion may occur.

5. Applications of Diffusion NMR Measurements in Combinatorial Chemistry

Combinatorial chemistry has become an important tool in organic and pharmaceutical research in recent years.[3,110,111] One of the main consequences of combinatorial chemistry is the generation of mixtures of a large number of products in minute concentrations that require high-throughput NMR methods. Therefore, methods that can be used to assign mixtures of compounds, preferably without their isolation, are needed. In addition, as one of the main concerns of combinatorial chemistry is finding new lead compounds and specific ligands for different receptors, efficient screening methods for the identification of the interaction of tentative ligands with their specific receptors are required. In addition, the kinetics of solid-phase reactions may depend on the ability of the solid support to swell and the ability of reagents to reach the interface of the solid support. Therefore, it seems only logical to use diffusion NMR spectroscopy in the context of combinatorial chemistry where mixture characterization and screening for potential new ligands are central issues. Herein, we outline some of these applications, emphasizing DOSY applications that were originally developed by the group of Johnson[33–36] and applied by Shapiro and co-workers[37,112] and several other research groups.[113] The next section emphasizes the potential and limitations of diffusion NMR techniques in the context of combinatorial chemistry by focusing on only two issues, mixture characterization and ligand screening.

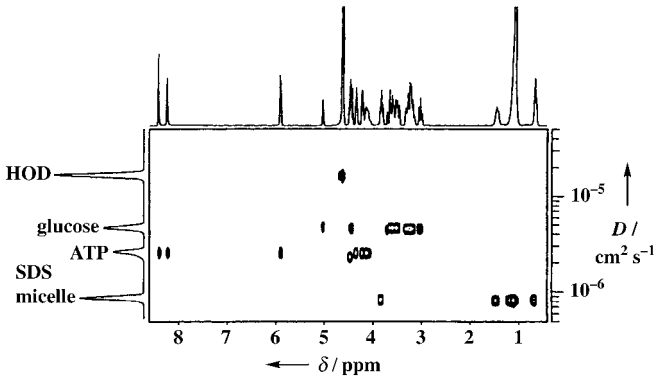

Figure 23. 2D DOSY spectrum of a mixture containing HOD, glucose, ATP, and SDS micelles. Reproduced with permission from Ref. [36a].

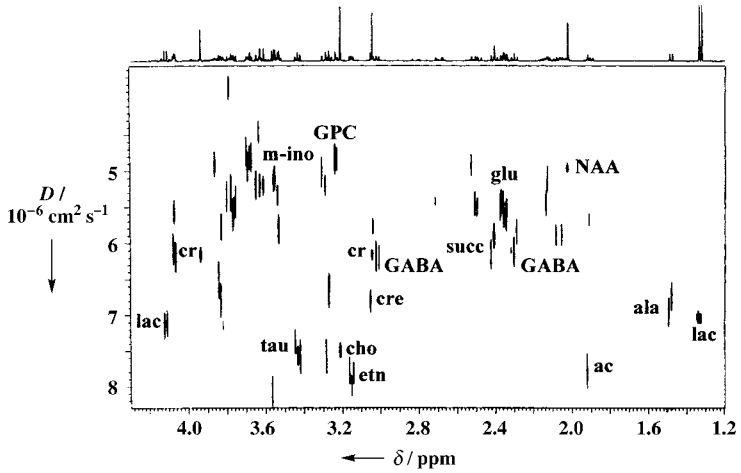

Figure 24. 2D DOSY spectrum (500 MHz) of the perchloric acid extract of a gerbil brain in D_2O. The assignments are as follows: ac = acetate, ala = alanine, cho = choline, cr = creatinine, etn = ethanolamine, GABA = γ-aminobutyric acid, glu = glutamine, GPC = glycerophosphocholine, lac = lactate, *m*-ino = myo-inositol, NAA = *N*-acetylaspartate, succ = succinate, and tau = taurine. Reproduced with permission from Ref. [115].

5.1. DOSY for Mixture Evaluation

DOSY provides an efficient means for the "virtual separation" of compounds.[34,35,37,113] As already shown in Section 3.3, DOSY provides 2D maps in which one axis corresponds to the chemical shifts and the other the diffusion coefficients. In fact, the validation of the DOSY approach was first demonstrated on different mixtures.[34,37,112–115] Figure 23 shows one of the first applications of DOSY, where it was demonstrated that one could indeed "virtually separate" compounds on the basis of their molecular weights. In this study, compounds of significantly different sizes, such as water, glucose, ATP, and sodium dodecylsulfate SDS micelles, were identified.[36a] Subsequently, with the advance in gradient hardware as well as DOSY acquisition and processing schemes, more demanding mixtures were characterized[115–117] (Figure 24) by using high-resolution DOSY (HR-DOSY).[115] In this study, a handful of different metabolites, some of which are not very different in their molecular weights, were resolved.[115]

Diffusion coefficients that differ by only few percent can be resolved with the current conventional technology for non-overlapping peaks (in the same sample). However, it should be noted that, for overlapping peaks, one needs at least a factor of 2–3 in the diffusion coefficients to render them resolvable in a conventional DOSY spectrum.[34,112] The DOSY approach requires the acquisition of a number of 1D spectra with relatively good signal-to-noise ratios (SNR) and are therefore more easily performed by using proton NMR spectroscopy. Overlapping signals may present a real problem when mixtures of large numbers of compounds or complex compounds having many types of protons are present in the mixture. One way to alleviate this problem is to couple the DOSY approach with a 2D NMR sequence where overlapping signals are less of a problem; this affords a 3D sequence, referred to as 3D DOSY. Since diffusion can easily

be coupled to a 2D sequence, many 3D DOSY sequences were developed with relative ease.[34,38,39,112]

However, there are only limited applications of these techniques in real chemical or combinatorial systems besides those of the systems used to demonstrate that these sequences are indeed operable. One of the main reasons for this might be the fact that these 3D DOSY sequences require long acquisition times and larger data storages, with the former being the much more important. Figure 25 shows a 3D

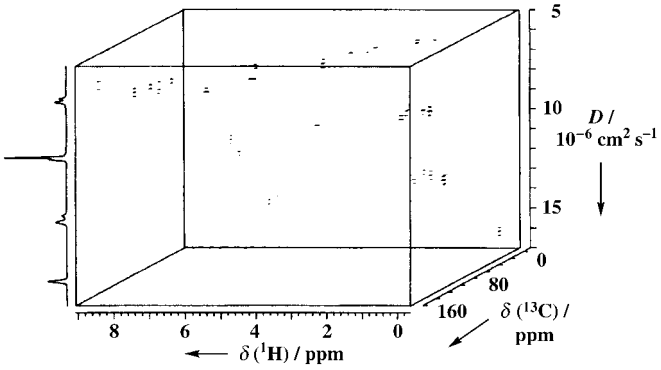

Figure 25. 3D DOSY-HMQC spectrum of quinine, camphene, and geraniol in CD_3OD. Left: projection of the integral onto the diffusion axis. Reproduced with permission from Ref. [39c].

DOSY-HMQC spectrum obtained on a simple mixture consisting of quinine (**100**), camphene (**101**), and geraniol (**102**) in CD_3OD as an example.[39c] This 3D DOSY spectrum

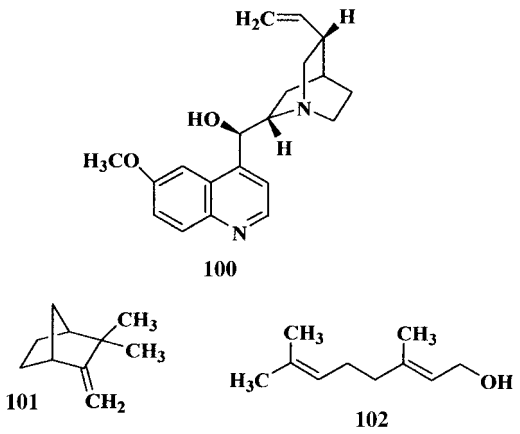

shows no overlap, and it is therefore much easier to extract the structural information from these maps and assign the different signals to the actual compounds present in the mixture. Although there is considerable potential for this type of spectrum, the acquisition schemes are only practical for relatively concentrated samples. A better solution is to use hybrid sequences, which introduce diffusion weighting into the 2D NMR spectrum without elongation of the acquisition time.[116b] Another way to overcome this problem is to use different nuclei whose chemical shifts extend over a larger range. An example was recently provided by the research group of Morris, who demonstrated that a mixture of silicon compounds can indeed be identified and assigned by performing a ^{29}Si DOSY experiment.[117] There was clear resolution of the four principle species in the system, namely, the monomeric silicate **103**, the cyclic trimer **105**, the prismatic hexamer **107**, and the cubic octamer **108** (Figure 26). It also seems that the dimer **104** and the cyclic tetramer **106** are also resolved. A good resolution of compounds was achieved in this study, but it should be noted that it was performed on a concentrated sample using enriched silicates (99.35 % $^{29}SiO_2$) and required several hours.

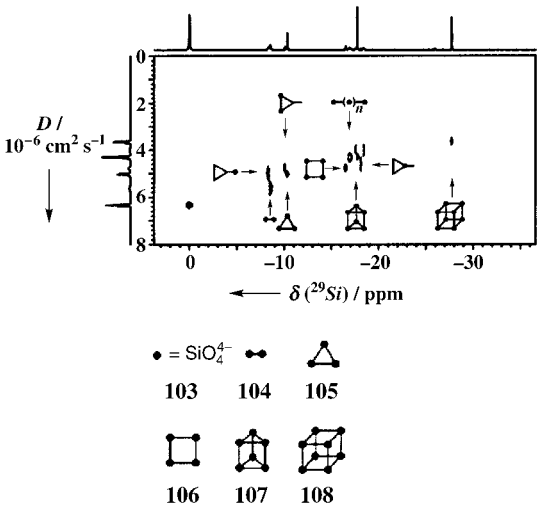

Figure 26. ^{29}Si DOSY spectrum (99.34 MHz) of silicates (0.5 M (99.35 % with 99.35 % ^{29}Si); top: ^{29}Si spectrum, side: projection of the integral onto the diffusion axis. The ten bipolar STE spectra acquired with 320 transients each were measured in a total time of 7 h. Reproduced with permission from Ref. [117].

These recent examples, which were obtained by using conventional instruments, demonstrate that the current technology is already suitable for identifying relatively subtle differences in molecular weights as a means to virtually separate different compounds spectroscopally.

5.2. Ligand Screening by Diffusion and Affinity NMR Spectroscopy

A number of NMR parameters that change upon complex formation, such as chemical shift, transferred nuclear Overhauser effect (NOE), relaxation, and diffusion, were suggested as a screening method.[118] The most widely used NMR screening method is the structure/activity relationships (SARs) introduced by Fesik and co-workers.[119] Diffusion coefficients can be used to screen for the interaction between small molecules and specific receptors, thus separating the spectra of different compounds without really physically separating the compounds in the mixture. As already demonstrated in Section 4.1.1, one can translate the fast change in the diffusion coefficient into an association constant. The calculation of the association constant requires

quantitative determination of the diffusion coefficients, and hence requires the full characterization of the signal decay as a function of the diffusion weighting. However, for screening purposes, where the indication of binding or relative binding is the required information, one can use only a few gradient points to screen for the possible binding of a certain ligand to a given receptor.[120a,b]

An approach where only one gradient point is measured was provided by Shapiro and co-workers and is depicted in Figure 27.[120b] These researchers first measured the 1D ^{1}H spectrum of the mixture of the eight potential ligands (**109**–**116**) and hydroquinine 9-phenanthryl ether (**117**) as the receptor (Figure 27a). They then found the experimental PFG conditions (gradient strength and duration) needed to eliminate the spectrum of the mixture of the eight tentative ligands in the absence of **117** (Figure 27b). They then repeated the same PFG 1D ^{1}H NMR spectrum after addition of **117** to the mixture and indeed observed, in addition to the signals of **117**, signals originating from compounds **109** and **110** that interact with the receptor molecule **117** (Figure 27c). Only the compounds which interact with the receptor experience a decrease in their diffusion coefficients and, hence, their signals reappear under the previously selected PFG conditions.

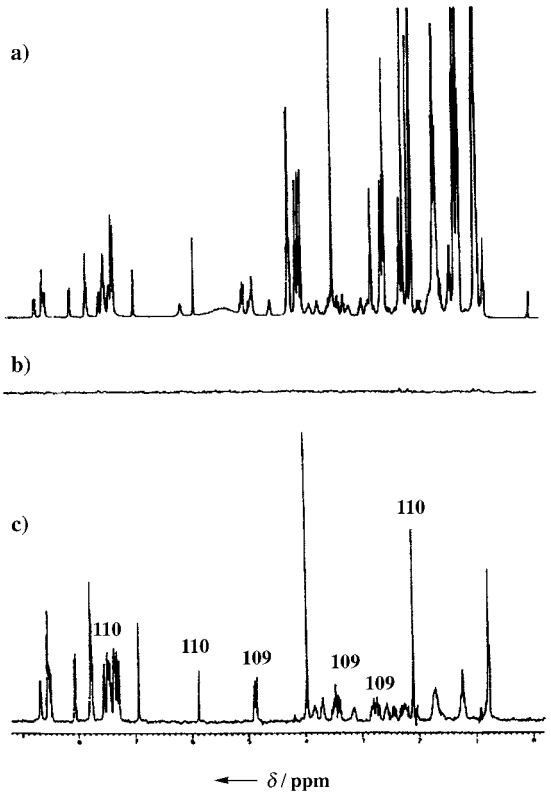

Figure 27. Screening by NMR methods: a) 1D ^{1}H NMR spectrum (400 MHz) of the nine-component mixture (**109**–**117**) in $CDCl_3$ at concentrations of 10 mM; b) 1D pulse gradient ^{1}H NMR spectrum of the mixture without **117** using the LED sequence; and c) 1D pulse gradient ^{1}H NMR spectrum of the eight-component mixture after addition of **117** using the same experimental conditions as (b). Signals arising from compounds **109** and **110** are labeled. All other signals are from compound **117**. Reproduced with permission from Ref. [120b].

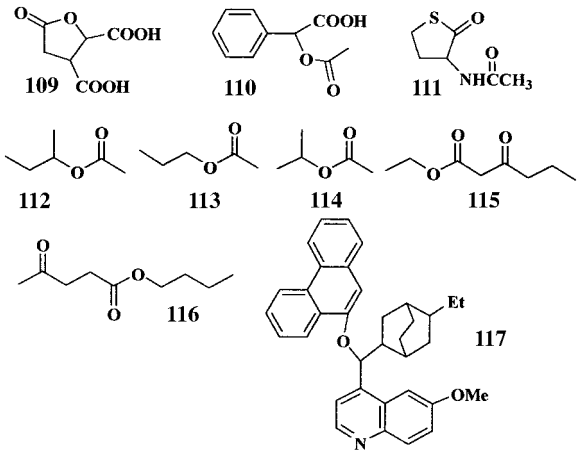

This simple method for screening potential ligands and receptors has the following advantages: The measured parameter, that is, the diffusion coefficient, is intuitively related to the followed phenomenon; the expected decrease in the diffusion coefficient for the compounds that interact with the receptor is indeed observed. This is in contrast to other (non-NMR) parameters and NMR chemical shifts and relaxation times, where the sign of the changes can be both positive or negative. Additionally, this quantitative result can be obtained in a matter of a few minutes from a mixture of several ligands. An important advantage of screening by diffusion NMR spectroscopy is the fact that the method is applicable to all receptors, even to systems of unknown ligands and receptors. This is in clear contrast to the main competing NMR approach for ligand screening, namely, SAR-NMR spectroscopy,[118–119] which is based on monitoring the changes in the ^{15}N/^{1}H hetreonuclear single quantum coherence (HSQC) of a uniformly ^{15}N-labeled receptor after the addition of a mixture of potential ligands. This method is, therefore, only applicable to known receptors for which a large quantity (about 200 mg) of labeled compounds is available. The receptor should have a relatively high solubility, with a molecular weight not more that about 20000–30000 Da.[121] Diffusion NMR spectroscopy, on the other hand, is a nonspecific method and, as such, can be used for the screening of possible ligands for possible receptors with practically no limitation in the size of the receptor. This technique can, in principle, also be applied in combination with other NMR sequences and using all NMR-active nuclei. As in all NMR methods, screening by diffusion NMR spectroscopy is less prone to complications arising from impurities as compared with non-NMR methods. In addition, it should be noted that the larger the difference in the size of the screened ligands and receptors, the higher the sensitivity of the method and, in fact, it may even be easier to monitor ligand association to larger receptors which are NMR silent. The major drawback of the simple approach for ligand screening by diffusion NMR spectroscopy, as outlined in Figure 27, is the fact that both the signals of the ligands interacting with the receptor and the receptor signals are all observed in the final spectrum.[120a] This implies that there is a good chance for signal overlap that will preclude the identification of the interacting ligand(s). However, the

identification of interacting ligands may be even simpler in cases where relatively large receptors, which have a short T_2 value that renders them NMR silent under the conditions used, are screened by this diffusion NMR screening method.[121] In such systems only the signals of the interacting ligand(s) will appear in the final spectrum.

Several approaches to increase the assignment capability of the diffusion NMR screening method were proposed to identify the interacting ligand(s). Fesik and co-workers suggested using diffusion editing to simplify the spectrum of the interacting ligand by eliminating the signals of the receptor, thus leaving only the signals of the interacting ligands after few spectra subtractions.[122] They demonstrated this approach for ligands of the FK506 binding protein and the catalytic domain of stromelysin. For the stromelysin system, the ligand **118** and an additional eight small molecules

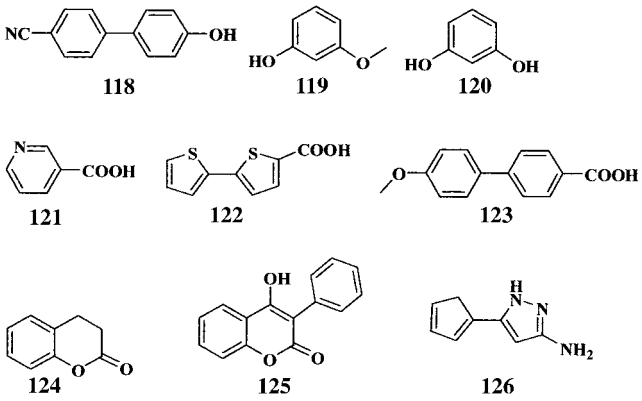

119–126 that were not expected to interact with FK506 were examained (Figure 28). First, they measured the ^{1}H NMR spectra at low gradient strengths of compounds **118–126** in the absence (Figure 28a) and presence of stromelysin. The signal of the protein was then eliminated by subtracting the spectrum of the mixture of the ligands in the presence of stromelysin, obtained at high gradient strengths (data not shown), from the spectrum of the same mixture obtained at low gradient strengths (Figure 28b). Then by subtracting the spectra shown in Figure 28a and Figure 28b, they could identify the peaks of the interacting ligand, namely, compound **118** as shown in Figure 28c. This approach is likely to be operational only in cases in which there are no dramatic changes in the chemical shifts of the compounds involved in the complexation, and it is likely to be more efficient for systems in which the ligands and the receptors differ greatly in size. In fact, Shapiro and co-workers reported that the Fesik approach did not work well in the screening of a mixture of ten different tetrapeptides (two ligands and eight nonbonding tetrapaptides) for their affinity with respect to vancomycin.[123a] They suggested another approach to identify the interacting ligands, namely, to couple the diffusion weighting with a 2D TOCSY sequence (TOCSY = total correlation spectroscopy) which they named DECODES (diffusion encoded spectroscopy).[123b] They showed by comparing the DECODES and TOCSY spectra of the series of ten

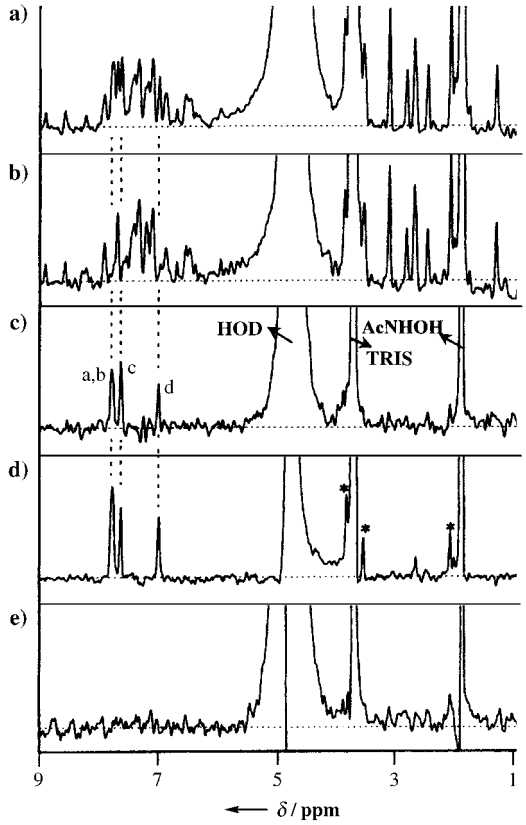

Figure 28. Analysis of ligand binding to the catalytic domain of stromelysin by using a diffusion-edited approach.[122] a) PFG-STE spectrum of a mixture of **118–126** in the absence of stromelysin using pulse gradients of low strength. b) The same spectrum as (a) after removal of protein signals by subtracting a spectrum obtained with strong pulse gradients of the same sample. c) Difference spectrum (a) − (b). The signals of **118** at $\delta = 7.84$, 7.70, and 7.06 ppm in the absence of the protein are indicated by the vertical dashed lines. The signals from 2-amino-2-(hydroxymethyl)propan-1,3-diol) (tris; $\delta = 3.74$ ppm) and acetohydroxamic acid (AcNHOH, $\delta = 1.94$ ppm) were significantly attenuated in the difference spectrum, but not eliminated. d) Reference spectrum of **118** alone. Asterisks (*) indicate impurities in the buffer. e) Difference spectrum obtained in an analogous fashion to the spectrum shown in (c), but on a mixture of eight compounds (**119–126**) which do not bind to stromelysin. Reproduced with permission from Ref. [122].

tetrapaptides in the presence of vancomycin that only signals from amino acids D, F, S, and A remain in the spectrum, thus indicating that only the two peptides DDFA and DDFS bind to vancomycin (see Figure 29). This system, in which there is relatively weak binding and in which the different ligands are of very similar size and not always very different from that of the small receptor of the vancomycin, clearly demonstrates the potential of this simple approach.[123b] Recently, such an approach was used to decode the binding affinity to a DNA dodecamer.[123c]

In fact, few DOSY spectra can, in principle, be used to screen for potential ligands for known or unknown receptors.[34] All that has to be done is obtain the DOSY spectra of a mixture of the potential ligands in the absence and presence of the alleged receptor—it must, however, be ensured that the addition of the receptor has no effect on the viscosity of the

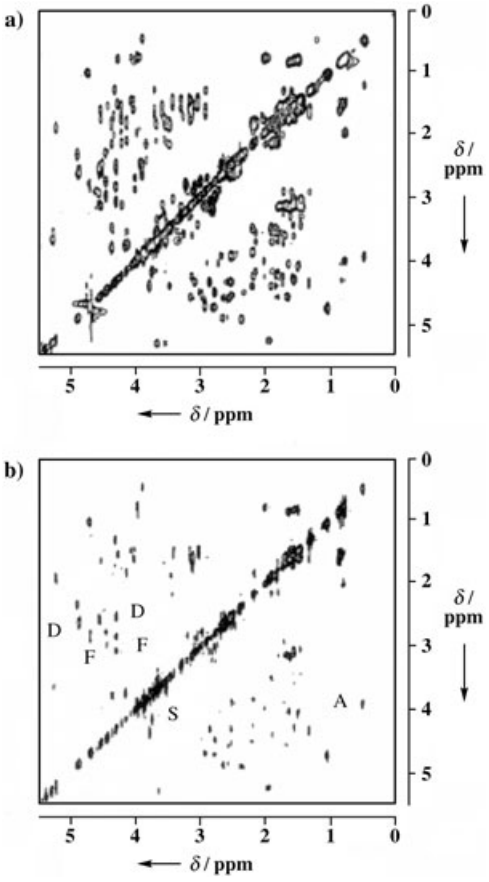

Figure 29. a) TOCSY NMR spectrum for the tetrapeptide mixture containing DDFA, YPFV, GLGG, GPRP, RGDS, GRGD, RGFF, KDEL, DASV, and DDFS in the presence of vancomycin. b) The corresponding DECODES spectrum highlighting the amino acids that remain: D, F, S, and A. Adapted with permission from Ref. [123b].

sample. It should then be possible to identify the interacting ligands by comparing the change in the DOSY spectra. In this approach, the signal separation should be significantly increased since the information is now spread in two dimensions and one has to compare the two 2D spectra of the DOSY experiment. If signal overlap does occur, one can resort to any of the 3D DOSY sequences to try to alleviate the signal overlap at the cost of a longer acquisition time.

6. Summary and Outlook

High-resolution diffusion NMR spectroscopy is a very simple, flexible, and accurate method to obtain diffusion coefficients in solution. With this method it is possible to analyze ensembles of signals simultaneously by using standard NMR spectroscopic technology, thus allowing the addition of the diffusion coefficient into the set of parameters used to characterize systems in solution. In this Review we attempted to describe, through the use of examples, the range of chemical problems that can be addressed with diffusion NMR spectroscopy, including determination of association constants, aggregation, encapsulation, solvation, hydration, ion pairing, estimation of mutual interaction in multicomponent systems, determination of effective size and structures of reactive intermediates, organometallic systems, and other supramolecular systems such as rotaxanes, catenanes, and molecular capsules. The combination of diffusion NMR spectroscopy with other NMR methods provides an improved tool for mapping the different interactions between the different components of the multicomponent systems in solution. Diffusion coefficients can also be used to probe the kinetic stability of multicomponent systems by merely monitoring the effect of a small excess of one of the components on the diffusion coefficient of the supramolecular system. In addition, diffusion NMR spectroscopy can be used for "virtual separation" of mixtures or libraries of compounds of modest size, and provides an efficient and general means, which imposes no requirement on the investigated system, to screen for lead compounds and also potential ligands for unknown receptors. An important feature of diffusion NMR spectroscopy is that the measured parameter, that is, the diffusion coefficient, is intuitively related to many of the phenomena that are studied in a much more direct way than many of the more conventional and heavily used NMR parameters, such as chemical shifts and relaxation times. Diffusion is also a filter, which can be obtained relatively easy and can easily be coupled to nearly any known NMR sequence.

In this Review we have not elaborated on technical issues and the theory of diffusion, which can be found in the many extensive technical reviews recently written on the subject (some of which were cited), since we have focused on applications relevant to supramolecular and combinatorial chemistry. Although we avoided technical issues, it is clear that current technology (conventional instruments and programs) allows easy, simple, and accurate determination of diffusion coefficients in high-resolution probes. In fact, the systems studied, which are characterized by a relatively long T_2 relaxation time and large diffusion coefficients, are simple cases for the current technology. We foresee continuous improvement in gradient technology, mainly arising from its important role in other MR applications. Current gradient technology with conventional PGSE and STE diffusion sequences already gives very good results on not very demanding systems that do not have very short T_2 relaxation times. Therefore, there is much less need for the LED and BPLED sequences, which were so important in the early days of DOSY when much less developed gradient technology was available in many laboratories. Currently, commercial instruments already have DOSY packages and there are ample sequences which can be installed that incorporate diffusion weighting. It therefore seems plausible to speculate that the application of diffusion NMR spectroscopy in the context of supramolecular and combinatorial chemistry will flourish in the coming years.

The main problem of diffusion NMR spectroscopy, like all NMR spectroscopic techniques in general, is its relative low sensitivity, which requires relatively concentrated samples and a long acquisition time. In addition, diffusion weighting means that a filtering out of the signal occurs. Moreover, in conventional DOSY sequences 1D and 2D NMR sequences are transformed into 2D and 3D NMR experiments, respec-

tively. This implies that relatively long acquisition times are required, but this will probably be partially alleviated in the future by using gradient systems on high-field magnets (more than 600 MHz) in combination with cryoprobes. This limitation is not very severe, however, and with current technology the PGSE or the STE diffusion experiments can be performed on host–guest or supramolecular systems having molecular weights of a few kilodaltons and a reasonable lineshape (that is, $\Delta\tilde{\nu}_{1/2} = 10$ Hz) within one hour on a conventional 400 or 500 MHz spectrometer when the concentration is in the range of about 5 mM.

Two additional areas of application of diffusion NMR spectroscopy, not dealt within the present Review because of space limitations, that deserve mentioning are: biochemistry and protein research,[124] as well as the newly emerging field of semisolid samples, where diffusion NMR spectroscopy is used in combination with magic angle spinning (MAS).[125] Diffusion measurements have been used in the context of biochemistry and protein research to study self-aggregation, the association of different ligands and DNA, as well as protein folding.[124,126] However, a very exciting recent development is the use of diffusion NMR spectroscopy to study protein folding in real time.[127] Buevich and Baum used the much more sophisticated ^{1}H-^{15}N LED-HSQC diffusion sequence to measure the protein-folding process in real time for residue-specific ^{15}N-labeled T1-892. They followed the disappearance of the monomer, the appearance of the trimer, and other kinetic intermediates by using diffusion NMR spectroscopy. This exciting demonstration was performed on a relatively slow folding process, but with the advent of high-sensitivity cryoprobes in combination with high-field magnets and fast 2D sequences, one may anticipate the study of much faster processes in the future.

The other field which is currently emerging is the measurement of diffusion by MAS probes on semisolid samples.[125] These probes, which only recently became available, have been used to distinguish between trapped or covalently bonded small molecules in swollen Wang resin beads. The combination of the bipolar LED and CPMG sequences (CPMG = Carr–Purcell–Meiboom–Gill) is useful for studying the interaction of different molecules with resins—an area vital to combinatorial chemistry.[125a,b]

With the above applications already published in the literature and in view of the rapid advancement of instruments and software, which will make diffusion NMR spectroscopy more accurate and efficient, it is possible to speculate that diffusion NMR spectroscopy will, in the near future, become a popular tool in the hands of chemists interested in molecular interactions in solution. The triumph of diffusion NMR spectroscopy will be when it becomes as commonplace as other NMR methods. Our aim in this Review was to convince organic, inorganic, organometallic and supramolecular chemists to add diffusion NMR spectroscopy to their arsenal of analytical tools used to study molecular interactions in solution.

We thank the Israel Science Foundation administered by the Israel Academy of Science and Humanities, Jerusalem, Israel, for supporting the early stage of this research. We also wish to thank Professors S. E. Biali, V. Böhmer, R. Ungaro, and D. N. Reinhoudt for collaborative efforts and Professor S. E. Biali for reading and commenting on the manuscript.

Received: October 23, 2003

[1] a) J.-M. Lehn, *Supramolecular Chemistry Concepts and Perspectives*, VCH, Weinheim, **1995**; b) J. W. Steed, J. L. Atwood, *Supramolecular Chemistry*, Wiley, New York, **2000**.

[2] a) *Comprehensive Supramolecular Chemistry*, *Vols. 1–10* (Eds.: J. L. Atwood, J. E. D. Davis, D. D. MacNicol, F. Vögtle, J.-M. Lehn), Pergamon, Oxford, **1996**; b) *Proc. Natl. Acad. Sci. USA* **2002**, *99*, 4755–5750, (special issue on supramolecular chemistry and self-assembly (Ed.: J. Halpern).

[3] *Combinatorial Chemistry: a Practical Approach* (Eds.: W. Bannwarth, E. Felder), Wiley-VCH, Weinheim, **2000**.

[4] E. L. Hahn, *Phys. Rev.* **1950**, *80*, 580–594.

[5] a) O. E. Stejskal, J. E. Tanner, *J. Chem. Phys.* **1965**, *42*, 288–292; b) it should be noted that the diffusion time depends on the shape of the pulse gradients used, as expected from Equation (9). For example, for the PGSE or the STE diffusion sequence with sine-shape gradient pulses, the effective diffusion time is $\Delta - \delta/4$. When $\Delta \gg \delta$ the diffusion time is $\approx \Delta$.

[6] a) J. Jeener, Ampére International Summer School, Basko Polje, Yugoslavia, **1971**; b) W. P. Aue, E. Bartholdi, R. R. Ernst, *J. Chem. Phys.* **1976**, *64*, 2229–2246.

[7] A. Bax, *Two-Dimensional Magnetic Resonance in Liquids*, Delft University Press, D. Reidel Publishing Company, **1982**.

[8] R. R. Ernst, G. Bodenhausen, A. Wokaun, *Principles of Nuclear Magnetic Resonance in One and Two Dimensions*, Oxford University Press, Oxford, **1987**; b) T. D. W. Claridge, *High-Resolution NMR Techniques in Organic Chemistry*, Pergamon, Amsterdam, **1999**.

[9] P. Stilbs, *Prog. Nucl. Magn. Reson. Spectrosc.* **1987**, *17*, 1–45, and references therein.

[10] a) J. Kärger, H. Pfeifer, W. Heink, *Adv. Magn. Reson.* **1988**, *12*, 1–88; b) for a recent volume concerning the use of diffusion NMR spectroscopy in chemical systems see: *Magn. Reson. Chem.* **2002**, *40*, S15–S152; c) for a recent volume regarding the use of diffusion NMR spectroscopy in chemical and biological systems see: *Diffusion NMR and MRI: Basic Concepts and Applications* (Eds.: Y. Cohen, M. Neeman), *Israel. J. Chem.* **2003**, *43*, 1–163.

[11] W. S. Price in *Annual Reports on NMR spectroscopy* (Ed.: G. A. Webb), Academic, London, **1996**, pp. 51–142; b) T. Parella, *Magn. Reson. Chem.* **1996**, *34*, 329–347; c) T. Parella, *Magn. Reson. Chem.* **1998**, *36*, 467–495.

[12] a) P. C. Lauterbur, *Nature* **1973**, *242*, 190–191; b) D. D. Stark, W. G. Bardley, *Magnetic Resonance Imaging*, 2nd ed., Mosby Company, St. Louis, **1992**; c) *Methods of Magnetic Resonance Imaging and Spectroscopy* (Ed.: I. R. Young), Wiley, Chichester, **2000**.

[13] *Perfusion and Diffusion Magnetic Resonance Imaging: Applications to functional MRI* (Ed.: D. Le Bihan), Raven Press, New York, **1995**.

[14] M. E. Moseley, Y. Cohen, J. Mintorovitch, L. Chileuitt, H. Shimizu, J. Kucharczyk, M. F. Wendland, P. R. Weinstein, *Magn. Reson. Med.* **1990**, *16*, 330–346.

[15] P. J. Basser, *NMR Biomed.* **1995**, *8*, 333–344; P. J. Basser, J. Mattiello, D. Le Bihan, *Biophys. J.* **1994**, *66*, 259–267; for a recent special volume on DTI see: *NMR Biomed.* **2002**, *15*, 431–593.

[16] a) J. Kärger, D. M. Ruthven, *Diffusion in Zeolites and Other Microporous Solids*, Wiley, New York, **1992**; b) T. Nose, *Annu. Rep. NMR Spectrosc.* **1993**, *27*, 218–253.

[17] a) W. S. Price, *Concepts Magn. Reson.* **1997**, *9*, 299 – 336; b) P. T. Callaghan, S. L. Codd, J. D. Seymour, *Concepts Magn. Reson.* **1999**, *11*, 181 – 202; c) W. S. Price, *Concepts Magn. Reson.* **1998**, *10*, 197 – 237.

[18] a) J. Kärger, H. Pfeifer, *NMR and Catalysis*, (Eds.: A. Pines, A. Bell), Dekker, New York, **1994**; b) P. T. Callaghan, A. Coy in *NMR Probes and Molecular Dynamics* (Ed.: R. Tycko), Kluwer, Dordrecht, **1993**, pp. 490 – 523.

[19] O. Söderman, P. Stilbs, *Prog. Nucl. Magn. Reson. Spectrosc.* **1994**, *26*, 445 – 482.

[20] G. Lindblom, G. Oradd, *Prog. Nucl. Magn. Reson. Spectrosc.* **1994**, *26*, 483 – 515.

[21] A. R. Waldeck, P. W. Kuchel, A. J. Lennon, B. E. Chapman, *Prog. Nucl. Magn. Reson. Spectrosc.* **1997**, *30*, 39 – 68.

[22] a) D. G. Corry, D. N. Garroway, *Magn. Reson. Med.* **1990**,*14*, 435 – 444; b) P. T. Callaghan, D. MacGowan, K. J. Packer, F. O. Zelaya, *J. Magn. Reson.* **1990**, *90*, 177 – 182; c) P. T. Callaghan, A. Coy, D. MacGowan, K. J. Packer, F. O. Zelaya, *Nature* **1991**, *351*, 467 – 469.

[23] P. W. Kuchel, A. Coy, P. Stilbs, *Magn. Reson. Med.* **1997**, *37*, 637 – 643.

[24] A. M. Torres, A. T. Taurins, D. G. Regan, B. E. Chapman, P. W. Kuchel, *J. Magn. Reson.* **1999**, *138*, 135 – 143.

[25] P. W. Kuchel, C. J. Durrant, *J. Magn. Reson.* **1999**, *139*, 258 – 272.

[26] a) Y. Assaf, A. Mayk, Y. Cohen, *Magn. Reson. Med.* **2000**, *44*, 713 – 722; b) Y. Assaf, D. Ben-Bashat, J. Chapman, S. Peled, I. E. Biton, M. Kafri, Y. Segev, T. Hendler, A. D. Korczyn, M. Graif, Y. Cohen, *Magn. Reson. Med.* **2002**, *47*, 115 – 126; c) Y. Assaf, Ph.D. Thesis, Tel Aviv University, **2001**.

[27] Y. Cohen, Y. Assaf, *NMR Biomed.* **2002**, *15*, 516 – 542.

[28] P. T. Callaghan, *Rep. Prog. Phys.* **1999**, *62*, 599 – 670, and references therein.

[29] a) U. Tallarek, D. van Dusschoten, H. Van As, E. Bayer, G. Guiochon, *J. Phys. Chem. B* **1998**, *102*, 3486 – 3497; b) U. Tallarek, F. J. Vergeldt, H. Van As, *J. Phys. Chem. B* **1999**, *103*, 7654 – 7664; c) U. Tallarek, E. Rapp, A. Seidel-Morgenstern, H. Van As, E. Bayer, G. Guiochon, *J. Phys. Chem. B* **2002**, *106*, 12709 – 12721.

[30] The theory of molecular diffusion and transport is highly developed and details can be found in the following excellent monograph: a) J. Crank, *The Mathematics of Diffusion*, 2nd ed., Claxendon Press, Oxford, **1975**; b) E. L. Cussler, *Diffusion: Mass Transfer in Fluid Systems*, Cambridge University Press, Cambridge, **1984**.

[31] A. Einstein, *Ann. Phys.* **1906**, *19*, 289 – 306.

[32] J. E. Tanner, *J. Chem. Phys.* **1970**, *52*, 2523 – 2526.

[33] S. J. Gibbs, C. S. Johnson, Jr., *J. Magn. Reson.* **1991**, *93*, 395 – 402.

[34] C. S. Johnson, Jr., *Prog. Nucl. Magn. Reson. Spectrosc.* **1999**, *34*, 203 – 256, and references therein.

[35] a) D. Wu, A. Chen, C. S. Johnson, Jr., *J. Magn. Reson. Ser. A* **1995**, *115*, 123 – 126; b) to further reduce the eddy currents sine-shaped gradient pulses rather than the classical rectangular gradient pulses can be used.

[36] a) D. Wu, A. Chen, C. S. Johnson, Jr., *J. Am. Chem. Soc.* **1993**, *115*, 4291 – 4299; b) D. Wu, A. Chen, C. S. Johnson, Jr., *J. Magn. Reson. Ser. A* **1996**, *123*, 215 – 218.

[37] J. S. Gounarides, A. Chen, M. J. Shapiro, *J. Chromatogr. B* **1999**, *725*, 79 – 90, and references therein.

[38] E. Gozansky and D. G. Gorenstein, *J. Magn. Reson. Ser. B* **1996**, *111*, 94 – 96.

[39] a) D. Wu, A. Chen, C. S. Johnson, Jr., *J. Magn. Reson. Ser. A* **1996**, *121*, 88 – 91. These authors have not inverted the third dimension to obtain the diffusion coefficients. b) A. Jerschow and N. Müller, *J. Magn. Reson. Ser. A* **1996**, *123*, 222 – 225; c) H. Barjat, G. A. Morris, A. G. Swanson, *J. Magn. Reson.* **1998**, *131*, 131 – 138.

[40] a) K. A. Connors, *Binding Constants*, Wiley, New York, **1987**; b) H. Tsukube, H. Furuta, A. Odani, Y. Takeda, Y. Kudo, Y. Inoue, Y. Liu, H. Sakamoto, K. Kimura in *Comprehensive Supramolecular Chemistry*, *Vol. 3* (Eds.: J. L. Atwood, J. E. D. Davis, D. D. MacNicol, F. Vögtle), Pergamon, Oxford, **1996**, chap. 10; c) H.-J. Schneider, A. Yatsimirsky, *Principle and Methods in Supramolecular Chemistry*, Wiley, New York, **2000**, pp. 137 – 226.

[41] For some selected examples and the compilation of association constants, see: a) J. J. Christensen, D. J. Eatough, R. M. Izatt, *Chem. Rev.* **1974**, *74*, 351 – 384; b) R. M. Izatt, J. S. Bradshaw, S. A. Nielsen, J. D. Lamb, J. J. Christensen, *Chem. Rev.* **1985**, *85*, 271 – 339; c) K. E. Krakowiak, J. S. Bradshaw, D. J. Zamecka-Krakowiak, *Chem. Rev.* **1989**, *89*, 929 – 972; d) R. M. Izatt, K. Pawlak, J. S. Bradshaw, *Chem. Rev.* **1991**, *91*, 1721 – 2085; e) H. An, J. S. Bradshaw, R. M. Izatt, *Chem. Rev.* **1992**, *92*, 543 – 572.

[42] a) T. Wang, J. S. Bradshaw, R. M. Izatt, *J. Heterocycl. Chem.* **1994**, *31*, 1097 – 1114; b) Y. Inoue, *Annu. Rep. NMR Spectrosc.* **1993**, *31*, 59 – 101; c) K. A. Connors, *Chem. Rev.* **1997**, *97*, 1325 – 1357; d) C. S. Wilcox in *Frontiers of Supramolecular Chemistry and Photochemistry* (Eds.: H.-J. Schneider, H. Durr) Weinheim, **1991**, pp. 123 – 143.

[43] a) L. Fielding, *Tetrahedron* **2000**, *56*, 6151 – 6170; b) L. Fielding, *Curr. Top. Med. Chem.* **2003**, *3*, 39 – 53.

[44] B. Lévay, *J. Chem. Phys.* **1973**, *77*, 2118 – 2121.

[45] For some early diffusion measurements by the Stilbs research group, see: P. Stilbs, M. E. Moseley, *Chem. Scr.* **1979**, *13*, 26 – 30; P. Stilbs, M. E. Moseley, *Chem. Scr.* **1980**, *15*, 215 – 217; P. Stilbs, B. Lindman, *J. Phys. Chem.* **1981**, *85*, 2587 – 2589; W. Brown, R. M. Johnsen, P. Stilbs, B. Lindman, *J. Phys. Chem.* **1983**, *87*, 4548 – 4553; M. Jansson, P. Stilbs, *J. Phys. Chem.* **1985**, *89*, 4868 – 4873.

[46] R. Rydén, J. Carlfors, P. Stilbs, *J. Inclusion Phenom.* **1983**, *1*, 159 – 167.

[47] O. Mayzel, Y. Cohen, *J. Chem. Soc. Chem. Commun.* **1994**, 1901 – 1902.

[48] For example, fluorescence was used to calculate the association constant of 5,10,15,20 tetrakis(4-carboxyphenyl) porphyrin with β-CD. The discrepancy was not only in the values obtained but also in the sign of the changes in the fluorescence observed upon complex formation: in one report, S. S. Zhao, J. H. T. Luong, *J. Chem. Soc. Chem. Commun.* **1994**, 2307 – 2308, an increase in the fluorescence is reported, while in another, F. Venema, A. E. Rowan, R. Nolte, *J. Am. Chem. Soc.* **1996**, *118*, 257 – 258, a decrease in fluorescence was reported.

[49] F. Vögtle, W. M. Muller, *Angew. Chem.* **1979**, *91*, 676 – 677; *Angew. Chem. Int. Ed. Engl.* **1979**, *18*, 623 – 624.

[50] S. Kamitori, K. Hirotsu, T. Higuchi, *J. Chem. Soc. Chem. Commun.* **1986**, 690 – 691.

[51] a) S. Kamitori, K. Hirotsu, T. Higuchi, *J. Am. Chem. Soc.* **1987**, *109*, 2409 – 2414; b) S. Kamitori, K. Hirotsu, T. Higuchi, *Bull. Chem. Soc. Jpn.* **1988**, *61*, 3825 – 3830.

[52] A. Gafni, Y. Cohen, *J. Org. Chem.* **1997**, *62*, 120 – 125.

[53] The hydrophobic interaction is the major driving force for most organic molecule complexes containing cyclodextrins in aqueous solutions. Only a few cases are known in which the addition of alcohol brings about an increase in the association constant of CD complexes in water and, even there, a decrease in the K_a value was observed for high alcohol concentrations; see, for example: G. Nelson, G. Patonay, I. M. Warner, *J. Inclusion Phenom.* **1988**, *6*, 277 – 289; K. A. Connors, M. J. Mulski, A. Paulson, *J. Org. Chem.* **1992**, *57*, 1794 – 1798.

[54] A. Gafni, Y. Cohen, R. Kataky, S. Palmer, D. Parker, *J. Chem. Soc. Perkin Trans. 2* **1998**, *19*–23.

[55] K. S. Cameron, L. Fielding, *J. Org. Chem.* **2001**, *66*, 6891 – 6895.

[56] a) L. Avram, Y. Cohen, *J. Org. Chem.* **2002**, *67*, 2639 – 2644; b) for an additional paper in which diffusion NMR spectroscopy was used to corroborate the formation of rotaxanes, see: P. J. Skinner, S. Blair, R. Kataky, D. Parker, *New J. Chem.* **2000**, *24*, 265 – 268.

[57] It was suggested that protonation of nitrogen atoms in nitrogen-containing pseudorotaxanes might convert them into rotaxanes: Y. Kawaguchi, A. Harada, *J. Am. Chem. Soc.* **2000**, *122*, 3797 – 3798.

[58] L. Frish, F. Sansone, A. Casnati, R. Ungaro, Y. Cohen, *J. Org. Chem.* **2000**, *65*, 5026 – 5030.

[59] a) A. Casnati, M. Fabbi, N. Pelizzi, A. Pochini, F. Sansone, R. Ungaro, *Bioorg. Med. Chem. Lett.* **1996**, *6*, 2699 – 2704; b) A. Casnati, F. Sansone, R. Ungaro, *Acc. Chem. Res.* **2003**, *36*, 246 – 254.

[60] a) B. K. Hubbard, C. T. Walsh, *Angew. Chem.* **2003**, *115*, 752 – 789; *Angew. Chem. Int. Ed.* **2003**, *42*, 730 – 765; b) D. H. Williams, B. Bardsley, *Angew. Chem.* **1999**, *111*, 1264 – 1286; *Angew. Chem. Int. Ed.* **1999**, *38*, 1172 – 1193, and references therein.

[61] C. T. Walsh, S. L. Fisher, I. S. Park, M. Prahaland, Z. Wu, *Chem. Biol.*, **1996**, *3*, 21 – 28.

[62] O. Mayzel, O. Aleksiuk, F. Grynszpan, S. E. Biali, Y. Cohen, *J. Chem. Soc. Chem. Commun.* **1995**, 1183 – 1184.

[63] J. M. Harrowfield, M. I. Odgen, W. R. Richmond, A. H. White, *J. Chem. Soc. Chem. Commun.* **1991**, 1159 – 1160.

[64] a) D. J. Cram, *Nature* **1992**, *356*, 29 – 36; b) R. G. Chapman, J. C. Sherman, *Tetrahedron* **1997**, *53*, 15911 – 15945; c) A. Jasat, J. C. Sherman, *Chem. Rev.* **1999**, *99*, 931 – 967.

[65] a) M. M. Conn, J. Rebek, Jr., *Chem. Rev.* **1997**, *97*, 1647 – 1668; b) M. Fujita, K. Umemoto, M. Yoshizawa, N. Fujita, T. Kusukawa, K. Biradha, *Chem. Commun.* **2001**, 509 – 518; c) F. Hof, S. L. Craig, C. Nuckolls, J. Rebek, Jr., *Angew. Chem.* **2002**, *114*, 1556 – 1578; *Angew. Chem. Int. Ed.* **2002**, *41*, 1488 – 1508.

[66] a) K. D. Shimizu, J. Rebek, Jr., *Proc. Natl. Acad. Sci. USA* **1995**, *92*, 12403 – 12407; b) V. Böhmer, O. Mogck, M. Pons, E. F. Paulus in *NMR in Supramolecular Chemistry* (Ed.: M. Pons), Kluwer Academic Publishers, Dordrecht, **1999**, pp. 45 – 60; c) J. Rebek, Jr., *Acc. Chem. Res.* **1999**, *32*, 278 – 286; d) J. Rebek, Jr., *Chem. Commun.* **2000**, 637 – 643; e) V. Böhmer, M. O. Vysotsky, *Aust. J. Chem.* **2001**, *54*, 671 – 677.

[67] a) R. Warmuth, *J. Inclusion Phenom. Macrocyclic Chem.* **2000**, *37*, 1 – 38; b) J. Chen, S. Körner, S. L. Craig, D. M. Rudkevich, J. Rebek, Jr., *Nature* **2002**, *414*, 385 – 386; c) J. Chen, S. Körner, S. L. Craig, S. Lin, D. M. Rudkevich, J. Rebek, Jr., *Proc. Natl. Acad. Sci. USA* **2002**, *99*, 2593 – 2596.

[68] L. Frish, S. E. Matthews, V. Böhmer, Y. Cohen, *J. Chem. Soc. Perkin Trans. 2* **1999**, 669 – 671.

[69] a) D. A. Dougherty, D. A. Stauffer, *Science* **1990**, *250*, 1558 – 1560; b) J. C. Ma, D. A. Dougherty, *Chem. Rev.* **1997**, *97*, 1303 – 1324.

[70] a) L. Frish, M. O. Vysotsky, S. E. Matthews, V. Böhmer, Y. Cohen, *J. Chem. Soc. Perkin Trans. 2* **2002**, 88 – 93; b) L. Frish, M. O. Vysotsky, V. Böhmer, Y. Cohen, *Org. Biomol. Chem.* **2003**, *1*, 2011 – 2014.

[71] L. Avram, Y. Cohen, *J. Am. Chem. Soc.* **2002**, *124*, 15148 – 15149.

[72] L. R. MacGillivray, J. L. Atwood, *Nature* **1997**, *389*, 469 – 472.

[73] a) A. Shivanyuk, J. Rebek, Jr., *Proc. Natl. Acad. Sci. USA* **2001**, *98*, 7662 – 7665; b) A. Shivanyuk, J. Rebek, Jr., *Chem. Commun.* **2001**, 2424 – 2425.

[74] A. Shivanyuk, J. Rebek, Jr., *J. Am. Chem. Soc.* **2003**, *125*, 3432 – 3433.

[75] a) L. Avram, Y. Cohen, *Org. Lett.* **2002**, *4*, 4365 – 4368; b) L. Avram, Y. Cohen, *Org. Lett.* **2003**, *5*, 1099 – 1102; c) L. Avram, Y. Cohen, *Org. Lett.* **2003**, *5*, 3329 – 3332; d) T. Gerkensmeier, W. Iwanek, C. Agena, R. Fröhlich, S. Kotila, C. Näther, J. Mattay, *Eur. J. Org. Chem.* **1999**, 2257 – 2262; e) J. L. Atwood, L. J. Barbour, A. Jerga, *Chem. Commun.* **2001**, 2376 – 2377; f) L. Avram, Y. Cohen, *J. Am. Chem. Soc.* **2003**, *125*, 16180 – 16181.

[76] I. P. Gerothanassis, *Prog. Nucl. Magn. Reson. Spectrosc.* **1994**, *26*, 171 – 237, and references therein.

[77] G. Otting, *Prog. Nucl. Magn. Reson. Spectrosc.* **1997**, *31*, 259 – 285, and references therein.

[78] B. Halle, V. P. Denisov, *Methods Enzymol.* **2001**, *338*, 178 – 201.

[79] O. Mayzel, A. Gafni, Y. Cohen, *Chem. Commun.* **1996**, 911 – 912.

[80] T. Iwachido, M. Minami, M. Kimura, A. Sadakane, M. Kawasaki, K. Toei, *Bull. Chem. Soc. Jpn.* **1980**, *53*, 703 – 708.

[81] For a recent volume regarding NMR spectroscopy of H-bonded systems, see: *Magn. Reson. Chem.* **2001**, *39*, S5–S213.

[82] a) R. Konrat, M. Tollinger, G. Kontaxis, B. Kräutler, *Monatsh. Chem.* **1990**, *130*, 961 – 967; b) H. B. Seba, B. Ancian, *J. Chem. Soc. Chem. Commun.* **1990**, 996 – 997; c) F. Cordier, S. Grzesiek, *J. Am. Chem. Soc.* **1999**, *121*, 1601 – 1602.

[83] a) G. S. Kapur, E. J. Cabrita, S. Berger, *Tetrahedron Lett.* **2000**, *41*, 7181 – 7185; b) E. J. Cabrita, S. Berger, *Magn. Reson. Chem.* **2001**, *39*, S142 – S148.

[84] G. M. Whitesides, E. E. Simanek, J. P. Mathias, C. T. Seto, D. N. Chin, M. Mammen, D. M. Gorden, *Acc. Chem. Res.* **1995**, *28*, 37 – 44.

[85] a) R. H. Vreekamp, J. P. M. van Duynhoven, M. Hubert, W. Verboom, D. N. Reinhoudt, *Angew. Chem.* **1996**, *108*, 1306 – 1309; *Angew. Chem. Int. Ed. Engl.* **1996**, *35*, 1215 – 1218; b) P. Timmerman, R. H. Vreekamp, R. Hulst, W. Verboom, D. N. Reinhoudt, K. Rissanen, K. A. Udachin, J. Ripmeester, *Chem. Eur. J.* **1997**, *3*, 1823 – 1832; c) K. A. Jolliffe, P. Timmerman, D. N. Reinhoudt, *Angew. Chem.* **1999**, *111*, 983 – 986; *Angew. Chem. Int. Ed.* **1999**, *38*, 933 – 937.

[86] P. Timmerman, J. L. Weidmann, K. A. Jolliffe, L. J. Prins, D. N. Reinhoudt, S. Shinkai, L. Frish, Y. Cohen, *J. Chem. Soc. Perkin Trans. 2* **2000**, 2077 – 2089.

[87] a) B. Olenyuk, M. D. Levin, J. A. Whiteford, J. E. Shield, P. J. Stang, *J. Am. Chem. Soc.* **1999**, *121*, 10434 – 10435; b) S. Viel, L. Mannina, A. Segre, *Tetrahedron Lett.* **2002**, *43*, 2515 – 2519.

[88] a) M. Greenwald, D. Wessely, I. Goldberg, Y. Cohen, *New J. Chem.* **1999**, *23*, 337 – 344; b) M. Shaul, Y. Cohen, *J. Org. Chem.* **1999**, *64*, 9358 – 9364; c) W. H. Otto, M. H. Keefe, K. E. Splan, J. T. Hupp, C. K. Larive, *Inorg. Chem.* **2002**, *41*, 6172 – 6174.

[89] G. R. Neukome, C. N. Morefield, F. Vogtle, Dendritic Macromolecules, 2nd ed., VCH, New York, **2001**.

[90] a) G. R. Newkome, J. K. Young, G. R. Baker, R. L. Potter, L. Audoly, D. Cooper, C. D. Weis, K. Morris, C. S. Johnson, Jr., *Macromolecules* **1993**, *26*, 2394 – 2396; b) J. K. Young, G. R. Baker, G. R. Newkome, K. F. Morris, C. S. Johnson, Jr., *Macromolecules* **1994**, *27*, 3464 – 3471.

[91] H. Ihre, A. Hult, E. Söderlind, *J. Am. Chem. Soc.* **1996**, *118*, 6388 – 6395.

[92] C. B. Gorman, J. C. Smith, M. W. Hager, B. L. Parkhurst, H. Sierzputowska-Gracz, C. A. Haney, *J. Am. Chem. Soc.* **1999**, *121*, 9958 – 9966.

[93] J. M. Riley, S. Alkan, A. Chen, M. Shapiro, W. A. Khan, W. R. Murphy, Jr., J. E. Hanson, *Macromolecules* **2001**, *34*, 1797 – 1809.

[94] a) S. Hecht, N. Vladimirov, J. M. J. Fréchet, *J. Am. Chem. Soc.* **2001**, *123*, 18 – 25; b) A. I. Sagidullin, A. M. Muzafarov, M. A. Krykin, A. N. Ozerin, V. D. Skirda, G. M. Ignat'eva, *Macromolecules* **2002**, *35*, 9472 – 9479; c) S. W. Jeong, D. F. O'Brien, G. Orädd, G. Lindblom, *Langmuir* **2002**, *18*, 1073 – 1076.

[95] a) D. Bratko, P. Stilbs, M. Bester, *Macromol. Rapid Commun.* **1985**, *6*, 163 – 168; b) R. Rymden, P. Stilbs, *J. Phys. Chem.* **1985**, *89*, 3502 – 3505.

[96] a) L. G. Longsworth, *J. Am. Chem. Soc.* **1952**, *74*, 4155 – 4159; b) L. G. Longsworth, *J. Phys. Chem.* **1960**, *64*, 1914 – 1917.
[97] H. J. Tyrell, K. R. Harris, *Diffusion in Liquids*, Butterworth, London, **1984**.
[98] Y. Cohen, A. Ayalon, *Angew. Chem.* **1995**, *107*, 888 – 890; *Angew. Chem. Int. Ed. Engl.* **1995**, *34*, 816 – 818.
[99] A. Ayalon, A. Sygula, P.-C. Cheng, M. Rabinovitz, P. W. Rabideau, L. T. Scott, *Science* **1994**, *265*, 1065 – 1067.
[100] a) R. E. Hoffman, E. Shabtai, M. Rabinovitz, V. S. Iyer, K. Müllen, A. K. Rai, E. Bayrd, L. T. Scott, *J. Chem. Soc. Perkin Trans. 2* **1998**, 1659 – 1664; b) E. Shabtai, R. E. Hoffman, P. Cheng, E. Bayrd, D. V. Preda, L. T. Scott, M. Rabinovitz, *J. Chem. Soc. Perkin Trans. 2* **2000**, 129 – 133.
[101] a) T. C. Pochapsky, P. M. Stone, *J. Am. Chem. Soc.* **1990**, *112*, 6714 – 6715; b) T. C. Pochapsky, A. P. Wang, P. M. Stone, *J. Am. Chem. Soc.* **1993**, *115*, 11 084 – 11 091.
[102] a) S. S. Pochapsky, H. Mo, T. C. Pochapsky, *J. Chem. Soc. Chem. Commun.* **1995**, 2513 – 2514; b) H. Mo, T. C. Pochapsky, *J. Phys. Chem. B* **1997**, *101*, 4485 – 4486.
[103] I. Keresztes, P. G. Williard, *J. Am. Chem. Soc.* **2000**, *122*, 10 228 – 10 229.
[104] M. Valentini, H. Rüegger, P. S. Pregosin, *Helv. Chim. Acta* **2001**, *84*, 2833 – 2853.
[105] S. Beck, A. Geyer, H.-H. Brintzinger, *Chem. Commun.* **1999**, 2477 – 2478.
[106] a) S. Beck, M. H. Prosenc, H. H. Brintzinger, R. Goretzki, N. Herfert, G. Fink, *J. Mol. Catal.* **1996**, *11*, 67 – 79; b) N. G. Stahl, C. Zuccaccia, T. R. Jensen, T. J. Marks, *J. Am. Chem. Soc.* **2003**, *125*, 5256 – 5257.
[107] C. Zuccaccia, G. Bellachioma, G. Cardaci, A. Macchioni, *Organometallics* **2000**, *19*, 4663 – 4665.
[108] a) M. Valentini, P. S. Pregosin, H. Rüegger, *Organometallics* **2000**, *19*, 2551 – 2555; b) M. Valentini, P. S. Pregosin, H. Rüegger, *J. Chem. Soc. Dalton Trans.* **2000**, 4507 – 4510.
[109] N. E. Schöler, E. J. Cabrita, S. Berger, *Angew. Chem.* **2002**, *114*, 114 – 116; *Angew. Chem. Int. Ed.* **2002**, *41*, 107 – 109.
[110] R. A. Fecik, K. E. Frank, E. J. Gentry, S. R. Menon, L. A. Mitscher, H. Telikepalli, *Res. Lab.* **1998**, *18*, 149 – 185.
[111] *Combinatorial Chemistry: Synthesis, Analysis, Screening* (Ed.: G. Jung), Wiley-VCH, Weinheim, **1999**.
[112] M. J. Shapiro, J. S. Gounarides, *Prog. Nucl. Magn. Reson. Spectrosc.* **1999**, *35*, 153 – 200, and references therein.
[113] H. Barjat, G. A. Morris, S. C. Smart, A. G. Swanson, S. C. R. Williams, *J. Magn. Reson. Ser. B* **1995**, *108*, 170 – 172; b) M. D. Palta, H. Barjat, G. A. Morris, A. L. Davis, S. J. Hammond, *Magn. Reson. Chem.* **1998**, *36*, 706 – 714; c) A. M. Dixon, C. K. Larive, *Anal. Chem.* **1997**, *69*, 2122 – 2128.
[114] For an early example of mixture evaluation by using DOSY see: K. F. Morris, P. Stilbs, C. S. Johnson, Jr., *Anal. Chem.* **1994**, *66*, 211 – 215.
[115] For high-resolution DOSY applications see: G. A. Morris, H. Barjat in *Methods for Structure Elucidation by High-Resolution NMR* (Eds.: Gy. Batta, K. E. Köveŕ, Cs. Szántay, Jr.), Elsevier, Amsterdam, **1997**, pp. 209 – 226.
[116] a) H. Barjat, G. A. Morris, A. G. Swanson, *J. Magn. Reson.* **1998**, *131*, 131 – 138; b) for hybrid sequences, see: N. Birlirakis, E. Guittet, *J. Am. Chem. Soc.* **1996**, *118*, 13 083 – 13 084.
[117] R. K. Harris, K. A. Kinnear, G. A. Morris, M. J. Stchedroff, A. Samadi-Maybodi, N. Azizi, *Chem. Commun.* **2001**, 2422 – 2423.
[118] a) P. J. Hajduk, R. P. Meadows, S. W. Fesik, *Q. Rev. Biophys.* **1999**, *32*, 211 – 240; b) M. van Dongen, J. Weight, J. Uppenberg, J. Schultz, M. Wikström, *Drug Discovery Today* **2002**, *7*, 471 – 478c) B. Meyer, T. Peters, *Angew. Chem.* **2003**, *115*, 890 – 918; *Angew. Chem. Int. Ed.* **2003**, *42*, 864 – 890.
[119] a) S. B. Shuker, P. J. Hajduk, R. P. Meadows, S. W. Fesik, *Science* **1996**, *274*, 1531 – 1534; b) P. J. Hajduk, R. P. Meadows, S. W. Fesik, *Science* **1997**, *278*, 497 – 499.
[120] a) M. Lin, M. J. Shapiro, *J. Org. Chem.* **1996**, *61*, 7617 – 7619; b) M. Lin, M. J. Shapiro, J. R. Wareing, *J. Am. Chem. Soc.* **1997**, *119*, 5249 – 5250; c) A. Chen, M. J. Shapiro, *Anal. Chem.* **1999**, *71*, 669A – 675A; d) the research groups of Lindon and Nicholson suggested in parallel a similar approach to study complex biofluids, see: M. Liu, J. K. Nicholson, J. A. Parkinson, J. C. Lindon, *Anal. Chem.* **1997**, *69*, 1504 – 1509; for a recent review from these research groups concerning the use of diffusion NMR spectroscopy in biochemicals and pharmacological applications, see: J. C. Lindon, M. Liu, J. K. Nicholson, *Rev. Anal. Chem.* **1999**, *18*, 23 – 66.
[121] The determination of SARs by NMR spectroscopy is currently applicable for proteins having a molecular weight of 20–30 kDa although transverse relaxation-optimized spectroscopy (TROSY) can extend the molecular weights amenable to NMR investigation beyond 100 kDa, see: K. Pervushin, R. Riek, G. Wider, K. Wüthrich, *Proc. Natl. Acad. Sci. USA* **1997**, *94*, 12 336 – 12 371. In contrast, this size limitation does not exist for NMR screening methods based on diffusion filtering (see the text).
[122] P. J. Hajduk, E. T. Olejniczak, S. W. Fesik, *J. Am. Chem. Soc.* **1997**, *119*, 12 257 – 12 261.
[123] a) M. Lin, M. J. Shapiro, J. R. Wareing, *J. Org. Chem.* **1997**, *62*, 8930 – 8931; b) K. Bleicher, M. Lin, M. J. Shapiro, J. R. Wareing, *J. Org. Chem.* **1998**, *63*, 8486 – 8490; c) R. C. Anderson, M. Lin, M. J. Shapiro, *J. Comb. Chem.* **1999**, *1*, 69 – 72.
[124] a) J. A. Jones, D. K. Wilkins, L. J. Smith, C. M. Dobson, *J. Biomol. NMR* **1997**, *10*, 199 – 203; b) S. L. Mansfield, D. A. Jayawickrama, J. S. Timmons, C. K. Larive, *Biochim. Biophys. Acta* **1998**, *1382*, 257 – 265; c) X. Gao, T. C. Wong, *Biophys. J.* **1998**, *74*, 1817 – 1888; d) W. Zhang, T. E. Smithgall, W. H. Gmeiner, *Biochemistry* **1998**, *37*, 7119 – 7126; e) M. L. Tillett, M. A. Horsfield, L.-Y. Lian, T. J. Norwood, *J. Biomol. NMR* **1999**, *13*, 223 – 232; f) W. S. Price, F. Tsuchiya, Y. Arata, *J. Am. Chem. Soc.* **1999**, *121*, 11 503 – 11 511; g) W. S. Price, F. Tsuchiya, C. Suzuki, Y. Arata, *J. Biomol. NMR* **1999**, *13*, 113 – 117; h) X. Gao, T. C. Wong, *Biopolymers* **1999**, *50*, 555 – 568; i) S. Yao, G. J. Howlett, R. S. Norton, *J. Biomol. NMR* **2000**, *16*, 109 – 119; j) X. Chang, D. Keller, S. I. O'Donoghue, J. J. Led, *FEBS. Lett.* **2002**, *515*, 165 – 170; k) T. S. Derrick, E. F. McCord, C. K. Larive, *J. Magn. Reson.* **2002**, *155*, 217 – 225; l) A. M. Weljie, A. P. Yamniuk, H. Yoshino, Y. Izumi, H. J. Vogel, *Protein Sci.* **2003**, *12*, 228 – 236.
[125] a) M. J. Shapiro, J. Chin, A. Chen, J. R. Wareing, Q. Tang, R. A. Tommasi, H. R. Marepalli, *Tetrahedron Lett.* **1999**, *40*, 6141 – 6143; b) J. A. Chin, A. Chen, M. J. Shapiro, *J. Comb. Chem.* **2000**, *2*, 293 – 296; c) J. Chin, A. Chen, M. J. Shapiro, *Magn. Reson. Chem.* **2000**, *38*, 782 – 784.
[126] a) J. Lapham, J. P. Rife, P. B. Moore, D. M. Crothers, *J. Biomol. NMR* **1997**, *10*, 255 – 262; b) W. H. Gmeiner, C. J. Hudalla, A. M. Soto, L. Marky, *FEBS. Lett.* **2000**, *465*, 148 – 152; c) X. Yang, Y. S. Sanghvi, X. Gao, *J. Biomol. NMR* **1997**, *10*, 383 – 388.
[127] a) J. Balbach, *J. Am. Chem. Soc.* **2000**, *122*, 5887 – 5888; b) A. V. Buevich, J. Baum, *J. Am. Chem. Soc.* **2002**, *124*, 7156 – 7162.

